Hydrodesulfurization of Benzothiophene and Dibenzothiophenes over Phosphorus Modified $CoMo/Al_2O_3$

BY

Khaja Wahab Ahmed

A Thesis Presented to the

DEANSHIP OF GRADUATE STUDIES

KING FAHD UNIVERSITY OF PETROLEUM & MINERALS

DHAHRAN, SAUDI ARABIA

In Partial Fulfillment of the
Requirements for the Degree of

MASTER OF SCIENCE

In

CHEMICAL ENGINEERING

April, 2011

KING FAHD UNIVERSITY OF PETROLEUM & MINERALS

DHAHRAN- 31261, SAUDI ARABIA

DEANSHIP OF GRADUATE STUDIES

This thesis, written by **KhajaWahab Ahmed** under the direction his thesis advisor and approved by his thesis committee, has been presented and accepted by the Dean of Graduate Studies, in partial fulfillment of the requirements for the degree of **MASTER OF SCIENCE IN CHEMICAL ENGINEERING.**

Thesis Committee

Dr. Usamah A. Al-Mubaiyedh
Department Chairman

29/01/2011

Dr. Muhammad A. Al-Saleh
(Advisor)

Dr. Salam A. Zummo
Dean of Graduate Studies

Dr. ShakeelAhmed(Member)

1/4/11

Date

Dr. Mohammad
MozaharHossain(Member)

Dedicated

To

My Family

ACKNOWLEDGMENTS

In the name of ALLAH, the Most Beneficent, the Most Merciful.

Praise and gratitude to ALLAH, the Almighty, with whose gracious help, I was able to complete this work with patience and endurance.

Acknowledgement is due to King Fahd University of Petroleum and Minerals, Saudi Arabia for providing the support and also for the Center of Research Excellence in Petroleum Refining and Petrochemicals KFUPM

I am deeply grateful to my thesis advisor Dr. Muhammad A. Al Saleh for his support, guidance and encouragement throughout this study. His wide knowledge and logical way of thinking have been great value for me. I would also like to thank my committee member Dr. Shakeel Ahmed for his inspiring guidance, motivation and for his extensive discussions.

I would like to express my profound gratitude and appreciation to Dr. Syed Ahmed Ali whose complete support was with me in every step of this study and I learned a lot and feel fortunate to work with him. I would also like to thanks my committee member Dr. Mohammad Mozahar Hossain for his cooperation, reviews and comments. I also wish to thank Dr. Muhammad Ashraf Ali for his support for GC analysis.

I would also like to thank the staff of CRP, KFUPM-RI, specially Mr Khursheed Alam, Mr Abdul bari and Mr Owais for their help during the experimental work.

Very special thanks to parents and other family members for their unconditional and endless support, love, sacrifices, prayers and understanding throughout my academic career. You all have been a constant support for me and showed never wavering belief in me and understanding during the last 2 years.

I am grateful to all my colleagues for their help and friendship especially to Saad, Jamal, Shahid and Wajahat for their motivational support and exchanging ideas. I want to express my thanks to some of my dearest friends especially specially Usman, Imran, Hanif, Babar, Faraz, Zeehasham, Salman, Asad, Asif, Kashif and all others for their friendship and for being there for me when I needed someone to help clear my thoughts and to give me much needed bout of laughter.

Contents

ACKNOWLEDGMENTS iv

Contents vi

List of Tables ix

List of Figures xiii

Abstract (English) xix

Abstract (Arabic) xx

Chapter 1. INTRODUCTION 1

1.1 Hydrotreating of Refinery Streams 1

1.2 Sulfur Compounds in Refinery Streams 3

1.2.1 Origin of sulfur compounds in Gasoline 4

1.2.2 Origin of sulfur compounds in Diesel 4

1.3 Different Sulfur Compounds encountered in HDS 4

1.4 Reaction Pathways of Model Compounds 5

1.4.1 Thiophene 5

1.4.2 Benzothiophene 6

1.4.3 Dibenzothiophene 7

1.5 Hydrodesulfurization Catalyst 9

1.5.1 Structure of the oxide catalyst precursor 10

1.5.2 Structure of the sulfided catalyst 11

Chapter 2. LITERATURE REVIEW 14

2.1 Reactivity of Model Compounds 14

2.2 Possible Reaction Pathways for 4,6-DMDBT. 17

2.3 Comparison of $CoMo/Al_2O_3$ with $NiMo/Al_2O_3$ for HDS of 4,6-DMDBT 19

2.4 Phosphorus Modified CoMoS and NiMoS Catalyst 20

2.5 Objectives 27

Chapter 3. EXPERIMENTAL 28

3.1 Experimental Design 28

3.2 Catalyst Preparation 29

3.3 Catalyst Characterization 34

3.3.1 Surface Area Measurement 34

3.3.2 X-Ray Diffraction 36

3.4 Batch Reactor Evaluation 38

3.5 Product analysis 39

Chapter 4. RESULTS AND DISCUSSIONS 40

4.1 Catalyst Characterization 41

4.1.1 Pore size distribution 41

4.1.2 X-Ray Diffraction. 42

4.2 Batch Reactor Evaluation 43

4.2.1 Preliminary Runs 43

4.2.2 Blank Runs 47

4.2.3 Reproducibility Runs. 47

4.3 Simultaneous HDS of Benzothiophene and Dibenzothiophene over $CoMo/Al_2O_3$ 48

4.3.1 Reaction Rate constants for simultaneous HDS of BT and DBT 51

4.3.2 Selectivity of Biphenyl and CHB 54

4.3.3 Apparent Activation energy 60

4.4 Simultaneous HDS of Dibenzothiophene and 4-Methyl Dibenzothiophene over Phosphorus modified CoMoP/Al_2O_3 62
4.4.1 Reaction Rate constants for Simultaneous HDS of DBT and 4-MDBT over phosphorus modified CoMo/Al_2O_3 68
4.4.2 Reaction pathways for DBT and 4-MDBT 73
4.4.3 Rate of Formation for HDS product of DBT and 4-MDBT 80
4.4.4 Apparent Activation energy for DBT and 4-MDBT. 88

4.5 Simultaneous HDS of Dibenzothiophene and 4,6-dimethyl dibenzothiophene over Phosphorus modified CoMoP/Al_2O_3. 89
4.5.1 Reaction Rate constants for Simultaneous HDS of DBT and 4,6-DMDBT over phosphorus modified CoMo/Al_2O_3 98
4.5.2 Reaction Pathways for DBT and 4,6-DMDBT 102
4.5.3 Rate of Formation for HDS product of DBT and 4,6-DMDBT 109

4.6 Comparison of CoMoP(0.5)/Al_2O_3 and NiMo(0.5)/Al_2O_3 in simultaneous HDS of DBT and 4-MDBT. 116
4.6.1 Reaction pathways of DBT and 4-MDBT over NiMoP (0.5)/Al_2O_3 120
4.6.2 Rate of Formation for HDS product of DBT and 4-MDBT 122

4.7 Comparison of CoMoP (0.5)/Al_2O_3 and NiMo (0.5)/Al_2O_3 in simultaneous HDS of DBT and 4,6-DMDBT 127
4.7.1 Reaction Pathways for DBT and 4,6-DMDBT over NiMoP(0.5)/Al_2O_3. 129
4.7.2 Rate of Formation for HDS product of DBT and 4,6-DMDBT 133

Chapter 5. CONCLUSIONS AND RECOMENDATIONS 136
5.1 Conclusions 136
5.2 Recommendations 137

APPENDICES 138

References 142

List of Tables

Table 1.1 Properties of various straight run refinery fractions. 4

Table 1.2 Reaction rate constants for different model compounds. 9

Table 2.1 Literature available for Phosphorus modified Catalysts. 25

Table 3.1 Composition of $CoMo/Al_2O_3$ catalysts. 28

Table.3.2. Catalysts Compositions and experiments at various temperatures with different feeds. 29

Table 4.2.1 Total sulfur (ppm) remaining in the reaction mixture 45

Table 4.2.2 Reaction rate constant kx1000 over Commercial $CoMo/Al_2O_3$ and $NiMo/Al_2O_3$ 46

Table 4.3.1 Composition of Catalysts with different Co/ (Co+Mo) ratio. 48

Table 4.3.2 Total Sulfur Conversion over different $CoMo/Al_2O_3$. 50

Table 4.3.3 Reaction rate constants of benzothiophene and dibenzothiophene over $CoMo/Al_2O_3$ Catalysts. 53

Table 4.3.4 Rate constants of biphenyl and cyclohexyl benzene obtained from initial transformation of DBT 60

Table.4.3.5 Activation energies of Benzothiophene and Dibenzothiophene over $CoMo/Al_2O_3$. 61

Table 4.4.1 Composition of Phosphorus modified catalysts. 62

Table 4.4.2 Sulfur (ppm) remaining in the reaction mixture over CoMoP(0) $/Al_2O_3$ catalyst 63

Table 4.4.3 Sulfur remaining in the reaction mixture over CoMoP(0.5)/Al2O3 catalyst 65

Table 4.4.4 Sulfur remaining in the reaction mixture over CoMoP(1)/Al_2O_3 catalyst 66

Table 4.4.5 Sulfur remaining in the reaction mixture over CoMoP(1.5)/Al_2O_3 catalyst. 67

Table 4.4.6 Reaction rate constants kx1000 (min^{-1}) of dibenzothiophene over different catalysts. 71

Table 4.4.7 Reaction rate constants kx1000 (min^{-1}) of 4 methyl dibenzothiophene over different catalysts. 71

Table 4.4.8 $k_{DBT}/k_{4\text{-}MDBT}$ ratio at two different temperatures 72

Table.4.4.9 Formation rate constant kx1000 (min^{-1}) of biphenyl at different temperatures..... 85

Table.4.4.10 Formation rate constant of kx1000 (min^{-1}) Cyclohexyl benzene at different temperatures. 85

Table.4.4.11 k_{BP}/k_{CHB} ratio at two different temperatures 86

Table.4.4.12 Formation rate constant of kx1000 (min^{-1}) methyl biphenyl benzene at different temperatures. 86

Table.4.4.13 Formation rate constant of kx1000 (min^{-1}) methyl cyclohexyl benzene at different temperatures. 87

Table.4.4.14 k_{MBP}/k_{MCHB} ratio at two different temperatures 87

Table 4.4.15 Activation Energies (KJ/mole). 88

Table 4.5.1 Sulfur (ppm) remaining in the reaction mixture over CoMoP(0)/Al_2O_3 catalyst. 91

Table 4.5.2 Sulfur (ppm) remaining in the reaction mixture over CoMoP (0.5)/Al_2O_3 catalyst. 92

Table 4.5.3 Sulfur (ppm) remaining in the reaction mixture over CoMoP(1)/Al_2O_3 catalyst. 94

Table 4.5.4 Sulfur (ppm) remaining in the reaction mixture over CoMoP(1.5)/Al_2O_3 catalyst. 95

Table 4.5.5 rate constants kx1000 of DBT and 4,6-DMDBT over different catalysts at 350°C. 101

Table 4.5.6 Foramtion rate constants kx1000 of Biphenyl and Cyclohexyl benzene and the ratio of formation rate constants at 350°C..... 114

Table 4.5.7 Rate constant kx1000 and Relative rate of formation of Biphenyl and Cyclohexyl benzene..... 115

Table 4.5.8 Foramtion rate constants kx1000 of Dimethyl biphenyl and Cyclohexyl benzene and the ratio of formation rate constants at 350°C..... 115

Table 4.6.1 Composition of Catalysts. 116

Table 4.6.2 Sulfur remaining in the reaction mixture over NiMoP(0.5)/Al_2O_3 catalyst. 117

Table 4.6.3 Reaction rate constants kx1000 (min^{-1}) of dibenzothiophene over different catalysts..... 118

Table 4.6.4 Reaction rate constants kx1000 (min^{-1}) of 4 methyl dibenzothiophene over different catalysts..... 119

Table 4.6.5 $k_{DBT}/k_{4\text{-}MDBT}$ ratio at two different temperatures. 119

Table.4.6.6 Formation rate constant kx1000 (min^{-1}) of biphenyl at different temperatures..... 124

Table.4.6.7 Formation rate constant of kx1000 (min^{-1}) Cyclohexyl benzene at different temperatures. 124

Table.4.6.8 k_{BP}/k_{CHB} ratio at two different temperatures..... 125

Table.4.6.9 Formation rate constant of kx1000 (min^{-1}) methyl biphenyl benzene at different temperatures..... 125

Table.4.6.10 Formation rate constant of kx1000 (min^{-1}) methyl cyclohexyl benzene at different temperatures..... 125

Table.4.6.11 k_{MBP}/k_{MCHB} ratio at two different temperatures. 126

Table 4.7.1 Sulfur (ppm) remaining in the reaction mixture over NiMoP(0.5)/Al_2O_3 catalyst. 128

Table 4.7.2 rate constants kx1000 of DBT and 4-MDBT over different catalysts at 350^oC..... 129

Table 4.7.3 Foramtion rate constants k x1000 of Biphenyl and Cyclohexyl benzene and the ratio formation rate constants at 350^oC..... 134

Table 4.7.4 Rate constant kx1000 and Relative rate of formation of dimethyl biphenyl and methyl cyclohexyl toluene..... 135

List of Figures

Figure 1.1: Various sulfur compounds encountered in HDS reaction..... 5

Figure 1.2 Reaction pathways for Thiophene. 6

Figure 1.3 Reaction pathways for Benzothiophene HDS. 7

Figure 1.4: Reaction pathways for Dibenzothiophene. 8

Figure 1.5. Orientation of small MoS_2 particles on (111) - (a) and (100)- (b) γ-Al_2O_3 surface. 12

Figure 1.6. Three forms of nickel present in a sulfided NiMo/Al2O3 catalyst: as active sites on the MoS_2 edges (the Ni-Mo-S phase), as segregated Ni3S2, and as Ni^{2+} ions in the support lattice. 13

Figure 1.7. Structure of different forms in which cobalt ion present in Co-promoted MoS_2/Al_2O_3. 13

Figure 2.1: Different Reaction pathways to increase the reactivity of 4,6-DMDBT 17

Figure 2.2: Enhancement of flexibility due to partial hydrogenation. 18

Figure 3.1 Steps in the preparation $CoMo/Al_2O_3$ Catalysts. 32

Figure 3.2 Steps in the preparation of phosphorus modified Catalyst ($CoMoP/Al_2O_3$)..... 33

Figure 3.3 Batch reactor used for HDS study. 38

Figure 4.1.1 Pore size distribution for $CoMo/Al_2O_3$ and phosphorus modified $CoMo/Al_2O_3$ 41

Figure 4.1.2 X-ray Diffraction patterns for $CoMo/Al_2O_3$ and phosphorus modified $CoMo/Al_2O_3$ 42

Figure 4.2.1 Conversion of BT and DBT in Competitive reaction over $CoMo/Al_2O_3$. 44

Figure 4.2.2 Conversion of BT and DBT in Competitive reaction over $NiMo/Al_2O_3$. 44

Figure 4.2.3 Rate constant of benzothiophene and dibenzothiophene at different temperatures over $CoMo/Al_2O_3$ catalyst. 45

Figure 4.2.4 Rate constant of benzothiophene and dibenzothiophene at different temperatures over $NiMo/Al_2O_3$ catalyst. 46

Figure 4.2.5 Reproducibiltiy Conversion of BT and DBT in Competitive reaction over $CoMo/Al_2O_3$. 47

Figure 4.3.1 Conversion of BT and DBT in Competitive reaction over $0.3CoMo/Al_2O_3$. 49

Figure 4.3.2 Conversion of BT and DBT in Competitive reaction over $0.4CoMo/Al_2O_3$. 49

Figure 4.3.3 Conversion of BT and DBT in Competitive reaction over $0.5CoMo/Al_2O_3$. 50

Figure 4.3.4 Rate constant of benzothiophene and dibenzothiophene at different temperatures over $0.3CoMo/Al_2O_3$ catalyst. 52

Figure 4.3.5 Rate constant of benzothiophene and dibenzothiophene at different temperatures over $0.4CoMo/Al_2O_3$ catalyst. 52

Figure 4.3.6 Rate constant of benzothiophene and dibenzothiophene at different temperatures over $0.5CoMo/Al_2O_3$ catalysts. 53

Figure 4.3.7 Transformation of DBT over $0.3CoMo/Al_2O_3$ catalyst. 54

Figure 4.3.8 Transformation of DBT over $0.4CoMo/Al_2O_3$ catalyst. 55

Figure 4.3.9 Transformation of DBT over $0.5CoMo/Al_2O_3$ catalyst. 55

Figure 4.3.10 Biphenyl to Cyclohexyl Benzene ratio over all $CoMo/Al_2O_3$ catalysts versus reaction time. 57

Figure 4.3.11 Biphenyl to Cyclohexyl Benzene ratio over all $CoMo/Al_2O_3$ catalysts versus total Conversion. 57

Figure 4.3.12 Formation rates of BP and CHB at 350°C over 0.3CoMo/Al_2O_3 catalyst. 58

Figure 4.3.13 Formation rates of BP and CHB at 350oC over 0.4CoMo/Al2O3 catalyst. 59

Figure 4.3.14 Formation rates of BP and CHB at 350°C over 0.5CoMo/Al_2O_3 catalyst. 59

Figure 4.3.15 Arrhenius plot for Benzothiophene and Dibenzothiophene hydrodesulfurization. 61

Figure 4.4.1 Conversion of DBT and 4-MDBT in Competitive reaction over CoMoP(0)/Al_2O_3 63

Figure 4.4.2 Conversion of DBT and 4-MDBT in Competitive reaction over CoMoP(0.5)/Al_2O_3 64

Figure 4.4.3 Conversion of DBT and 4-MDBT in Competitive reaction over CoMoP(1)/Al_2O_3 65

Figure 4.4.4 Conversion of DBT and 4-MDBT in Competitive reaction over CoMoP(1.5)/Al_2O_3. 67

Figure 4.4.5 Rate constant of DBT and 4-MDBT at different temperatures over CoMoP(0)/Al_2O_3. 69

Figure 4.4.6 Rate constant of DBT and 4-MDBT at different temperaturesover CoMoP(0.5)/Al_2O_3. 69

Figure 4.4.7 Rate constant of DBT and 4-MDBT at different temperatures over CoMoP(1)/Al_2O_3. 70

Figure 4.4.8 Rate constant of DBT and 4-MDBT at different temperatures over CoMoP(1.5)/Al_2O_3. 70

Figure 4.4.9 Transformation of DBT over CoMoP(0)/Al_2O_3 catalyst. 74

Figure 4.4.10 Transformation of 4-MDBT over CoMoP(0)/Al_2O_3 catalyst. 74

Figure 4.4.11 Transformation of DBT over CoMoP(0.5)/Al_2O_3 75

Figure 4.4.12 Transformation of 4-MDBT over CoMoP (0.5)/Al_2O_3 catalyst. 76

Figure 4.4.13 Transformation of DBT over CoMoP(1)/Al_2O_3 catalyst. 77

Figure 4.4.14 Transformation of 4-MDBT over CoMoP(1)/Al_2O_3 catalyst. 77

Figure 4.4.15 Transformation of DBT) over CoMoP(1.5)/Al_2O_3 catalyst. 78

Figure 4.4.16 Transformation of 4-MDBT over CoMoP(1.5)/Al_2O_3 catalyst. 79

Figure 4.4.17 Formation rates of BP and CHB over CoMoP (0)/Al_2O_3 catalyst. 80

Figure 4.4.18 Formation rates of MBP and MCHB over CoMoP(0)/Al_2O_3 catalyst. 81

Figure 4.4.19 Formation rates of BP and CHB over CoMoP (0.5)/Al_2O_3 catalyst. 81

Figure 4.4.20 Formation rates of MBP and MCHB over CoMoP(0.5)/Al_2O_3 catalyst. 82

Figure 4.4.21 Formation rates of BP and CHB over CoMoP(1)/Al_2O_3 catalyst. 82

Figure 4.4.22 Formation rates of MBP and MCHB over CoMoP(1)/Al_2O_3 catalyst. 83

Figure 4.4.23 Formation rates of BP and CHB over CoMoP (1.5)/Al_2O_3 catalyst. 83

Figure 4.4.24 Formation rates of MBP and MCHB over CoMoP(1.5)/Al_2O_3 catalyst. 84

Figure 4.5.1 Conversion of DBT and 4,6-DMDBT in Competitive reaction over CoMoP(0)/Al_2O_3. 90

Figure 4.5.2 Conversion of DBT and 4,6-DMDBT in Competitive reaction over CoMoP(0.5)/Al_2O_3. 91

Figure 4.5.3 Conversion of DBT and 4,6-DMDBT in Competitive reaction over CoMoP(1)/Al_2O_3. 93

Figure 4.5.4 Conversion of DBT and 4,6-DMDBT in Competitive reaction over CoMoP(1.5)/Al_2O_3. 95

Figure 4.5.5 Promotional effect of phosphorus with increasing P_2O_5 content for HDS of DBT and 4-MDBT at 350^oC 96

Figure 4.5.6 Promotional effect of phosphorus with increasing P2O5 content for HDS of DBT and 4,6-DMDBT at 350^oC..... 96

Figure 4.5.7 Rate constant of DBT and 4,6-DMDBT over CoMoP (0)/Al_2O_3. 99

Figure 4.5.8 Rate constant of DBT and 4,6-DMDBT over CoMoP (0.5)/Al_2O_3. 99

Figure 4.5.9 Rate constant of DBT and 4,6-DMDBT over CoMoP(1)/Al_2O_3. 100

Figure 4.5.10 Rate constant of DBT and 4,6-DMDBT over CoMoP(1.5)/Al_2O_3. 100

Figure 4.5.12 Transformation of 4,6-DMDBT over CoMoP (0)/Al_2O_3 catalyst. 104

Figure 4.5.13 Transformation of DBT over CoMoP (0.5)/Al_2O_3 catalyst..... 105

Figure 4.5.14 Transformation of 4,6-DMDBT over CoMoP (0.5)/Al_2O_3 catalyst. 106

Figure 4.5.15 Transformation of DBT over CoMoP(1)/Al_2O_3 catalyst. 107

Figure 4.5.16 Transformation of 4,6-DMDBT over CoMoP(1)/Al_2O_3 catalyst. 107

Figure 4.5.17 Transformation of DBT over CoMoP(1.5)/Al_2O_3 catalyst..... 109

Figure 4.5.18 Transformation of 4,6-DMDBT over CoMoP(1.5)/Al_2O_3 catalyst. 109

Figure 4.5.19 Formation rates of BP and CHB over CoMoP (0)/Al_2O_3 catalyst..... 110

Figure 4.5.20 Formation rates of DMBP and MCHT over CoMoP(0)/Al_2O_3 catalyst. 110

Figure 4.5.21 Formation rates of BP and CHB over CoMoP (0.5)/Al_2O_3 catalyst. 111

Figure 4.5.22 Formation rates of DMBP and MCHT over CoMoP(0.5)/Al_2O_3 catalyst. 111

Figure 4.5.23 Formation rates of BP and CHB over CoMoP (1)/Al_2O_3 catalyst..... 112

Figure 4.5.24 Formation rates of DMBP and MCHT over CoMoP(1)/Al_2O_3 catalyst. 112

Figure 4.5.25 Formation rates of BP and CHB over CoMoP (1.5)/Al_2O_3 catalyst. 113

Figure 4.5.26 Formation rates of DMBP and MCHT over CoMoP (1.5)/Al_2O_3 catalyst..... 113

Figure 4.6.1 Conversion of DBT and 4-MDBT in Competitive reaction over NiMoP(0.5)/Al_2O_3. 117

Figure 4.6.2 Rate constant of DBT and 4-MDBT at different temperature sover NiMoP(0.5)/Al_2O_3. 118

Figure 4.6.3 Transformation of DBT over NiMoP (0.5)/Al_2O_3 catalyst. 121

Figure 4.6.4 Transformation of 4-MDBT over NiMoP(0.5)/Al_2O_3 catalyst..... 122

Figure 4.6.5 Formation rates of BP and CHB over NiMoP (0.5)/Al_2O_3 catalyst 123

Figure 4.6.6 Formation rates of BP and CHB over NiMoP (0.5)/Al_2O_3 catalyst 123

Figure 4.7.1 Conversion of DBT and 4,6-DMDBT in Competitive reaction over NiMoP(0.5)/Al_2O_3. 127

Figure 4.7.2 Rate constant of DBT and 4,6-DMDBT over NiMoP(0.5)/Al_2O_3..... 128

Figure 4.7.3 Transformation of DBT over NiMoP (0.5)/Al_2O_3 catalyst. 130

Figure 4.7.4 Transformation of 4,6-DMDBT over NiMoP(0.5)/Al_2O_3 catalyst. 131

Figure 4.7.5 Formation rates of BP and CHBnover NiMoP(0.5)/Al_2O_3 catalyst. 133

Figure 4.7.6 Formation rates of MBP and MCHB over NiMoP(1.5)/Al_2O_3 catalyst..... 134

ABSTRACT

Name **Khaja Wahab Ahmed**

Thesis Title **HDS of Benzothiophene and Dibenzothiophenes over Phosphorus modified $CoMo/Al_2O_3$**

Degree **Masters of Science**

Major Field **Chemical Engineering**

Date of Degree **April 2011**

Deep desulfurization of middle distillate involves the removal of residual sulfur compounds such as alkyl substituted benzothiophenes, dibenzothiophenes. There is a renewed interest in study of hydrodesulphurization of these refractory sulfur compounds due to the requirement to use new feed stocks and the application of more severe environmental legislations. Therefore there is a need to study HDS of these refractory compounds to achieve very low sulfur levels. In this study reactivities, reaction pathways and reaction kinetics of benzothiophene and hindered dibenzothiophenes were studied. The focus was on 4,6-DMDBT and 4-MDBT which are considered as most refractory sulfur compounds to be desulfurized. $CoMo/Al_2O_3$ and Phosphorus modified $CoMo/Al_2O_3$ were synthesized by wet impregnation method. Catalysts were characterized by BET surface area and pore volume and by X-ray Diffraction. Reaction studies were carried out in a batch autoclave reactor system. $CoMo/Al_2O_3$ catalysts were prepared to achieve selective HDS properties and to enhance the favorable reaction pathway. The phosphorus modified $CoMo/Al_2O_3$ shows higher conversion as compared to unmodified catalysts. The reaction pathway study showed that the simultaneous Hydrodesulfurization (HDS) of DBT in a simultaneous reaction were influenced due to the presence of 4-MDBT and 4,6-DMDBT, the conversion of DBT was higher for the latter case. Simultaneous HDS of DBT also influenced the Direct desulfurization/Hydrogenation (DDS/HYD) ratio which was higher when DBT was desulfurized with 4,6-DMDBT.

خـــلاصـــــة الرســــــــالـــــــة

اسم الطالب : خواجه وهاب احمد

عنوان الرسالة: HDS **ل Benzothiophene وDibenzothiophenes على الفسفور المعدل ب $CoMo/Al_2O_3$**

التخصص: هندسه كيميائيه

تاريخ الرساله: أبريل ٢٠١١م

إزالة الكبريت من المشتقات الوسيطة في أعماق الأوسط ينطوي على إزالة مركبات الكبريت المتبقية مثل ألكيل استبدال benzothiophenes ، dibenzothiophenes. هناك اهتمام متجدد في دراسة السلفرة الهيدروجينية لهذه المركبات الكبريتية الحرارية بسبب شروط لاستخدام مخزونات تغذية جديدة وتطبيق مزيد من التشريعات البيئية المتشديدة. ولذلك هناك حاجة لدراسة (HDS) من هذه المركبات المقاومة للحرارة لتحقيق مستويات الكبريت منخفه جدا. في هذا البحث درست نشاطية ، ومسارات و كيناتيكيت التفاعل ل benzothiophene و dibenzothiophenes. وكان التركيز على 4,6-DMDBT و 4-MDBT التي تعتبر مركبات الكبريت الحرارية لتكون desulfurized. فقد تم تصنيع $CoMo/Al_2O_3$ والفوسفور المعدل ب $CoMo/Al_2O_3$ من قبل أسلوب التشريب الرطب. درست المساحة BET وحجم المسام وحيود الأشعة السينية للمحفزات . وأجريت دراسات عن التفاعل في مفاعل نظام دفعة الأوتوكلاف. وأعدت $CoMo/Al_2O_3$ المحفزات لتحقيق انتقائية HDS خصائص وتعزيز المسار رد فعل مفضله. ويظهر تعديل $CoMo/Al_2O_3$ الفوسفور تحويل أعلى بالمقارنة مع المواد الحفازة المعدلة. وأظهرت الدراسة أن رد فعل مسار السلفرة الهيدروجينية في وقت واحد (HDS) من DBT في رد فعل في وقت واحد تأثرت بسبب وجود 4,6-DMDBT و 4-MDBT وتحويل DBT كان أعلى لهذه الحالة الأخيرة. في وقت واحد HDS ل DBT أثرت أيضا إزالة الكبريت المباشر / الهدرجة (HYD / DDS) الذي كان أعلى نسبة عندما desulfurized DBT مع 4,6-DMDBT.

درجة الماجستير في علوم الهندسه الكيميائيه

جامعة الملك فهد للبترول والمعادن

الظهران- المملكه العربيه السعوديه

أبريل ٢٠١١م

Chapter 1. INTRODUCTION

1.1 Hydrotreating of Refinery Streams

The main task of refinery is to convert raw crude oil into valuable products efficiently by using different chemical and physical processes like distillation, extraction, reforming, hydrogenation, cracking and blending the refinery converts crude oil to higher value products. The main products from the refinery are liquid (LPG), Gasoline, jet fuel, diesel fuel, wax, lubricants, petrochemicals and bitumen. Energy and hydrogen for internal and external use are also produced in a refinery.

Petroleum products are presently consumed in vast quantities and this consumption continues to rise up with the increasing rates. Transportation fuels, the major petroleum products are receiving the highest inspection because of new more severe environmental restrictions regarding the quality of transportation fuels. The major pollutants are SOx, CO, NOx, particulates, Olefins and aromatic hydrocarbon

Hydrotreating or hydroprocessing refers to a variety of hydrogenation processes which saturate unsaturated hydrocarbons and remove Sulfur by hydrodesulfurization (HDS), Nitrogen [by hydrodenitrogenation (HDN)], Oxygen by hydrodeoxygenation (HDO) and metals by hydrodemetallization (HDM) from different petroleum streams in a refinery. The main aim of hydrotreating is to diminish air pollution emissions, to avoid poisoning of noble metals and acid catalysts used in catalytic reforming and cracking and to improve the fuel quality.

Catalytic HDS of refinery streams carried out at elevated temperature and hydrogen partial pressure to convert organanosulfur compounds to hydrogen sulfide (H_2S) and hydrocarbon [1,2].

The conventional HDS process is usually conducted over sulfided $CoMo/Al_2O_3$ or $NiMo/Al_2O_3$Catalyst. Their Performance in terms of desulfurization level, activity and selectivity depends on the properties of specific catalyst used (active species concentration, support properties, synthesis route), the reaction conditions (sulfiding protocol, temperature partial pressure of hydrogen and H_2S), nature and concentration of the sulfur compounds present in the feed stream, and reactor and process design.

Depending on the nature of refinery stream the process conditions and precise catalyst formulation varies [3]. Today, hydroprocessing is the most widely used refining process. Some oil fractions may pass a hydroprocessing catalyst several times before they end up in the product pool. The worldwide consumption of these catalysts is in the order of 100,000 tons per year.

Hydrotreating or hydroprocessing is an established process in the refinery, having been first practiced before the World War II, and the technology has progressively evolved during the past 70 years [4]. As with any major industrial technology, the original process and its catalyst have developed according to the needs of the time. As result, today a wide diversity of process conditions, configurations and catalyst exists, although remarkably, the components of the original catalyst have hardly changed. The Co, Ni, Mo and W transition metal sulfides are still the industry favorites due to their hydrodesulfurization, hydrodenitrogenation and hydrogenation activities, as well as their availability and low

cost. Other major catalyst ingredients such as alumina, silica-alumina and zeolites have also been in use for a number of decades now.

Hydroprocessing has been an active area of research for a very long period. However, there are major challenges still to be met in the fundamental study of hydroprocessing reactions and catalyst. The chemistry involved is complex and does not allow for easy solutions. In the past decade, clean fuel research including desulfurization has become a more important subject of environmental catalysis studies worldwide.

Recent trends in Deep HDS is influenced by following major factors

1) Availability of lighter sulfur content crudes is diminishing.
2) Strict Environmental legislation limits sulfur content in gasoline and diesel fuel to less than 10ppm.

1.2 Sulfur Compounds in Refinery Streams

Organanosulfur compounds are usually present in almost all fractions of crude oil distillation. Higher boiling point fractions contain relatively more sulfur and the sulfur compounds are of higher molecular weight. Therefore, a wide spectrum of sulfur containing compounds should be considered from the viewpoint of their reactivity in the hydrotreating processes. Various refinery streams are used to produce three major types of transportation fuels, gasoline, jet fuels and diesel fuels that differ in composition and properties.

1.2.1 Origin of sulfur compounds in Gasoline

Gasoline is formed by blending several refinery streams including straight run naptha (reformate, isomerate and alkylate products), Fluid Catalytic Cracking (FCC) Naptha and Coker Naptha. FCC Naptha is responsible for most of the sulfur in gasoline. The HDS of other gasoline forming streams is not a problem treatment of FCC gasoline is essential to bring down the sulfur level to lowest level.

1.2.2 Origin of sulfur compounds in Diesel

Straight run diesel, light cycle oil from FCC unit, hydrocracker diesel, and coker diesel blend to form Diesel fuel. Most sulfur comes from FCC and Coker units which accounts for 2.5wt.% sulfur.

Table 1.1 Properties of various straight run refinery fractions.

	Naptha	Kerosene	Gas Oil	Atm.residue	Vac. GO	Vac.Residue
B.P (C)	40-180	180-230	230-360	343+	343-500	500+
S (%)	0.01-0.05	0.1-0.3	0.5-1.5	2.5-5	1.5-3	3-6

1.3 Different Sulfur Compounds encountered in HDS

Organosulfur compounds are usually present in almost all fractions of crude oil distillation. Higher boiling point fractions contain relatively more sulfur and the sulfur compounds are of higher molecular weight. Therefore, a wide spectrum of sulfur containing compounds should be considered from the viewpoint of their reactivity in the hydrotreating processes

R-S-H R-S-S-R’ R-S-R’

Thiols(Merceptants) Disulfides Sulfides

Thiophenes

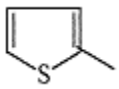

Benzothiophenes

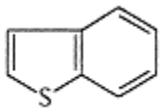

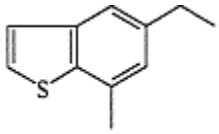

Dibenzothiophenes

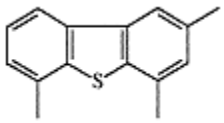

Figure 1.1: Various sulfur compounds encountered in HDS reaction.

1.4 Reaction Pathways of Model Compounds

1.4.1 Thiophene

Most of the thiophene studies have been conducted at atmospheric pressure. Thiophene HDS takes place by two parallel pathways [5].Thiophene is desulfurized prior to hydrogenation to give butadiene which is hydrogenated to butane [6].The other path is

through hydrogenation of thiophene prior to desulfurization to give Tetrahydro Thiophene(THT) which is desulfurized to butane [7].

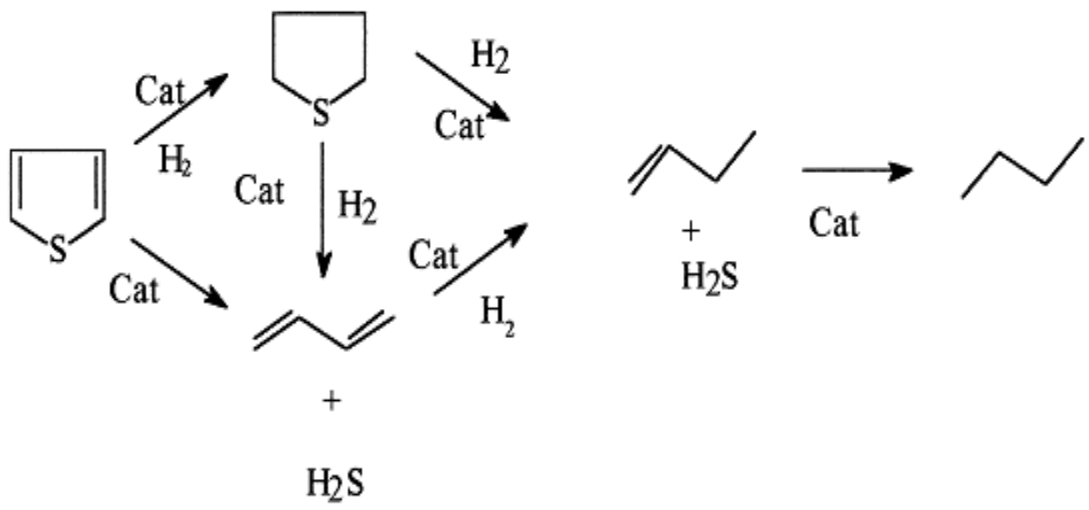

Figure 1.2 Reaction pathways for Thiophene.

1.4.2 Benzothiophene

There are two major reaction pathways that have been proposed in literature [8.9].The first path is by desulfurization of benzothiophenes prior to hydrogenation to dihydrobenzothiophene (DHBT) to give styrene, then styrene is further hydrogenated to ethylbenzene (EB). The Second path is by hydrogenation of Benzothiophene to DHBT, which is desulfurized to Ethyl Benzene. Figure 1.2 shows the benzothiophenes HDS mechanism.

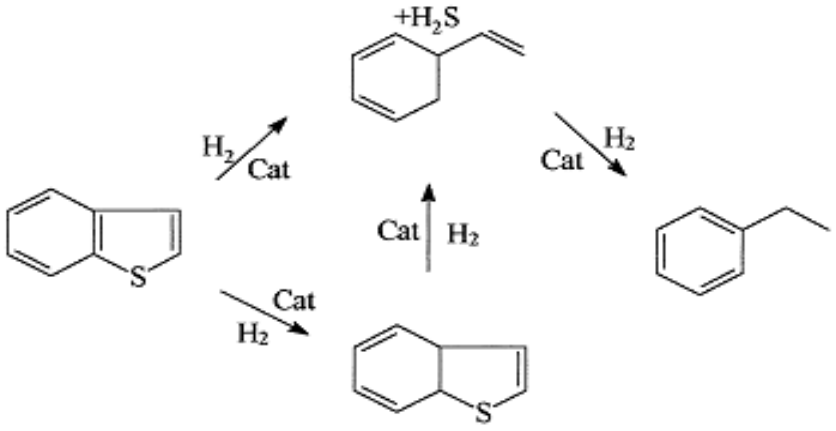

Figure 1.3 Reaction pathways for Benzothiophene HDS.

1.4.3 Dibenzothiophene

Houlla et.al [10] as proposed two parallel pathways for HDS of Dibenzothiophene (DBT). The first way is by direct desulfurization in which DBT directly desulfurized to give Biphenyl (BP). In other pathway DBT hydrogenate to yield Tetra hydro Dibenzothiophene (THDBT) or Hexaheydro Dibenzothiophene (HDBT), these intermediates then desulfurized to yield Cyclo Hexyl Benzene (CHB).

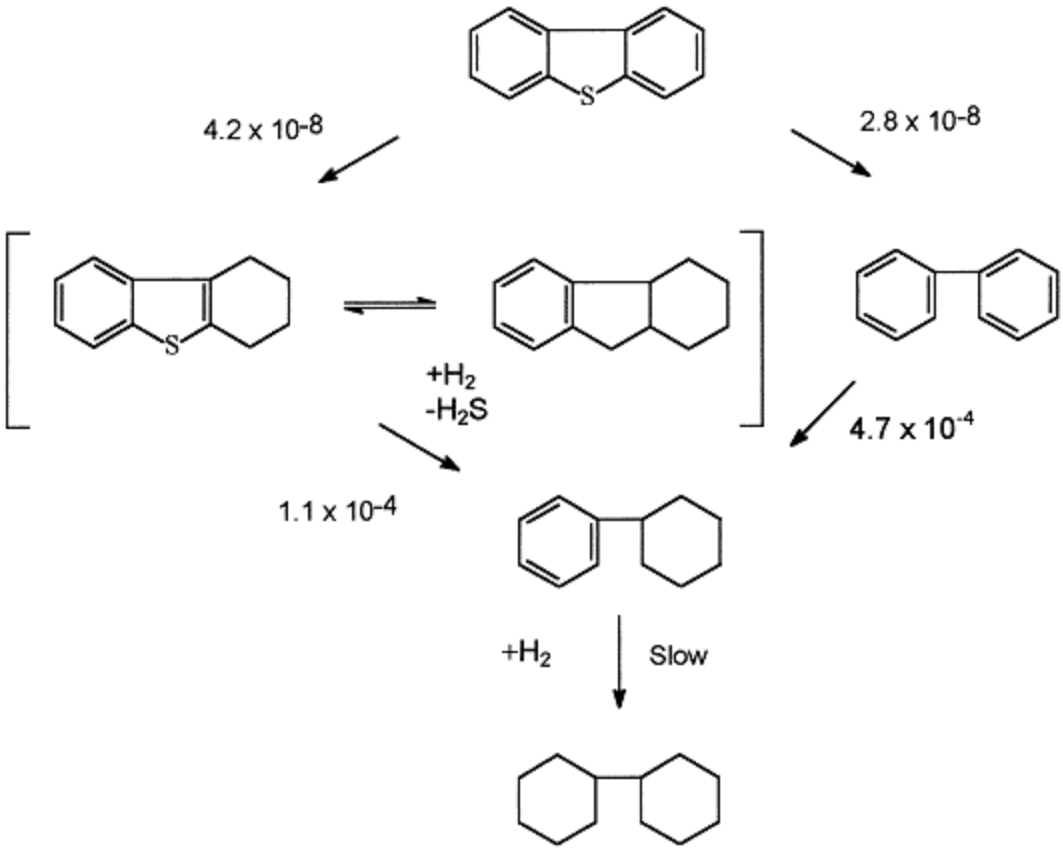

Figure 1.4: Reaction pathways for Dibenzothiophene.

Table 1.2 Reaction rate constants for different model compounds.

Compounds	Structure	Pseudo first order rate (1/g of catalyst s^{-1})
Thiophene		1.38x10-3
Benzothiophene	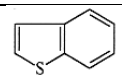	8.11x10-4
Dibenzothiophene	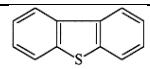	6.11x10-5
Benzon[b]naptho[2,3,d]thiophene	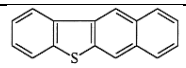	1.61x10-4
7,8,9,10-tetrahydro-Benzon[b]naptho[2,3,d]thiophene	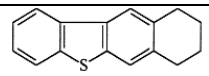	7.78x10-5

1.5 Hydrodesulfurization Catalyst

Industrial hydrotreating catalysts contain molybdenum and cobalt or nickel, supported on γ-Al_2O_3 [11, 12]. Since oil fractions always contain sulfur, a metal or metal oxide that would be introduced as a catalyst would quickly become sulfided by the H_2S that is produced during hydrotreating. In practice, one therefore sulfides supported metal oxides under controlled conditions before starting the hydrotreating process. When supported alone on alumina, molybdenum sulfide has a much higher activity for the removal of S, N and O atoms than cobalt or nickel sulfide. Therefore, molybdenum sulfide is traditionally considered to be the actual catalyst. Sulfided $CoMo/Al_2O_3$ and $NiMo/Al_2O_3$ catalysts, on the other hand, have substantially higher catalytic activities than Mo/Al_2O_3. Consequently, cobalt and nickel are referred to as promoters. Cobalt is used mainly as a promoter for sulfided Mo/Al_2O_3 in HDS, whereas nickel is most preferred choice for HDN.

1.5.1 Structure of the oxide catalyst precursor

Hydrotreating catalysts are usually prepared by a sequential pore volume impregnation procedure or by co-impregnation [13]. In the former method, the γ-Al_2O_3 support is first impregnated with an aqueous solution of ammonium heptamolybedate $(NH_4)_6Mo_7O_{24}$, followed by drying and calcination in air. In a second step, the resulting material is further impregnated with an aqueous solution of nickel nitrate $Ni(NO_3)_2$ or cobalt nitrate $Co(NO_3)_2$ and then dried and calcined. Alternatively in the industries all inorganic materials are co-impregnated in order to decrease the preparation time and lower the operation cost, and the resulting catalyst precursor is then dried and calcined.

Cobalt can be present in several forms in $CoMo/Al_2O_3$ catalysts. In Oxide form Cobalt ions interact very strongly with spinel type ɣ-Al_2O_3 lattice and occupy octahedral sites just below the Al_2O_3 surface or tetrahedral sites in the bulk of Al_2O_3. Co_3O_4 crystallites also form on the support at higher loading of cobalt.

The strong interaction between molybdenum with the hydroxyl groups on the Al_2O_3 surface has been assumed due to MoO_3 monolayer structure [14, 15]. This has been later proved by a thermodynamic study [16]. Massoth has suggested that the molybdenum is present in small patches or chains rather than a well-defined two-dimensional monolayer [17]. A similar conclusion was reached in a combined ^{1}H-NMR and low temperature chemisorption study [18], and in several EXAFS studies [19,20]. The latter studies show that Mo is present in structures without a significant order outside the first coordination shell. Even for relatively high-loading Mo/Al_2O_3 catalysts (15 wt.% MoO_3), infrared emission spectroscopy could not detect bands due to a MoO_3 phase [21], indicating that the molybdenum is present in a highly dispersed phase.

1.5.2 Structure of the sulfided catalyst

The oxide catalysts precursors, which are formed during the impregnation, drying and calcination steps, are transformed into the actual hydrotreating catalyst by sulfidation in a mixture of H_2 and one or more compounds containing sulfur. H_2S, thiophene, CS_2, dimethyl disulfide or the oil fraction to be hydrotreated can be used for the sulfidation. The properties of the final sulfided catalyst depend to a great extent on the calcination and sulfidation steps. Calcination at high temperature induces a strong interaction between molybdenum and cobalt or nickel cations and the Al_2O_3 support. Consequently, it is difficult to transform the oxidic species into sulfides. Mössbauer spectroscopy of $CoMo/Al_2O_3$ catalysts showed that, at increasingly high calcination temperatures, increasingly more Co^{2+} ions are incorporated into the bulk of the alumina [22]. The amount of that tetrahedrally coordinated Co increases at the expense of Octahedrally coordinated Co [23] and this Co specie is a precursor of CoMoS. This means by increasing the calcination temperature the amount of CoMoS decrease. The higher the calcination temperature, the higher the sulfidation temperature needed to bring these cations back to the surface to provide a high catalytic activity for hydrotreating. At temperatures that are too high, however, the metal sulfides particles sinter or do not form the catalytically active Co-Mo-S structure. Optimum calcination and sulfidation temperatures are in the range 673-773 K for Al_2O_3 supported catalysts [24].

The sulfidation mechanism was investigated by temperature-programmed sulfidation, in which the oxidic catalyst is heated in a flow of H_2S and H_2, and the consumption of H_2S and H_2 and the evolution of H_2O are measured continuously [25]. It was found that H_2S is taken up and H_2O given off, even at room temperature, indicating a sulfur-oxygen exchange reaction.

Investigations of model catalysts consisting of MoS_2 grown on γ-Al_2O_3 films on the surfaces of $MgAl_2O_4$ supports have shown that MoS_2 grows with its basal plane parallel to the (111) surface of γ-Al_2O_3 and perpendicular to the (100) γ-Al_2O_3 surface [26]. This observation suggests that the edges of the MoS_2 platelets are bonded to the (100) surface of γAl_2O_3 by Mo-O-Al bonds (Figure 1.5).

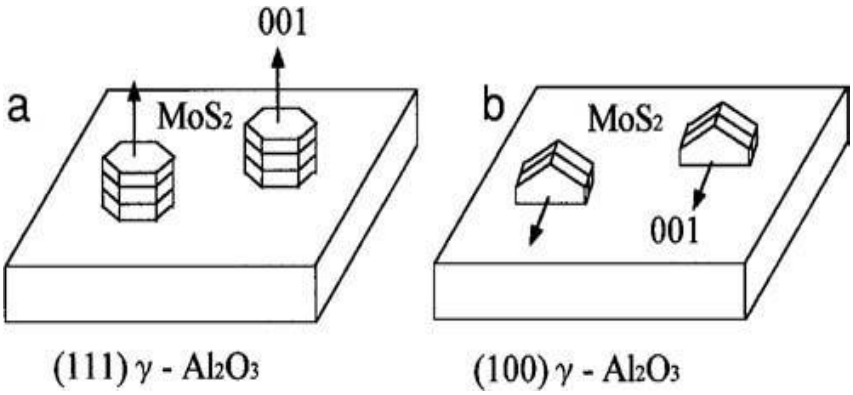

Figure 1.5. Orientation of small MoS_2 particles on (111) - (a) and (100)- (b) γ-Al_2O_3 surface.

Nickel may be present in three forms after sulfidation: as Ni_3S_2 crystallites on the support, as nickel atoms adsorbed on the edges of the MoS_2 crystallites (the so-called Ni-Mo-S phase) and as nickel cations at octahedral or tetrahedral sites in the γ-Al_2O_3 lattice (Figure 1.6). In the same way, cobalt can be present as segregated Co_9S_8, as Co-Mo-S and as cobalt cations in the support. Depending on the relative concentrations of nickel (or cobalt) and molybdenum and on the pretreatment conditions, a sulfided catalyst may contain a relatively large amount of either Ni_3S_2 (or Co_9S_8) or the Ni-Mo-S (or Co-Mo-S) phase.

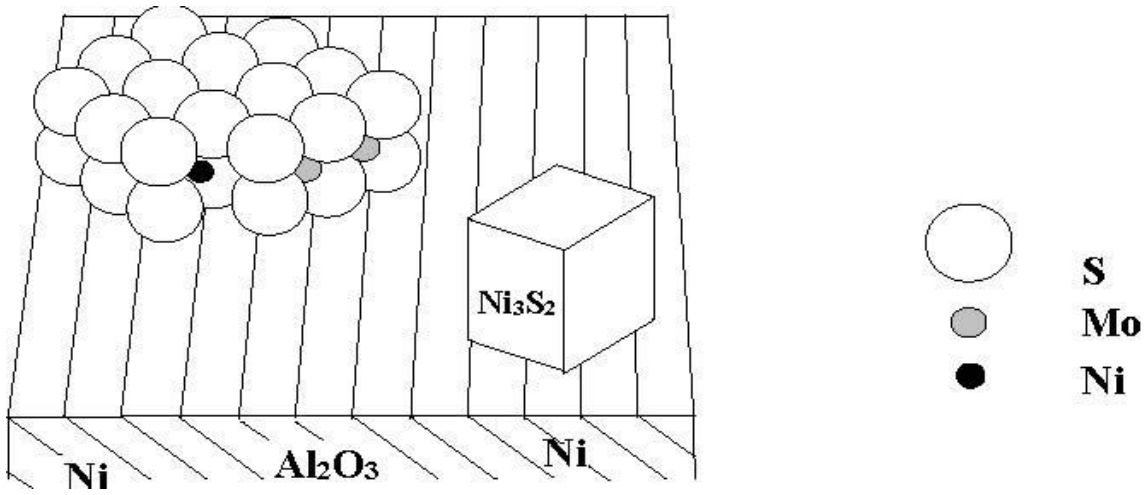

Figure 1.6. Three forms of nickel present in a sulfided NiMo/Al_2O_3 catalyst: as active sites on the MoS_2 edges (the Ni-Mo-S phase), as segregated Ni_3S_2, and as Ni^{2+} ions in the support lattice.

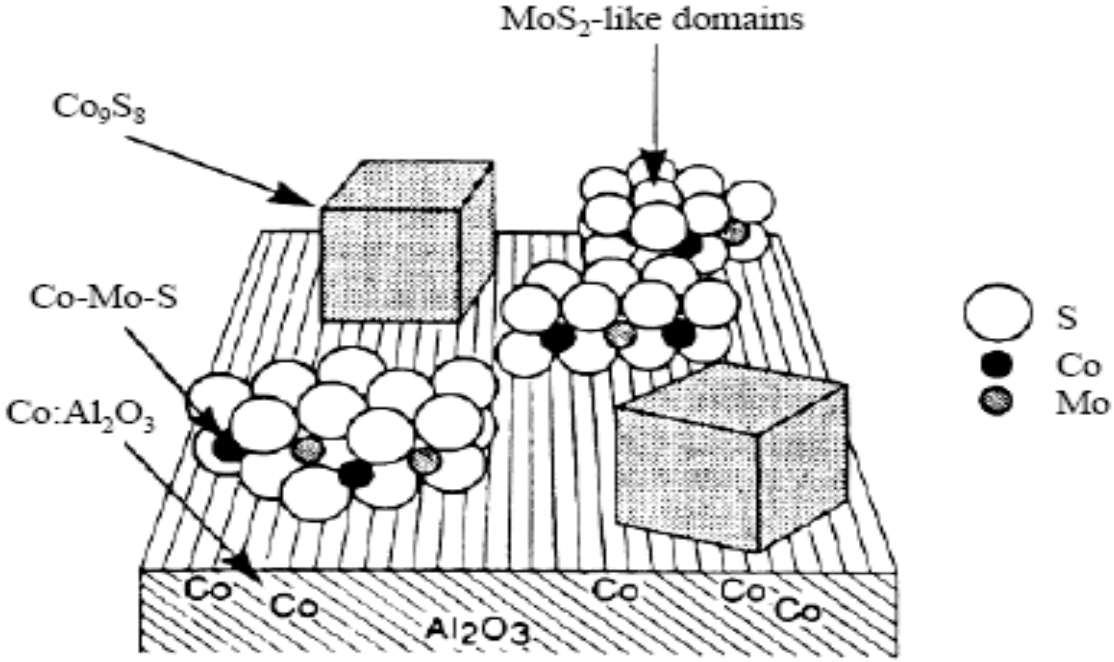

Figure 1.7. Structure of different forms in which cobalt ion present in Co-promoted MoS_2/Al_2O_3.

Chapter 2. LITERATURE REVIEW

2.1 Reactivity of Model Compounds

Hydrodesulfurization of thiophenic compounds is reported to proceed via two reaction pathways. In the first pathway, the sulfur atom is directly removed from the molecule (hydrogenolysis pathway). In the second pathway the aromatic ring is hydrogenated and sulfur is subsequently removed (hydrogenation pathway) as shown in the Figure 2.1.

It should be noted that there is a marked difference in these two pathways in terms of catalyst activity requirement, process conditions, and hydrogen consumption etc. Both pathways occur in parallel employing different active sites of the catalyst surface. Which reaction pathway pre-dominates depends on the nature of sulfur compounds, the reaction conditions, and the catalyst used. At the same reaction conditions, dibenzothiophene (DBT) reacts preferably via hydrogenolysis pathway whereas for alkylated DBT such as 4-MDBT and 4,6-DMDBT both the hydrogenation and hydrogenolysis routes are significant [27].

The reactivity of organosulfur compounds varies widely depending on their structure and local sulfur atom environment. In middle distillates, the organosulfur compounds predominantly contain thiophenic rings. These compounds include thiophenes and benzothiophenes and their alkylated derivatives. These thiophenic compounds are more difficult to desulfurize than merceptants and sulfides to convert by hydrotreating. The heaviest fractions blended to the diesel pool Fluid Catalytic Cracking (FCC) naptha, coker naptha, FCC and coker diesel, light cycle oil contain mainly alkylated benzothiophenes, dibenzothiophenes (DBT) and alkyldibenzothiophenes, as well as

polynuclear organic sulfur compounds, i.e the least reactive sulfur compounds in the HDS reaction.

Kilanowski et al. [28] studied the Hydrodesulfurization of alkylated Benzothiophenes and Dibenzothiophenes with methyl substitution in different positions. The compound chosen for the study were 3-methylbenzothiophene, 3,7-dimethylbenzothiophene, 2-methylbenzothiophene, 7-methylbenothiophene, 2,3-dihydro-benzothiophene, 4-methyldibenzothiophene, 2,8-DMDBT and 4,6 DMDBT. The HDS reactions were performed in a pulse microreactor at range of temperatures between 350°C and 450°C. The result suggested that the reactivity of these sulfur compounds decreases in the following order.

2,8-DMDBT > DBT > 4-MDBT > 4,6-DMDBT

For 2,8-MDBT the increase in reactivity was explained due to the electronic effect. They proposed that a combination of inductive and hyperconjugative effects of methyl groups *para* to the two α carbons could enrich the electron density and this increase the reactivity. For other substituted alkyl DBTs the decrease in the reactivity was due to steric effects. A similar study on hindered DBTs was carried out by Houalla et al. [29]. Hydrodesulfurization of different alkylated DBTs were studied. They found that the reactivity of 4-MDBT and 4,6-DMDBT were different .The yield of Cyclohexyl benzene (CHB) was found out to be 5-10 times greater than that from obtain from DBT at same experimental conditions. This suggest that 4-MDBT and 4,6-DMDBT were more hydrogenated before sulfur removal compared to other substituted DBTs. Mochida et al. [30] studied the various refractory sulfur compounds including hindered DBTs 4-MDBT

and 4,6-DMDBT. The result showed that out of all refractory sulfur compounds 4-MDBT and 4,6-DMDBT were most difficult to desulfurized. Pseudo first order reaction rate constant were calculated to compare the reactivites of sulfur compounds. This study also includes the inhibition effect of H_2S on HDS of sulfur compounds. As the Hydrodesulfurization starts Benzothiophene, which is more reactive comparatively to hindered DBTs, desulfurized to produce large amount of H_2S. The HDS was found out to be inhibited on both $CoMo/Al_2O_3$ and $NiMo/Al_2O_3$. Zhang et al.[31] investigated the HDS of DBT and 4,6-DMDBT over $CoMo/Al_2O_3$and $NiMo/Al_2O_3$. The DBTs used were 4-MDBT and 4,6-DMDBT, the HDS were carried out at temperature range of 190 to 340°C. The products obtained were corresponding Biphenyls and Cyclohexyl Benzene. HDS of DBT results in Bipheyl and Cyclohexyl Benzene and the products obtained from HDS of 4,6-DMDBT were 3, 3-DMBiPh and 3,3-DMCHB. Reactivities were found out to be decreased in the order of DBT > 4-MDBT > 4,6-DMDBT. When Biphenyl and 3,3-DMBiPh were added in the substrate, the concentration of CHB did not increase that suggest that CHBs were mostly coming from hydrogenation of DBTs before sulfur removal Lamuremeille et al. [32].

2.2 Possible Reaction Pathways for 4,6-DMDBT.

As discussed in the previous Chapter out of all DBTs, 4,6-DMDBT is most refractory sulfur compound to be desulfurized. Figure.2.1 showed the possible ways to effectively desulfurized 4,6-DMDBT.

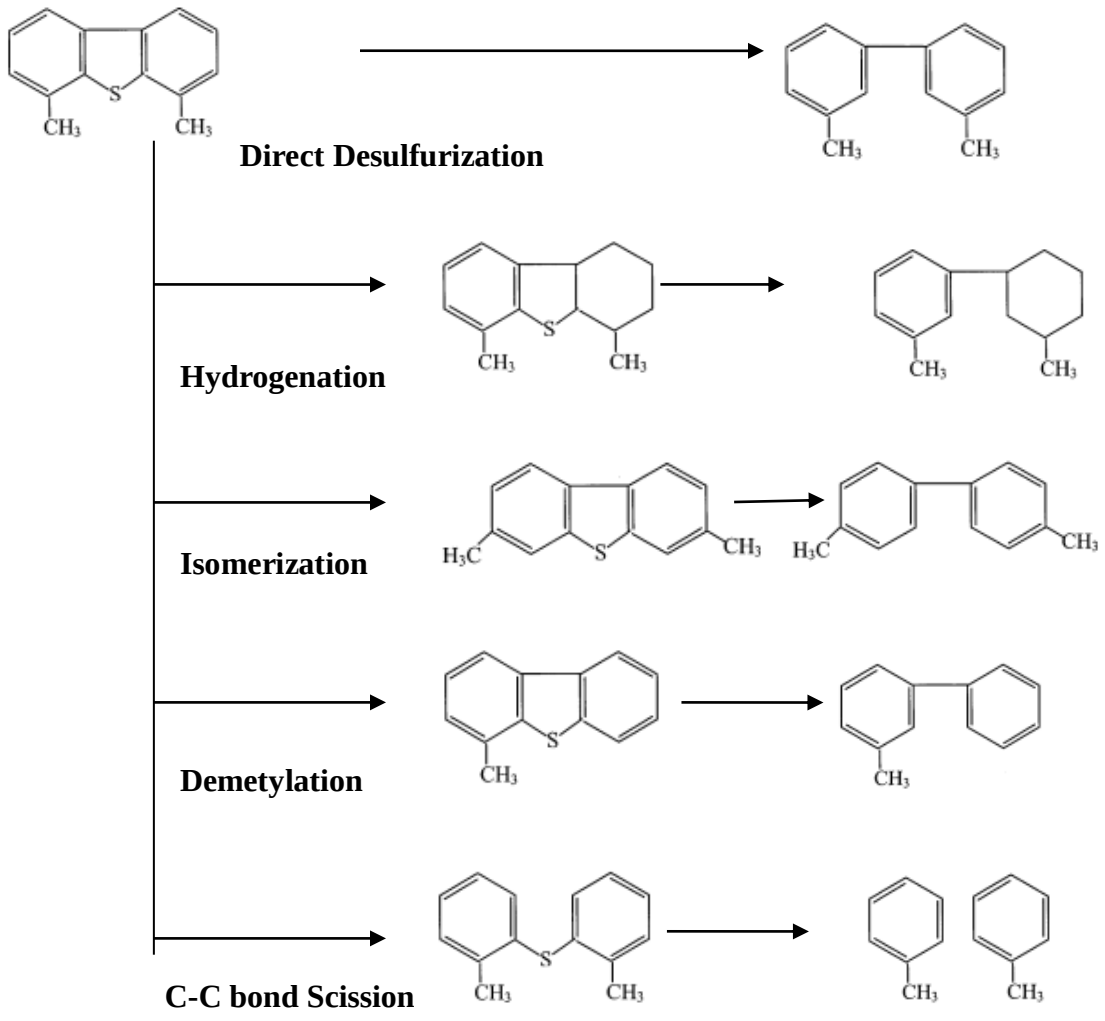

Figure 2.1: Different Reaction pathways to increase the reactivity of 4,6-DMDBT

Figure 2.1 shows 4 possible ways of desulfurization of 4,6-DMDBT. Except the Direct Desulfurization route all 3 other routes are based on the removing of steric hindrance of

the methyl groups attached to 4th and 6th positions of phenyl ring. The most important HDS pathway for 4,6-DMDBT is hydrogenation of one of the phenyl ring, before sulfur removal. The hydrogenation of one of the phenyl ring increases the flexibility of methyl group and hence decreases the steric hindrance [33]. Fig. 2.2 shows the enhancement of flexibility of partially hydrogenated 4,6-DMDBT.

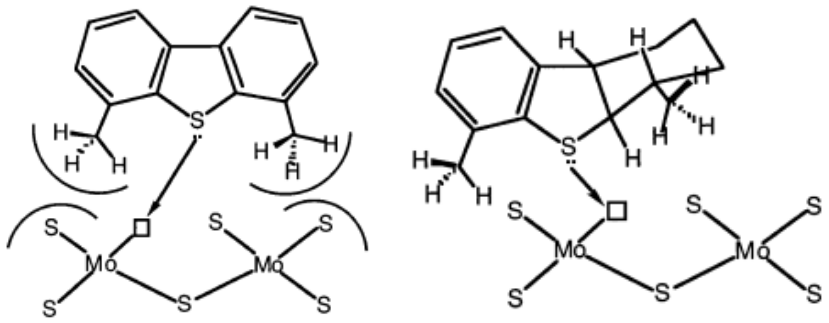

Figure 2.2: Enhancement of flexibility due to partial hydrogenation.

Isomerization is also useful to shift the position of 4, 6 to 3, 7 or 2, 8. As the product thus formed have relatively as compared to 4,6-DMDBT. Dealkylation of one or both methyl ring is also an option as the resulting DBTs. Dibenzothiophene and 4-MDBT are comparatively more reactive than 4,6-DMDBT [34,35]. C-C bond Scission in thiophenic ring is also an option.

The entire above reaction path shown in Fig.2.5 can be grouped as hydrogenative and non hydrogenative pathways. For hydrogenative pathway that takes place with the saturation of phenyl rings before sulfur removal depends on the catalyst ability to hydrogenate. This property can be increased by using metals with more hydrogenation potential like Ni, W, Pt, Pd and Ru and also increase the metal loading and the dispersion of active metal on support. The metal loading can be increased by using high surface area support. The other

HDS pathway i.e. non hydrogenative way which includes isomerization, Dealkylation and C-C bond scission depends on the acidic properties of catalyst [22].

2.3 Comparison of $CoMo/Al_2O_3$ with $NiMo/Al_2O_3$ for HDS of 4,6-DMDBT

It is generally believed that $NiMo/Al_2O_3$has higher hydrogenation ability as compared with $CoMo/Al_2O_3$. One of the study carried out by Isoda et al. [36]on 4,6-DMDBT by using $CoMo/Al_2O_3$ and $NiMo/Al_2O_3$ catalyst. The HDS of 4,6-DMDBT was carried out at same experimental, 270°C and 3 MPa hydrogen pressure. At these experimental conditions the conversion of 4,6-DMDBT over NiMo was 68% and over CoMo 49%. Hydrogenative pathway was found out to be the main route over both catalysts. Also further hydrogenation of second ring in MCHT was prominent only when the reaction took place over NiMo catalyst. In a similar study carried out by lecremamu et al. [37] the activity of CoMo and NiMo were compared. The CoO content of CoMo was 4.3wt.% and NiO content of NiMo was 3.1 wt.%. The reaction was carried out in decane and 4,6-DMBDT was used as a model compound. The first order rate constant of 4,6-DMDBT over CoMo catalyst were 0.006 min^{-1} g^{-1} and over NiMo based catalyst were 0.02 min^{-1} g^{-1}. The ratio of Hydrogenative product to direct desulfurization product (DDS/HDS) over CoMo catalyst at 270°C was 4 and over NiMo catalyst at same conditions was 12. They proposed that this enhancement of HDS activity is due to the more hydrogenation capability of NiMo catalyst. As from the above literature we can see that $NiMo/Al_2O_3$ performed better, but the aromatic content of the feedstock also affects the performance of the catalysts. In their study Isoda et al.[38] used a feed in which 4,6-DMDBT was

mixed with decane and Napthalene. Due to the presence of significant amount of naphthalene the conversion of 4,6-DMDBT over NiMo catalyst was decreased because of hydrogenation of naphthalene. On the other hand the conversion of 4,6-DMDBT over CoMo catalyst was not much retarded. In one of their study lecreany et al. [39] studied $CoMoS/Al_2O_3$ and $NiMoS/Al_2O_3$catalyst. The CoO and NiO content of the catalyst were 3wt.% and MoO content in both catalysts was 10wt.%. The CoMoS catalyst showed higher activity as compared to NiMoS for transalkylation of Isopropyl benzene. NiMoS catalyst was more active as compared to CoMoS catalyst for hydrogenation of naphthalene. The HDS of 4,6-DMDBT was carried over both catalyst at 270^oC in decane. The rate constant o over NiMoS was found out to be doubled that of CoMoS. By this result they concluded that for HDS of 4,6-DMDBT the hydrogenation property of NiMo is more important than the cracking property provided by the CoMoS catalyst.

2.4 Phosphorus Modified CoMoS and NiMoS Catalyst

In order to improve catalyst properties, Phosphorus addition to commercial Co(Ni)Mo catalyst is a common practice. J. M. Lewis et.al. [40] did HDS study of thiophene on $NiMo-Al_20_3$ catalyst modified with phosphorus the catalyst composition was MoO_3 15 wt. % and NiO 3wt. % by using three different methods (1) All the precursors AHM (Ammonium hepta molybedate) Nickel Nitrate and phosphoric acid were added in the same impregnation solution (2) Three separate impregnation solutions were used and catalyst were calcined prior to addition of phosphoric acid**.** (3) In third method separate impregnation solutions were used but phosphoric acid was added first and the metal salts were added after calcinations. The metal loading was kept constant and the different

catalyst was prepared by varying the phosphorus loading. The phosphorus loading was 0.3, 1, 3, 5, 7 wt. % phosphorus. The catalyst so formed is tested for HDS activity of thiophene and a promotional effect of phosphorus modification was observed for all three methods of preparation. They found out that 3rd preparation method yields best results. The optimum phosphorus loading was found out to be 1wt.% P. The effect of phosphorus addition on Co-MoS_2/Al_2O_3 was studied by Yasuaki Okamoto [41]. A series of MoO supported catalyst was prepared by co-Impregnating H_3PO_4, $(NH_4)_6Mo_7O_{24}.4H_2O$ followed by calcinations at 773K for 5 hours. The phosphorus content was 0, 0.2, 0.5, 1, 2, 3 and 5wt. %. The MoO_3 catalyst was presulfided at 673K for 1.5 hours. Cobalt was introduced by Chemical vapor deposition (CVD) technique. The HDS activity for thiophene with Co-MoS_2/Al_2O_3 was slightly increased by addition of 0.2wt.% P, followed by a slight decrease with further addition of phosphorus. The promotion effect of phosphorus modified $CoMo/Al_2O_3$ was also studied on HDS of DBT and 4,6-DMDBT. KWAK et.al. [42] did HDS study by using $CoMoS/Al_20_3$ Catalyst for DBT and 4,6DBT HDS. They concluded that phosphorus modified catalyst behaves in two ways one by increasing the metal dispersion and second increase the bronsted acidity. In DBT HDS phosphorous modification increase the formation of (CHB) cyclohexylbenzene than (BP). For 4,6-DMDBT the conversion also increases but more Dimetylbiphenyl (DMBP) is formed than metcylcyclohexyltoluene (MCHT). These are the opposite trends because HDS of DBT takes place by Direct desulphurization route and the main product is (BP) and for 4,6 DMDBT the hydrodesulphurization takes place by hydrogenation route .So Phosphorus modification allows migration of methyl groups in 4,6-DMDBT. The optimum phosphorus content was observed to be 0.5 wt. %. Other supports like MCM-41

were also modified by phosphorus to investigate its effects [43]. NiMo catalyst was used in this study with MoO_3 12 wt.% and NiO 3wt.% and Phosphorus content was (0-5wt.%P_2O_5). It was found out that incorporation of P on MCM-41 material increase the acidity. HDS of DBT and 4,6-DMDBT was also performed and the result showed that the modified NiMo/P-MCM-41 showed higher catalytic activity than reference NiMo/Al_2O_3 for 4,6-DMDBT. The highest activity was observed for MCM-41 modified with 1wt.% P_2O_5. For DBT at this optimum P loading the ratio of CHB to Biphenyl was 0.91 and for 4,6-DMDBT the ratio of MCHT/DMBiP was 4.70 where MCHT is (Methyl Cyclo hexyl toluene) hydrogenation product and DMBiP (Dimethyl Biphenyl) is direct desulfurization product.

The influence of catalyst acidity on the reaction mechanism of 4,6-DMDBT HDS over CoMo hydrotreating Catalyst was studied by B.Pawelec et.al. [44]. In this study P free Ti-HMS and P containing P/Ti-HMS mesoporous siliceous material were synthesized and used as support .Simultaneous Impregnation of Co and Mo phased was found out to be the best method. Phosphorous addition promotes the isomerization route of 4,6 DMDBT than the dealkylation route. On CoMoP/Al_2O_3 reference catalyst HDS of 4,6 DMDBT proceeded through Hydrogenation and DDS pathways and DDS pathway was the main route for HDS. For all the catalyst supported on Ti-HMS the catalyst composition was Co 3wt.% and Mo 9wt.%. .The phosphorus content for P containing catalyst was 0.64 wt.% . The HDS of 4,6-DMDBT over supported Ti-HMS catalyst took place by dealkylation and Isomerization followed by hydrogenation and DDS pathways. In one of the study Hexagonal mesoporous silica (HMS) were modified with phosphorus and used as a support for CoMo catalyst [45]. The activity of P containing CoMo catalyst was

examined by HDS of DBT and compared with $CoMo/Al_2O_3$. It was found out that dispersion of Co and Mo species depends on the presence of phosphate and also on the sequence of Co and Mo Order. Co-Impregnation method was favorable than sequential impregnation. The optimum P_2O_5 content was 1.5wt. % and give best results with catalyst prepared by co impregnation method. The maximum conversion with P(1.5)/HMS substrate for HDS of DBT was 84.5% as compared to 53.6% for commercial $CoMo/Al_20_3$catalyst .

F.Richard et.al [46] studied the HDS of 4,6-DMDBT over pure sulfide $NiMoP/Al_2O_3$ catalyst and mechanical mixtures containing $NiMoP/Al_20_3$ and an acidic component such as HY and H(B) zeolites at 340°C under 4MPa of total pressure in fixed bed reactor. The HDS of 4,6-DMDBT was also carried out on HY and Hβ zeolites at 350°C under atmospheric pressure. The HDS of 4,6-DMDBT over pure $NiMoP/Al_2O_3$ took place by direct desulfurization and Hydrogenation pathways. For pure zeolite 4,6-DMDBT transformed by both isomerization and disproportionation reactions. Hβ was found out to be more selective for Isomerization than HY zeolites. For bifunctional catalyst obtained by mechanical mixing of (sulfide $NiMoP/Al_2O_3$-Zeolite) increase the reactivity of 4,6-DMDBT. By bifunctional catalyst two new categories of product were obtained which were due to isomerization and disproportionation products owing to zeolite presence. These products were found to be more reactive than 4,6-DMDBT. Out of all the catalysts $NiMoP/Al_2O_3$ sulfided catalyst associated with HY-16 (Si/Al ratio =16) was most active of all. The level of improvement increases with amount of phosphorus addition Zhou et.al. [47] used different P/MoO ratio to make different $NiMoP/Al_2O_3$ catalyst with composition of NiO+MoO =25% and Ni/Mo ration of 3/7 for all the catalyst. The

optimum HDS activity of NiMoP//Al_2O_3 catalyst increase with the increase in P loading and reached maximum at P/MoO_3 ratio of 0.08 to 0.10.

The above literature shows different possible reaction pathways and enhancement in the reactivity of refractory sulfur compounds specially 4,6-DMDBT. The Phosphorus loading and optimum loading differ from one study to another. Except one or two studies most of the studies show the promotional effect of phosphorus.

Table 2.1 Literature available for Phosphorus modified Catalysts.

Catalyst	Composition Preparation method	Reaction Condition	Optimum phosphorus content	Results
$NiMo/Al_2O_3$ [40]	MoO 15wt. **%** and NiO 3wt.%.Phosphorus content 0.3, 1, 3, 5, 7%.	The HDS of Thiophene was carried out in flow reactor at 400^oC under atmospheric conditions.	1 wt.% P	The catalyst prepared by co-Impregnation gives best results.
$CoMo/Al_2O_3$ [42]	17wt. % MoO_3 and 4wt. %CoO. Ɣ-alumina was modified by H_3PO_4.	HDS of DBT and 4, 6- DMDBT was carried out in a 100 cm^3 autoclave at 623K under hydrogen pressure of 40MPa.	0.5wt.% P_2O_5	Conversion of DBT and 4,6-DMDBT was 75 and 51% respectively.
NiMo/MCM-41 [43]	MoO_3 12 wt. % and NiO 3 wt. % phosphorus content 0 to 5 wt. % $P_2O_5.H_3PO_4$ were used to impregnate the support.	The HDS of DBT and 4,6-DMDBT was carried out in batch reactor at 300C^o and 7.3MPa H_2 pressure for 8 hours.	1wt.% P_2O_5	CHB/BP =0.91 for DBT MCHT/DMBP= 4.70 for 4.6DMDBT
CoMo/Ti-HMS [44]	MoO_3 9wt. % and CoO 3wt. % .P_2O_5 content was 0.64wt. %.	The HDS of 4,6-DMDBT were carried out in batch and fixed bed reactor at 598K and H_2pressure of 5.5MPa.	0.64wt.% P_2O_5	The conversion of 4,6-DMDBT 92.2%.
CoMo/HMS [45]	Mo 10wt. % and Co 3wt. %. The HMS molecular sieves were modified by H_3PO_4 to achieve the P_2O_5 loading of 0.5, 1, 1.5, 2wt. %.	The HDS of DBT was carried out in batch reactor at 623K at 3.1MPa for 5 hours.	1.5wt.% P_2O_5	Conversion of 84.5% for DBT
$NiMo/Al_2O_3$ [47]	NiO+MoO = 25wt. % and Ni/Mo = 3/7. The Support was modified by H_3PO_4.	The HDS were performed in fixed bed reactor at 230^oC and 2MPa pressure.	P/MoO_3 =0.08-0.10	Conversion of DBT was 70% and BP/CHB =1.75

Abbreviation used in table 2.1.

(CHB)Cyclohexyl benzene, (BP) Biphenyl, (MCHT) Methyl cyclohexyl Toluene, (DMBP) Dimethyl Biphenyl

DDS/HYD = (BP) Biphenyl / (CHB) Cyclo Hexyl Benzene

(ISO/DA) Isomerization/ Dealkylation, Dealkylation (DA) route vs. isomerization (ISO) route products: [(DBT+THDBT+BP+CHB+DCH)/ (3, 4'-DMBP [(or 3, 3'-DMBP) +BP]

, (HMS) Hexagonal mesoporous Silica

2.5 Objectives

The overall objectives of this study is to investigate hydrodesulfurization of model compounds benzothiophene, dibenzothiophene, 4methyl dibenzothiophene and 4,6-dimethyldibenzothiophene over different metal oxide catalysts. However, the specific objectives of the study are as follows.

- Preparation of $CoMo/Al_2O_3$ catalysts with different Co/(Co+Mo) ratio.
- Preparation of $CoMo/Al_2O_3$ catalysts modified with phosphorus.
- Characterization of prepared Catalysts by X-ray diffraction and Sorption Analysis.
- Evaluation of prepared catalysts in batch autoclave reactor at various temperatures and using different feeds of Model Compounds (Benzothiophenes, Dibenzothiophenes)

Chapter 3. EXPERIMENTAL

3.1 Experimental Design

The first part of this study deals with the preparation of $CoMo/Al_2O_3$ Catalysts with different composition and Co/Co+Mo ratios. Benzothiophene and dibenzothiophene were desulfurized over these catalysts and the promising catalysts which give higher activity were selected for the preparation of phosphorus modified $CoMoP/Al_2O_3$ catalysts. Table 3.1 shows the composition of $CoMo/Al_2O_3$catalysts that were used for the first part of study i.e. for hydrodesulfurization of Benzothiophene and Dibenzothiophene.

By the 1st part catalyst evaluation a series of phosphorus modified $CoMoP/Al_2O_3$ catalysts were synthesized by keeping the metal oxide concentration constant and varying the phosphorus content. One $NiMoP/Al_2O_3$ and $CoNiMoP/Al_2O_3$catalysts were also prepared to compare the activity with $CoMoP/Al_2O_3$.

Table 3.1 Composition of $CoMo/Al_2O_3$ catalysts.

Catalyst	MoO_3(wt %)	CoO(wt %)	Al_2O_3(wt %)	Co/(Co+Mo)
$0.3CoMo/Al_2O_3$	15.4	3.6	81	0.3
$0.4CoMo/Al_2O_3$	14.0	5.0	81	0.4
$0.5CoMo/Al_2O_3$	12.4	6.6	81	0.5

Table.3.2. Catalysts Compositions and experiments at various temperatures with different feeds.

Catalysts	MoO_3 (wt %)	CoO (wt %)	NiO (wt %)	P_2O_5 (wt %)	Feed#1	Feed#2
CoMoP(0))/Al_2O_3	15	4		0	DBT + 4-MDBT At 300,325 and 350°C	DBT + 4,6-DMDBT At 350°C
CoMoP(0.5))/Al_2O_3	15	4		0.5		
CoMoP(1))/Al_2O_3	15	4		1		
CoMoP(1.5))/Al_2O_3	15	4		1.5		
NiMoP(0.5)/Al_2O_3	15	0	4	0.5		

3.2 Catalyst Preparation

In this work $CoMo/Al_2O_3$ catalysts were prepared by wet Impregnation method. One series of catalyst was prepared by keeping the total metal oxide (MoO_3 + CoO) concentration constant at 19 wt.%. Different catalysts were prepared by varying the Co/(Co+Mo) ratio. The other series of catalysts were prepared with the same metal oxide concentration but with variation in phosphorus content. In this way two series of $CoMo/Al_2O_3$ catalysts with and without phosphorus were synthesized. The first series of catalysts were prepared with the Co/(Co+Mo) ratio of 0.3, 0.4 and 0.5. The second series was prepared with Co/Co+Mo ratio of 0.4 and varying the P_2O_5 content to 0.5, 1 and 1.5wt.%.

Calcination of Catalyst Support Al_2O_3

Boehmite Alumina was calcined to change it into Gamma Phase (ɣ). The calcination temperature was 600^oC for 3 hours with the rate of 5C^o/minute.

Impregnation Step (for CoMo/Al_2O_3Catalyst)

The CoMo/Al_2O_3catalyst was prepared at room temperature by co impregnation of Ammonium heptamolybedate $(NH_4)_6Mo_7O_{24.}4H_2O$ and Cobalt nitrate $Co(NO_3)_{2.}6H_2O$ simultaneously on calcined ɣ-alumina. The catalyst was the heated at100^oC for 12 hours. Follow by calcination at 500 ^oC for 1 hour with a heating rate of 5^oC /min.

Impregnation Step (for CoMoP/Al_2O_3)

For Phosphorus modified CoMoP/Al_2O_3catalyst the ɣ-alumina support was first modified with H_3PO_4 to get the desired loading of P_2O_5. After Impregnation of H_3PO_4 the support was dried and calcined as above followed by the impregnation of $(NH_4)_6Mo_7O_{24.}4H_2O$ and $Co(NO_3)_{2.}6H_2O$ simultaneously and then dried and calcined with the same procedure as used for the CoMo/Al_2O_3.

Sulfiding

The catalyst formed after calcination is in the oxide form. The oxide catalysts are not active and therefore catalyst was sulfided before the HDS reaction in a flow reactor.

The steps for sulfiding are as follows

1. After catalyst loading, pressure testing was carried at room temperature.
2. The reactor was then slowly depressurized to 4 MPa pressure.
3. At 4 MPa, the gas flow was started and the temperature was slowly increased to 100^oC at max 25^oC /h. Care was taken to avoid temperature overshoot.

4. The prewetting of the catalyst was done using LGO at high liquid flow (LHSV = 3.5 h^{-1}). For 10 ml catalysts, it is 35 ml/h (~29 g/h). H_2-flow rate should be 100 Nm^3/m^3 (3.5 NL/h). The temperature was kept at 100 ^oC for a period of about one hour.

5. Presulfiding liquid was prepared using white kerosene spiked with dimethyl disulfide (DMDS) to a total sulfur level of 2.5 wt.%. In 1 kg white kerosene, add 36.7 g of DMDS.

6. After prewetting for one hour, the feed is switched from LGO to spiked feed.

7. Flow rate was decreased to LHSV of 2.5 (25 ml/h, ~21 g/h), and the H_2/oil was increased to 200 Nm^3/m^3 (5.0 L/h) and the temperature was increased from 100 ^oC to 320 ^oC. It is important to limit the temperature increase to 15^oC/hour to ensure sufficient presulfiding of the catalyst at low temperature.

8. These conditions (320 ^oC , 2.5h^{-1}, 4.0 MPa, 200 Nm^3/m^3) were maintained for at least 8 hours (normally overnight).

9. The feed is then switched to normal feed. Operating conditions are also changed to normal operating pressure, LHSV and H_2/oil. After stabilization for 3 hours, the temperature is increased/decreased for the first test. In case of increase, the maximum rate of increase was 3 ^oC /hour.

10. To avoid premature coking, the first test condition was carried out at lowest test severity (low temperature and high pressure).

11. For every next adjustment of the test temperature to a higher level, the maximum rate of temperature increase was kept at $3^{o}C$/hour, to avoid premature coking of the catalyst.

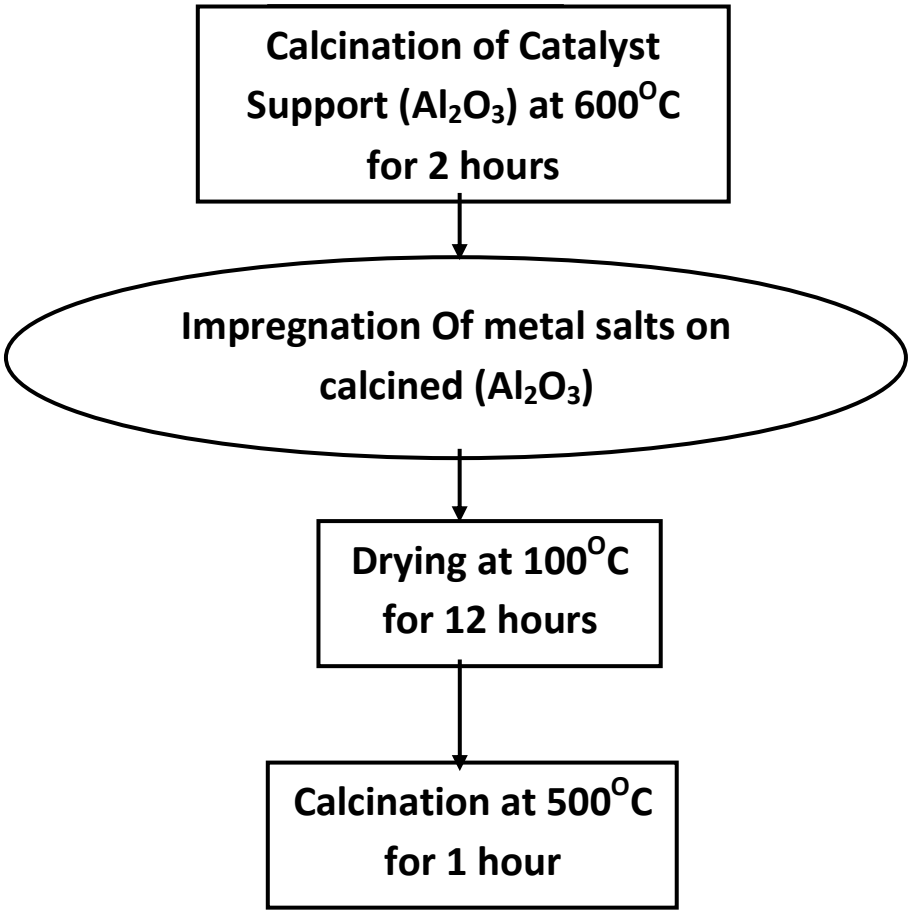

Figure 3.1 Steps in the preparation CoMo/Al_2O_3 Catalysts.

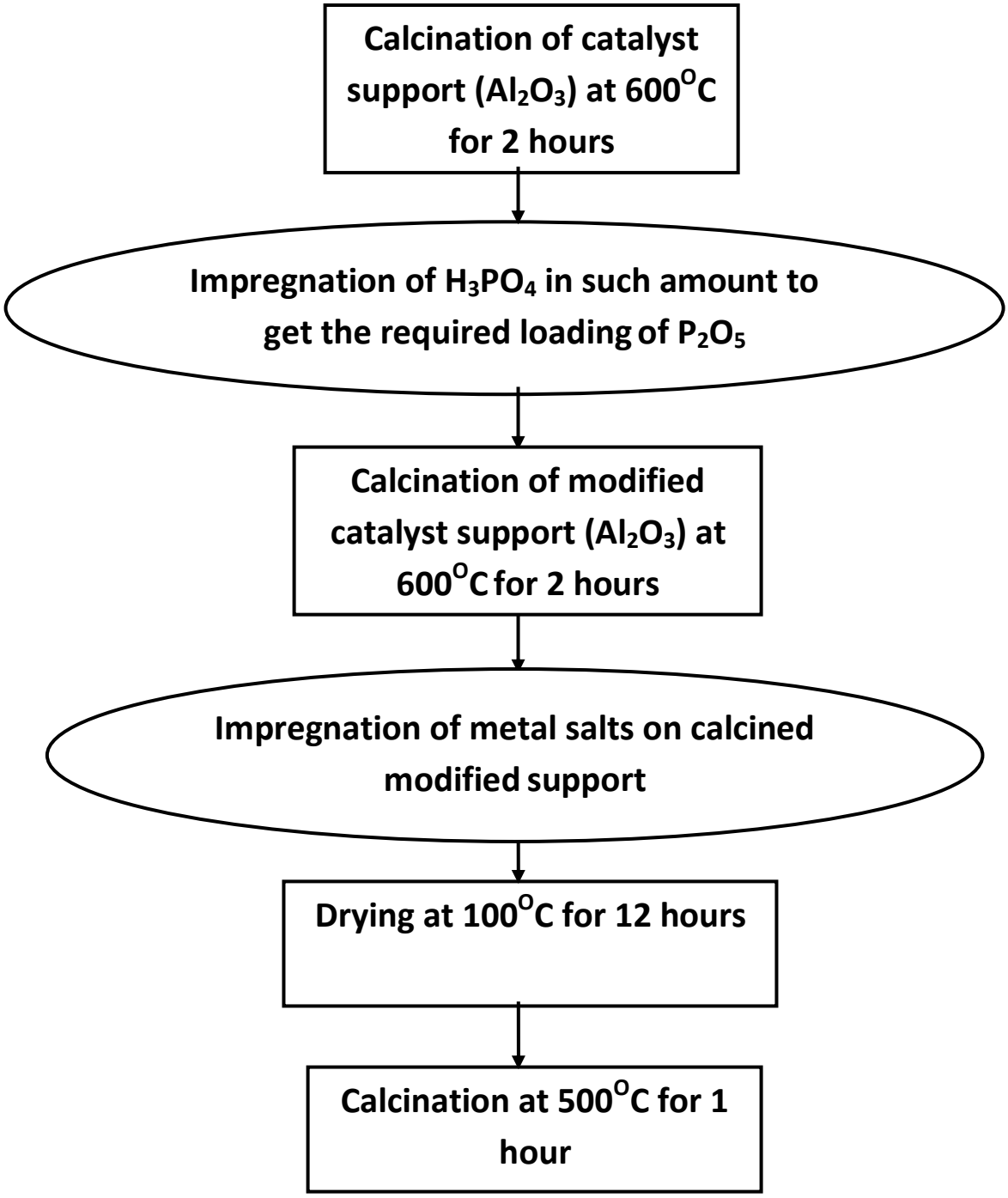

Figure 3.2 Steps in the preparation of phosphorus modified Catalyst ($CoMoP/Al_2O_3$)

3.3 Catalyst Characterization

3.3.1 Surface Area Measurement

Accurate sorption measurements of a gas on solids surface was carried out in NOVA 1200 system supplied by Quanta chrome Corporation. ANOVA is an acronym for NO VOID ANALYSIS which measure multipoint BET surface area, single point BET surface area, total pore volume, average pore radius, sample volume, density.

Operational Procedure for gas sorption analyzer

Procedure for pretreatment and subsequent experiment is as follows.

0.25gm of catalyst sample was weighed and placed in a sample cell assembly which was heated to 90°C in 10 min and temperature is maintained for 1 hour then the temperature is raised to 350 ^{o}C and is maintained for 2hr. Adsorbate source used is Nitrogen, as it serves to be most common adsorbate source and well characterized one. All measurement was fully programmed and fully automated.

Mesopore size calculations are done assuming cylindrical pore geometry using Kelvin equation.

$$r_k = \frac{-2\gamma Vm}{RTln(\frac{P}{Po})}$$

Where γ is the surface tension of nitrogen at its boiling point (8.85 ergs/cm^2 at 77K).

Vm is molar volume of liquid nitrogen (34.65cm^3/mol)

R is gas constant (8.314 x 10^7 ergs/degmol).

T is boiling point of nitrogen.

$P/P_o$is relative pressure of nitrogen

r_k is the Kelvin radius of the pore.

Kelvin radius rk is the radius of pore in which condensation occurs at a relative pressure of P/P_o. Since prior to condensation some adsorption has taken place on the walls of the pore rk is not actual pore radius. Actual pore radius is given by $r_p = r_k + t$, where t is the thickness of the adsorbed layer.

$$t(A^o) = 3.54\left[\frac{5}{2.303\log\left(\frac{p}{po}\right)}\right]^{\frac{1}{3}}$$

Total pore volume is derived from the amount of vapor adsorbed at a relative pressure by assuming that pores are filled with liquid adsorbate. Most common method in determining the total surface area of the catalyst is that developed by Braunner, Emmet and Teller (called BET method).

BET equation is given by

$$\frac{P}{Va(Po-P)} = \frac{1}{VmC} + \frac{c-1}{VmC}\left[\frac{P}{Po}\right]$$

Where

Va is the quantity of gas adsorbed at a relative pressure P/Po.

Vm is the quantity of adsorbate constituting a monolayer of surface coverage.

C (BET constant) is related to energy of adsorption in the first adsorbed layer and indicates the magnitude of the adsorbate/adsorbent interactions. In this technique, amount of nitrogen adsorbed at equilibrium at its normal boiling point (-195.8^{o}C) is measured over a range of partial pressure below 1 atmosphere. The volume of gas adsorbed is calculated by measuring pressure variation resulting from the adsorption of known volume of N_2 gas by test sample.

3.3.2 X-Ray Diffraction

X-ray diffraction is generally used to obtain information about structure and composition of crystalline material. XRD patterns are of great importance in identifying specific crystal structures of crystal planes within a complex catalyst. X-ray diffraction patterns from typical catalyst powders give information about interplanar lattice spacing through Bragg's equation

$$2d\sin\Theta = n\lambda$$

Where

d is interplanar spacing

Θ is angle between lattice plane and both the incident and diffracted X-ray beam

n is order of Braggs reflection

λ is the wavelength of the X-rays

Combined with fact that intensities of diffraction lines depend on the arrangement of atoms in unit cell of crystal lattice, this information in principle provides an almost unique description of nature of the crystalline phases present. However in practice the

interpretation of diffraction patterns may not always be trivial as catalyst often contains many different phases. The diffraction pattern is generated by a 2-theta/theta scanning diffractometer.

3.4 Batch Reactor Evaluation

Batch autoclave reactor is suitable for high exothermic reaction. The batch reactor has advantages like good control on Temperature so that reaction can be performed with very less temperature fluctuations. By using Batch reactor one can study Catalyst activity, selectivity, and kinetics and Activation energies of the reaction.

Batch Reactor Setup

The Reactor used in this study is A 100 ml Autoclave reactor with external heating system was used in this study. The heating system is controlled by the program which gives Precision in kinetic studies. The pressure of $H_2$was controlled manually. Figure 3.3 shows the Batch reactor used for the study.

Figure 3.3 Batch reactor used for HDS study.

Batch Reactor Feed

Model Compounds were dissolved in 50 gm. of decalin in order to get 500ppm sulfur concentration from each of two model compound. For all studies the catalyst concentration is kept at 1wt.% of the feed.

Experimental Procedure

A 100 ml autoclave was used as a stirred-batch reactor to conduct the catalyst evaluation experiments. The reactor was equipped with an impellor with controllable speed, thermo well, and product sampling system. The reactor was loaded with 50 g decalin and 0.105 g of benzothiophene and 0.144 gm. of dibenzothiophene. Hence, the model compounds contributed 500 ppm each of sulfur content, which resulted in a total sulfur content of 1,000 ppm in feedstock. Half a gram of fresh catalyst was used for each experiment, which amounted to a catalyst-to-feedstock ratio of 1 wt.%. Experiments were carried out for two hours under a hydrogen pressure of 900 psig and at temperatures of 300, 325 and 350 ^{o}C. The product samples were taken during the course of the experimental run through a specially-designed sampling tube after 15, 30, 45, 60, 90 and 120 minutes.

3.5 Product analysis

The sulfur species in reaction products were analyzed quantitatively by gas chromatography equipped with sulfur chemiluminescence detector (GC Agilent 7890A with SCD Sievers 355). GC-MS (Agilent 6890N with Mass Selective Detector 5973) was used for the identification of hydrocarbons such as biphenyls and cyclohexyl benzenes. PIONA analyzer (Shimadzu GC 2010 with Flame-ionization detector) was used for quantification of hydrocarbons present in the product samples.

Chapter 4. RESULTS AND DISCUSSIONS

In this chapter, experimental results are presented. This work is mainly based on the study of reactivities of different model compounds including Benzothiophene, Dibenzothiophene and hindered dibenzothiophenes such as 4-MDMDBT and 4,6-DMDBT. A detailed kinetic study of these compounds was done in batch autoclave reactor.

The model compounds were desulfurized over two series of Catalysts with different feeds which are as following.

1) $CoMo/Al_2O_3$ with different Co/Co+Mo ratio was used for the simultaneous desulfurization of benzothiophene and dibenzothiophene.
2) $CoMoP/Al_2O_3$ catalysts with different Phosphorus content were used to simultaneously desulfurized DBT and 4-MDBT at three different temperatures 300,325 and 350°C.
3) DBT and 4,6-DMDBT was desulfurized simultaneously over $CoMoP/Al_2O_3$.

Experimental results are presented in the following order.

Batch reactor evaluation

1) Simultaneous HDS of BT and DBT over $CoMo/Al_2O_3$ catalyst.
2) Simultaneous HDS of DBT and 4-MDBT over $CoMoP/Al_2O_3$.
3) Simultaneous HDS of DBT and 4,6-DMDBT over $CoMoP/Al_2O_3$.

4.1 Catalyst Characterization

4.1.1 Pore size distribution

Pore size distribution of unmodified CoMoP (0)/Al_2O_3 shows that the range of pores is from 9A^o to 81A^o. Figure 4.1.1 shows the pore size distribution of modified and unmodified CoMo/Al_2O_3. The radius of the pores was found to increase as the P_2O_5 content of the catalyst was increased as shown in the Figure. The phosphorus modified catalyst show higher range of pore size as compared to unmodified catalyst. The reason for this might be due to the dissolution of Al_2O_3 by the addition of phosphorus which leads to the elimination of small pores and results in microspores.

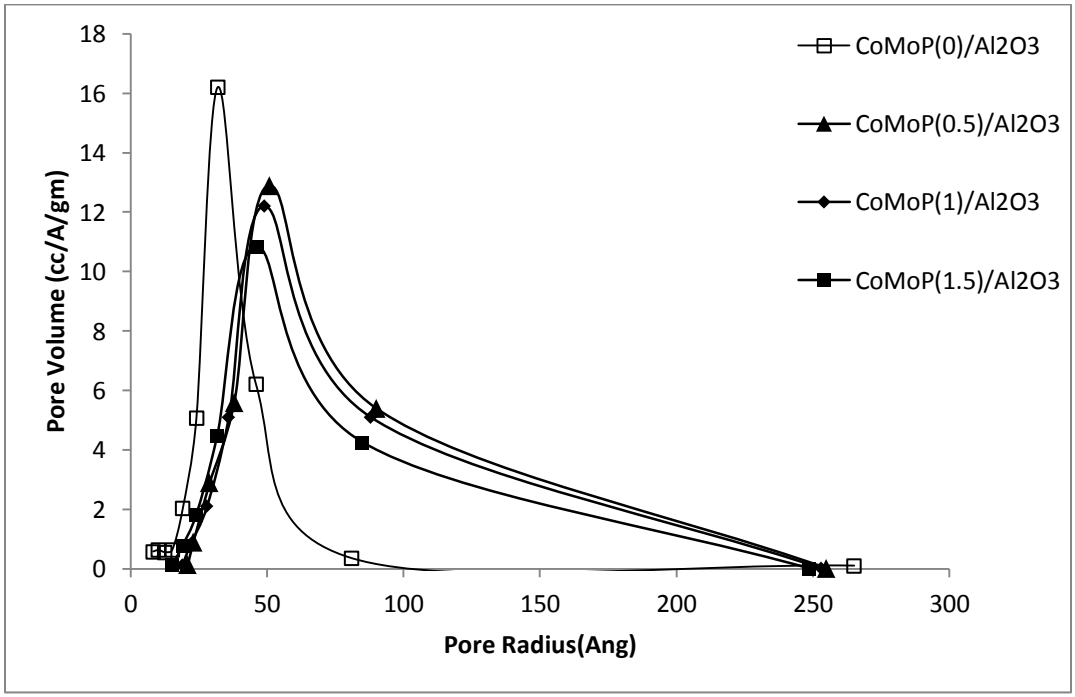

Figure 4.1.1 Pore size distribution for CoMo/Al_2O_3 and phosphorus modified CoMo/Al_2O_3

4.1.2 X-Ray Diffraction.

Figure 4.1.2 shows the XRD patterns of gamma-Al_2O_3 and CoMoP/Al_2O_3 catalysts. The diffraction peak at 2Θ = 26.2 was due to $CoMo_4$ phase. By increase in the phosphorus content the amount of the C,oMoO_4 increases and the peaks at 2Θ = 24 and 2Θ = 27 were attributed due to MoO_3 [48,49]. Both of the later peaks were absent in CoMoP(0)/Al_2O_3 and only found for phosphorus modified catalysts. This shows that the phosphorus incorporation influence the amount of active phases.

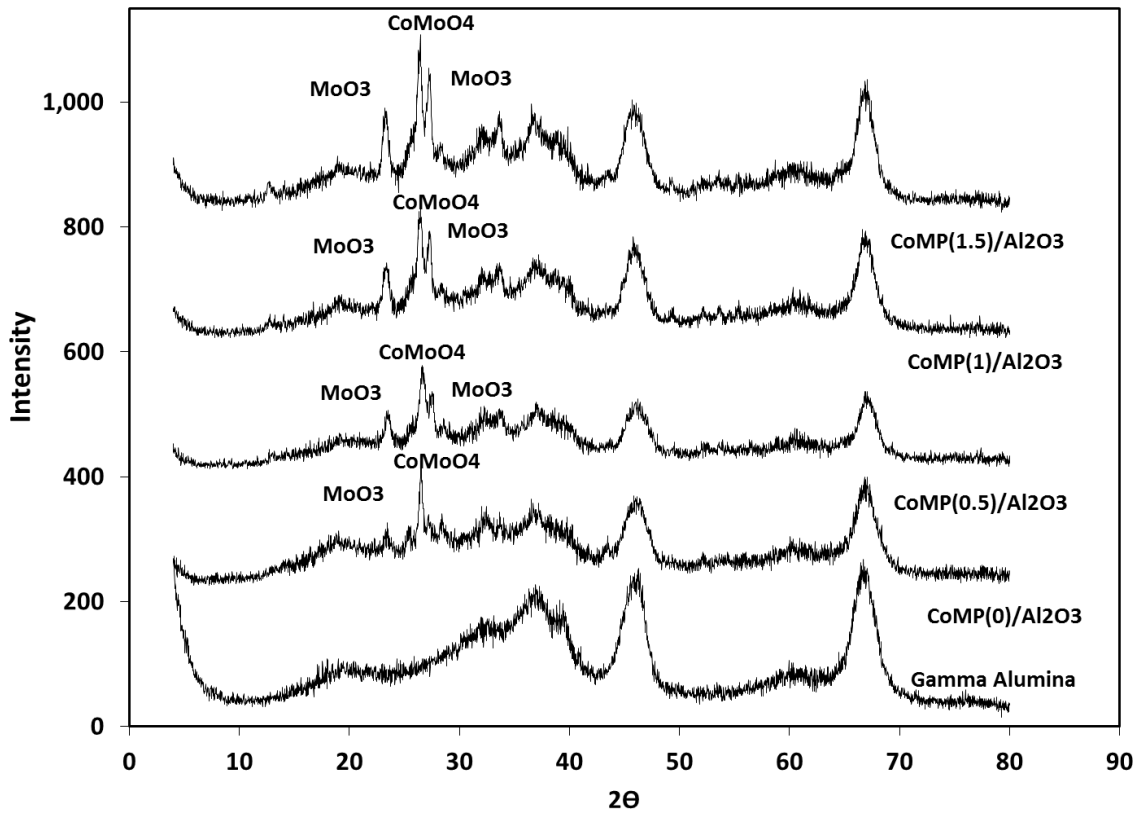

Figure 4.1.2 X-ray Diffraction patterns for CoMo/Al_2O_3 and phosphorus modified CoMo/Al_2O_3

4.2 Batch Reactor Evaluation

4.2.1 Preliminary Runs

Before performing experiments with the prepared modified and unmodified $CoMo/Al_2O_3$ catalysts. Some preliminary experiments were performed over commercial $CoMo/Al_2O_3$ and $NiMo/Al_2O_3$ to test our reaction system. The hydrodesulfurization of benzothiophene (BT) and Dibenzothiophene (DBT) were carried out together in a simultaneous HDS reaction over $CoMo/Al_2O_3$. The conversion of BT was higher as compared to DBT at a given temperature. Figure 4.2.1 and Figure 4.2.2 shows the conversion of BT and DBT over three different temperatures 300,325 and 350°C over commercial $CoMo/Al_2O_3$ and $NiMo/Al_2O_3$ respectively. Benzothiophene was very reactive and desulfurized 100% at all temperatures and over the both catalysts. Whereas HDS of DBT was difficult compared to BT the maximum conversion of DBT at 350°C over $CoMo/Al_2O_3$ and $NiMo/Al_2O_3$ were 77 % and 65% respectively.

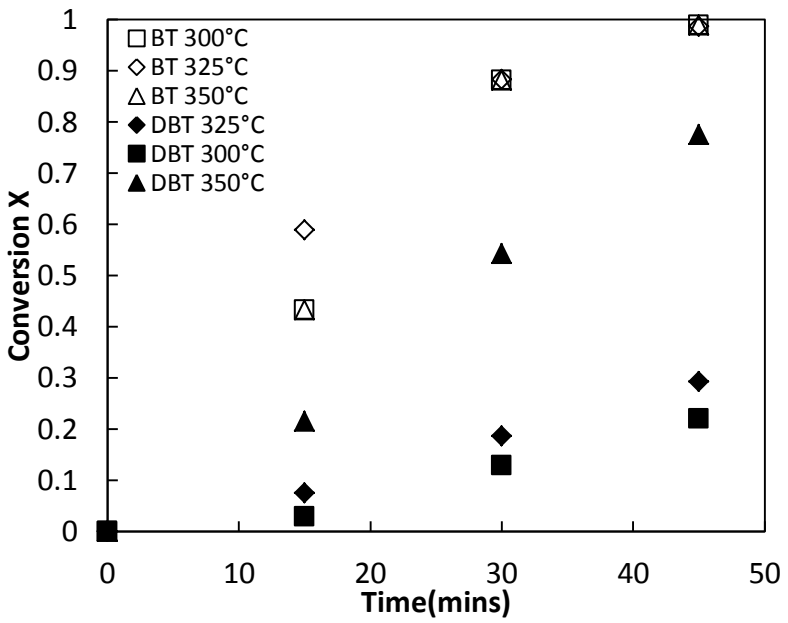

Figure 4.2.1 Conversion of BT and DBT in Competitive reaction over CoMo/Al_2O_3.

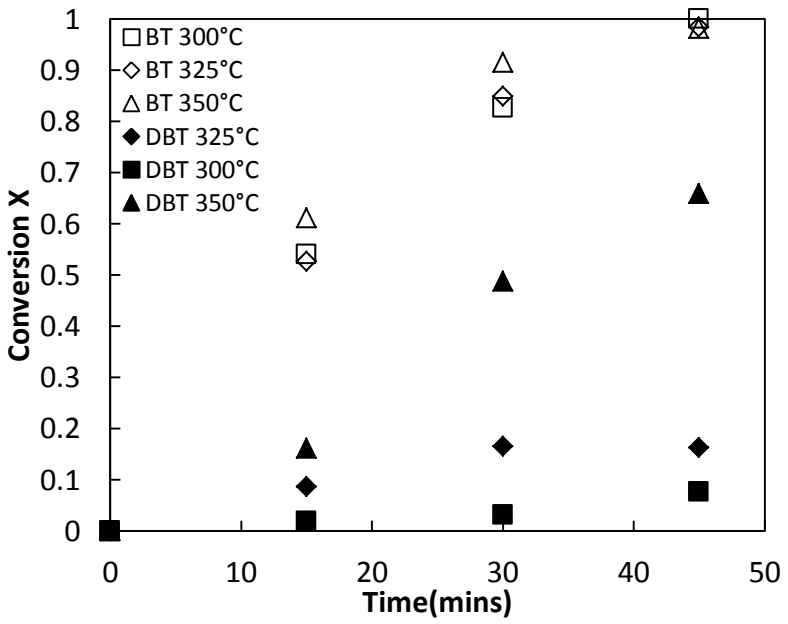

Figure 4.2.2 Conversion of BT and DBT in Competitive reaction over NiMo/Al_2O_3.

Table 4.2.1 shows the total sulfur content remaining in the reaction mixture due to BT and DBT.

Table 4.2.1 Total sulfur (ppm) remaining in the reaction mixture

Catalyst	Temp. (C)	Total Sulfur in feed	Product Sulfur(ppm) after x mins					
			15	30	45	60	90	120
NiMo	300	1000	696	529	411	379	353	317
	325	1000	720	510	440	370	305	245
	350	1000	613	299	180	155	71	35
CoMo	300	1000	718	541	441	398	380	300
	325	1000	668	465	361	300	255	163
	350	1000	676	288	117	60	39	10

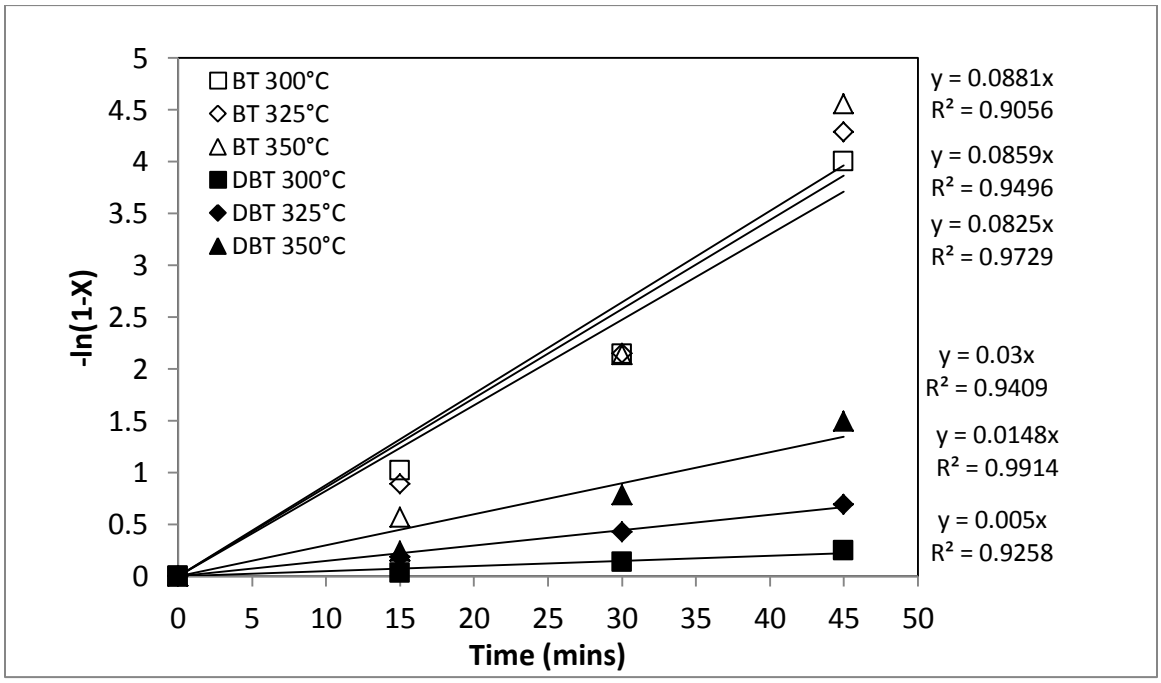

Figure 4.2.3 Rate constant of benzothiophene and dibenzothiophene at different temperatures over CoMo/Al_2O_3 catalyst.

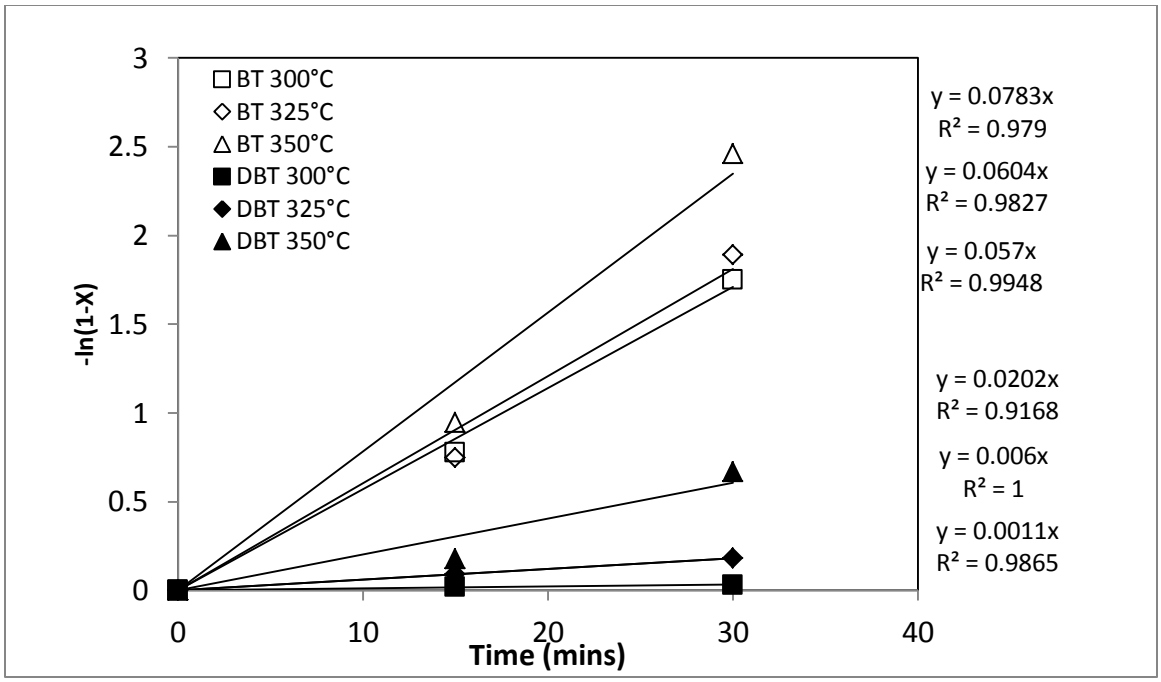

Figure 4.2.4 Rate constant of benzothiophene and dibenzothiophene at different temperatures over NiMo/Al_2O_3 catalyst.

Table 4.2.2 Reaction rate constant kx1000 over Commercial CoMo/Al_2O_3 and NiMo/Al_2O_3.

Catalyst Type	Temp. (C)	k x1000(1/min) BT	DBT
NiMo/Al_2O_3	300	58	1
	325	60	6
	350	78	20
CoMo/Al_2O_3	300	70	5
	325	85	6
	350	88	29

4.2.2 Blank Runs

The experiments were performed without the catalyst in order to see any thermal cracking for the benzothiophene and Dibenzothiophene. The results showed that there was no conversion for benzothiophene and dibenzothiophene.

4.2.3 Reproducibility Runs.

In order to check the accuracy and reproducibility of the results experiments were performed at same temperature and pressure more than 1 time. The reproducibility runs were performed over $CoMo/Al_2O_3$. The reproducibility was found out to be 3%.

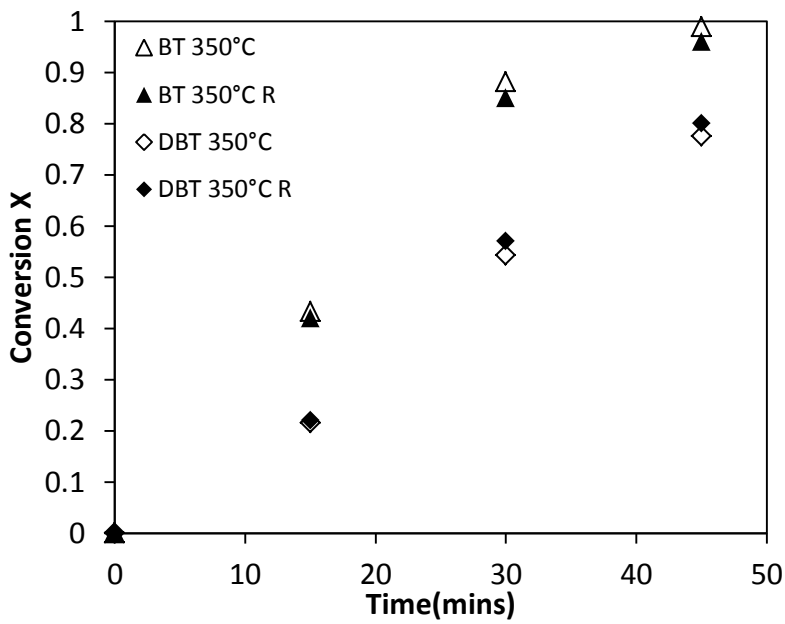

Figure 4.2.5 Reproducibiltiy Conversion of BT and DBT in Competitive reaction over $CoMo/Al_2O_3$.

4.3 Simultaneous HDS of Benzothiophene and Dibenzothiophene over $CoMo/Al_2O_3$

Benzothiophene and DBT were desulfurized over a series of $CoMo/Al_2O_3$ catalysts Table 4.3.1 shows the composition of the catalysts. The concentration of BT and DBT were 2100 and 2800 ppm respectively and this equals to 1000ppm of sulfur.

Table 4.3.1 Composition of Catalysts with different Co/ (Co+Mo) ratio.

Catalyst	MoO_3(wt.%)	CoO(wt.%)	Al_2O_3(wt.%)	Co/(Co+Mo)	Co/Mo
$0.3CoMo/Al_2O_3$	15.4	3.6	81	0.310	0.276
$0.4CoMo/Al_2O_3$	14	5	81	0.407	0.421
$0.5CoMo/Al_2O_3$	12.4	6.6	81	0.505	0.628

The hydrodesulfurization of benzothiophene and Dibenzothiophene were carried out together in a simultaneous HDS reaction over a series of $CoMo/Al_2O_3$ catalysts with the varying ratio of Co/Co+Mo. The conversion of BT was higher as compared to DBT at a given temperature and all benzothiophene desulfurized to 100% in 45 minutes. For DBT the maximum conversion at 350°C for three different catalysts at 0.3, 0.4 and 0.5 Co/Co+Mo ration were 64%, 84% and 66% respectively. Figure 4.4.1 to Figure 4.4.3 shows that HDS of simultaneous HDS of BT and DBT over three different temperatures 300,325 and 350°C.

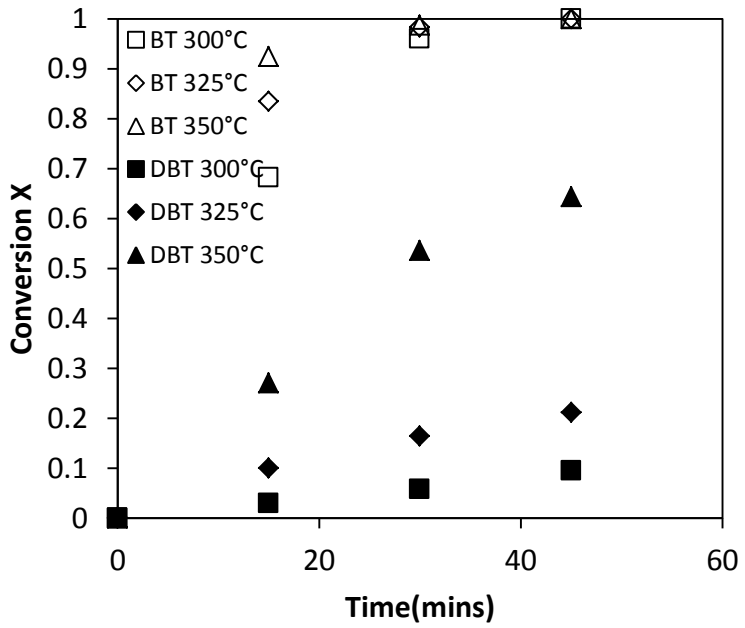

Figure 4.3.1 Conversion of BT and DBT in Competitive reaction over 0.3CoMo/Al_2O_3.

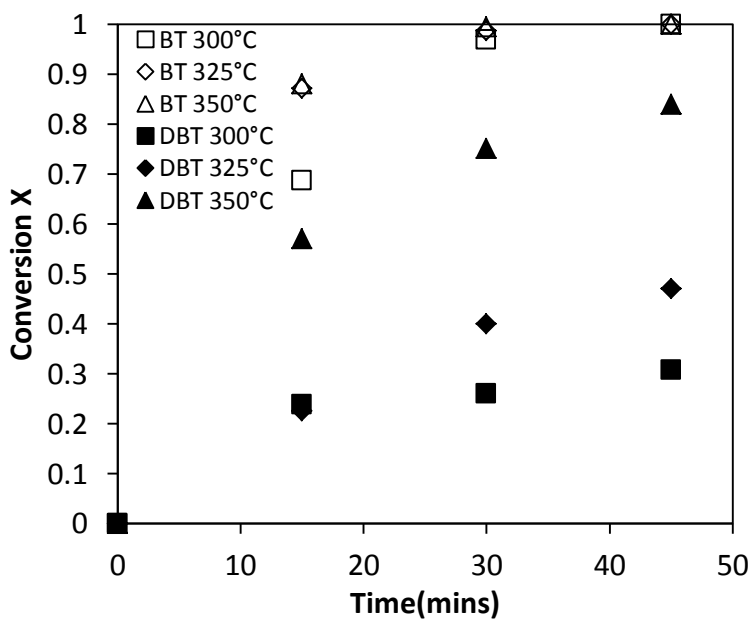

Figure 4.3.2 Conversion of BT and DBT in Competitive reaction over 0.4CoMo/Al_2O_3.

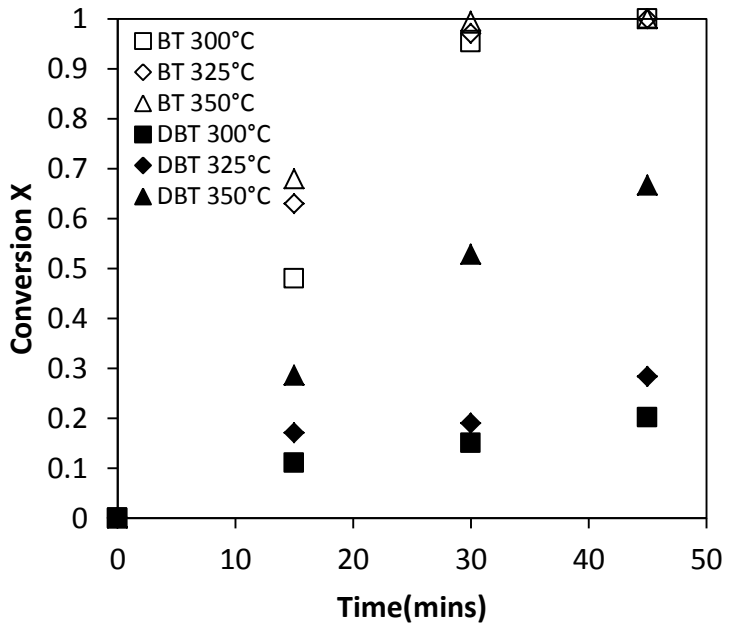

Figure 4.3.3 Conversion of BT and DBT in Competitive reaction over 0.5CoMo/Al_2O_3.

Table 4.3.2 Total Sulfur Conversion over different CoMo/Al_2O_3.

Catalyst	Temp. (^oC)	Total Sulfur in feed (ppm)	Product Sulfur(ppm) after x mins					
			15	30	45	60	90	120
(0.3CoMo)	300	1000	657	495	453	440	415	408
	325	1000	609	343	251	200	158	81
	350	1000	402	238	179	116	84	28
(0.4CoMo)	300	1000	538	398	347	331	296	262
	325	1000	452	307	265	234	161	103
	350	1000	275	128	80	49	32	7
(0.5CoMo)	300	1000	836	825	798	727	693	626
	325	1000	820	755	716	572	494	358
	350	1000	714	471	333	254	153	50

4.3.1 Reaction Rate constants for simultaneous HDS of BT and DBT

In order to compare the reactivities of sulfur compound, hydrodesulfurization behavior of benzothiophene and dibenzothiophene was analyzed according to the pseudo-first-order kinetic equation .The integral rate equation is shown below.

$-\ln(1-X) = kt$ Where X is the conversion of benzothiophene and dibenzothiophene and k is the rate constant (min^{-1}) .The Pseudo first order plots are given below

The rate constants obtained at different temperatures showed that benzothiophene conversion was much faster over all catalyst as compared to DBT. For Instance at 350 ^{o}C over 0.4CoMo/Al_2O_3 the ratio of k_{BT}/k_{DBT} was 3.45 whereas at 300°C over the same catalyst the ratio was 10.8. This suggest that DBT hydrodesulfurization, that predominantly takes place by DDS reaction was low at lower temperature and at higher temperature conversion increases so by this it can be infer that DDS reaction is favored by high temperatures which is similar to the results of Mochida et.al [50]**.**

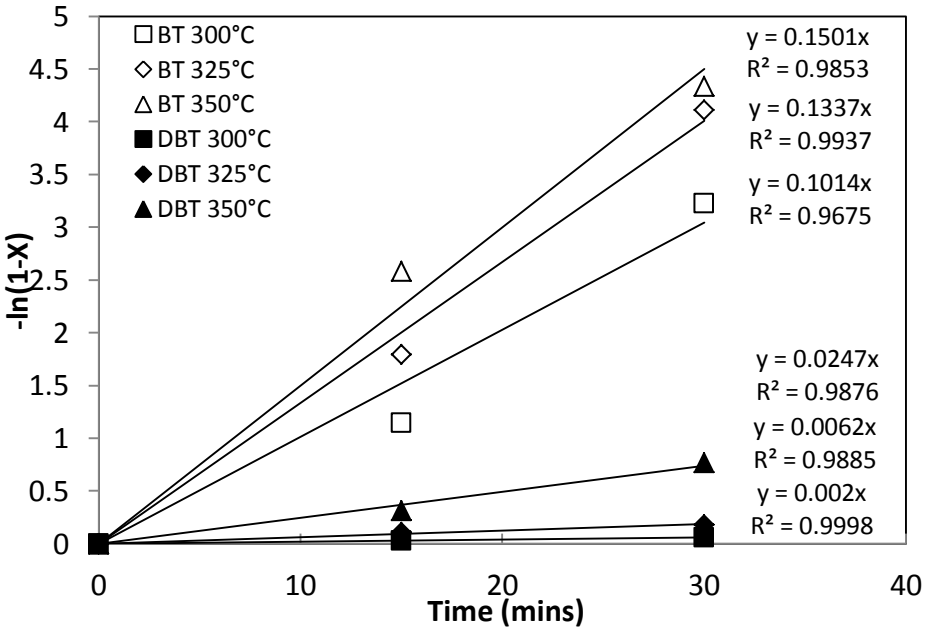

Figure 4.3.4 Rate constant of benzothiophene and dibenzothiophene at different temperatures over 0.3CoMo/Al_2O_3 catalyst.

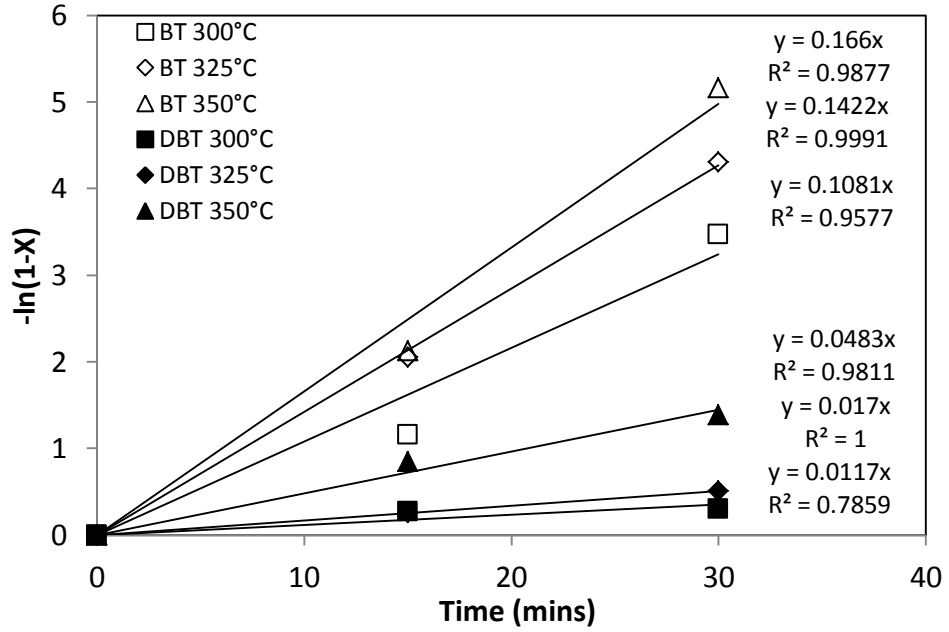

Figure 4.3.5 Rate constant of benzothiophene and dibenzothiophene at different temperatures over 0.4CoMo/Al_2O_3 catalyst.

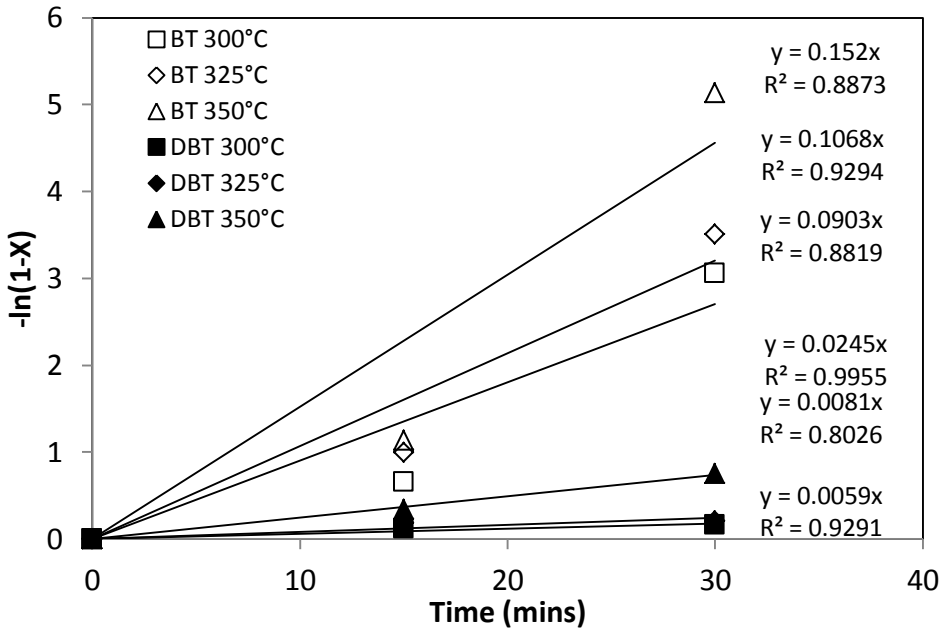

Figure 4.3.6 Rate constant of benzothiophene and dibenzothiophene at different temperatures over 0.5CoMo/Al_2O_3 catalysts.

Table 4.3.3 Reaction rate constants of benzothiophene and dibenzothiophene over CoMo/Al_2O_3 Catalysts.

Catalyst Type	Temp. (^oC)	k (1/min) BT	k (1/min) DBT	k_{BT}/k_{DBT}
(0.3CoMo) /Al_2O_3	300	0.101	0.001	100
	325	0.139	0.005	27.8
	350	0.15	0.024	6.25
(0.4CoMo) /Al_2O_3	300	0.108	0.01	10.8
	325	0.142	0.017	8.35
	350	0.166	0.048	3.45
(0.5CoMo) /Al_2O_3	300	0.090	0.005	18
	325	0.106	0.008	13.25
	350	0.152	0.024	6.33

4.3.2 Selectivity of Biphenyl and CHB

Figure 4.3.7 shows the transformation of DBT over $0.3CoMo/Al_2O_3$ at 350^oC into biphenyl (product of hydrogenolysis) and cyclohexyl benzene (product of hydrogenation). This result agrees with the study of Houlla et.al. [51] which reported that DBT HDS takes place preferentially by least hydrogen consumption (DDS) route and that hydrogenation of biphenyl and cyclohexyl Benzene is comparatively low. The intermediates tetrahydrodibenzothiophene and hexa hydrodibenzothiophene via hydrogenation pathway were observed in trace amounts. DBT conversion was 94% and the selectivity of biphenyl that is, Direct Desulfurization route was 85% and selectivity of cyclohexyl benzene that is hydrogenation route was 15% after 120 minutes.

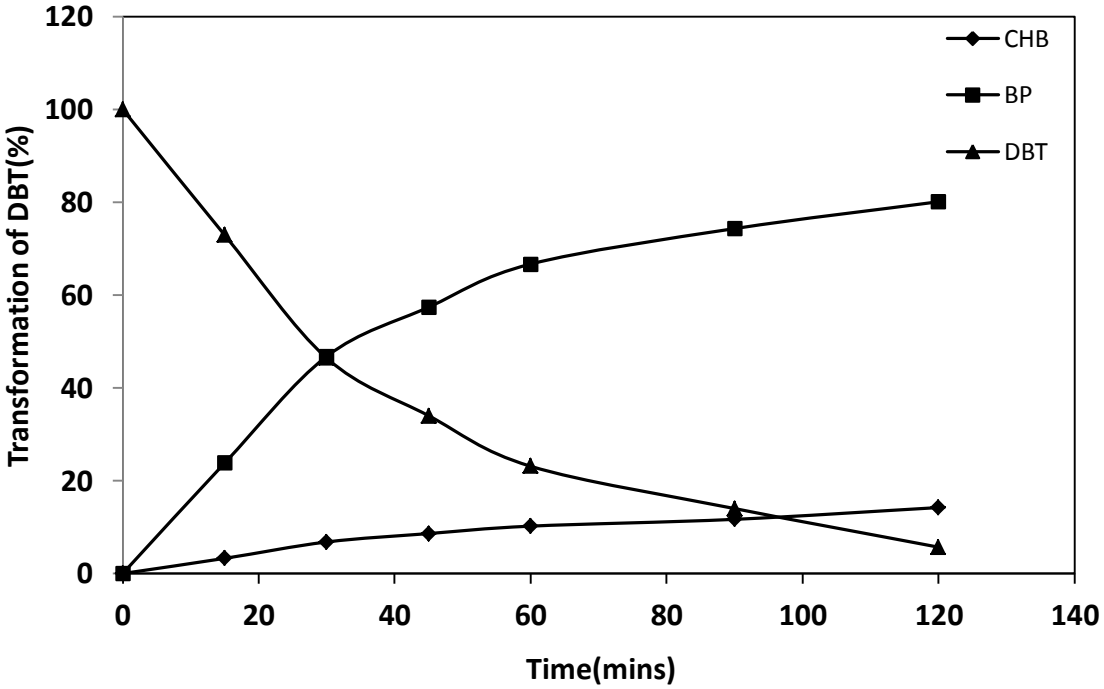

Figure 4.3.7 Transformation of DBT over $0.3CoMo/Al_2O_3$ catalyst.

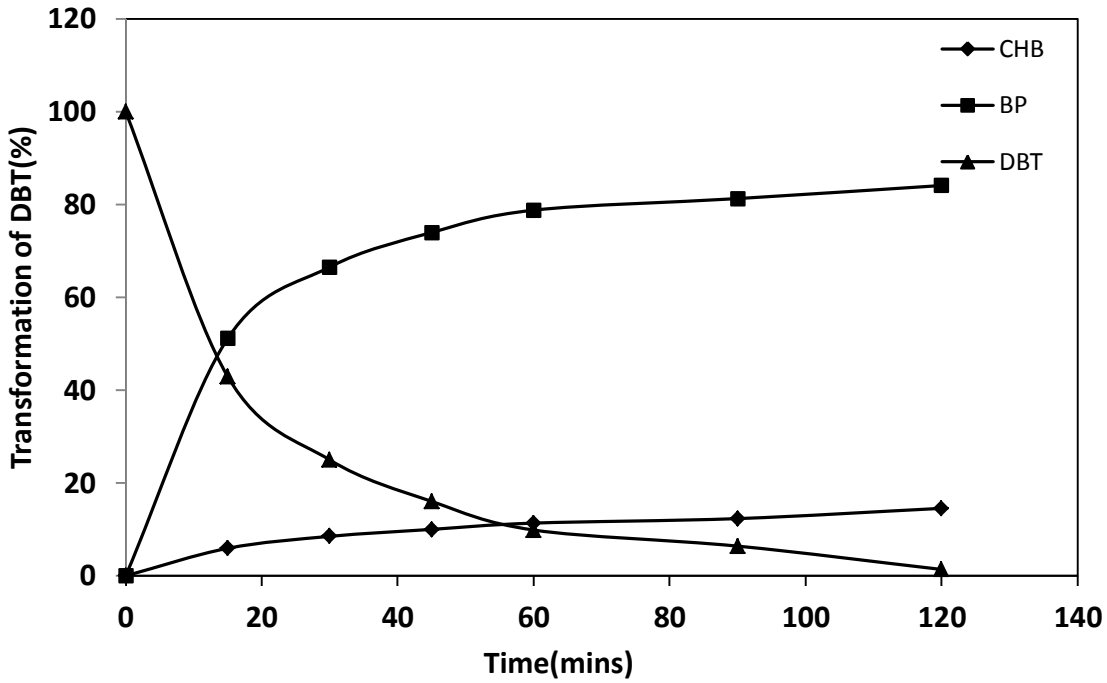

Figure 4.3.8 Transformation of DBT over 0.4CoMo/Al_2O_3 catalyst.

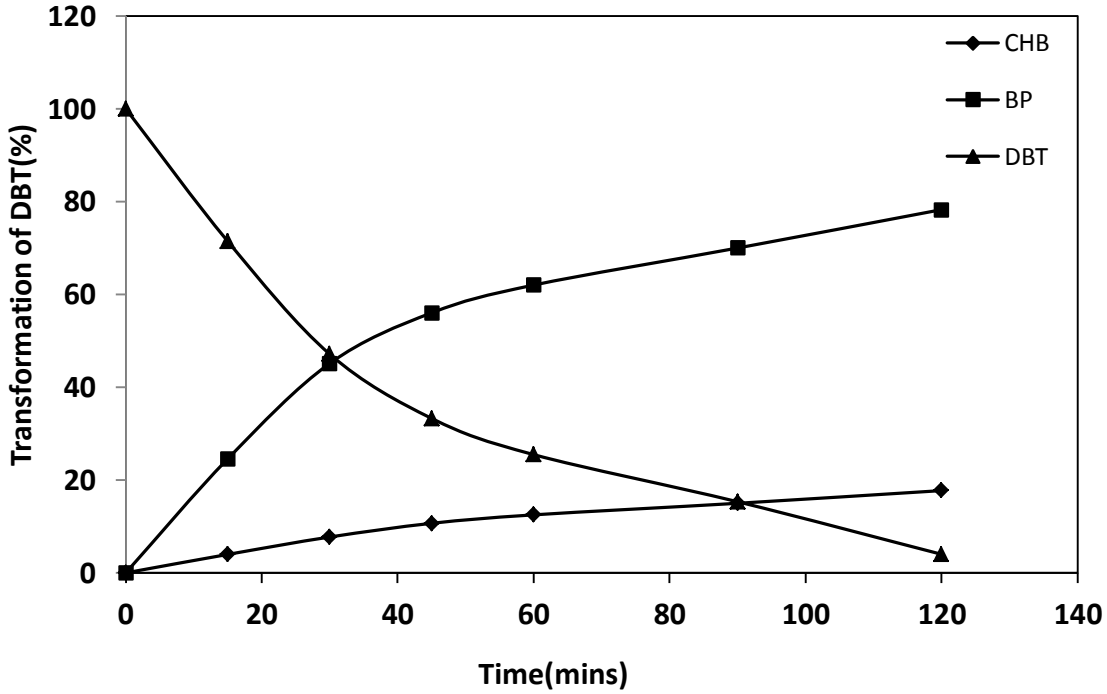

Figure 4.3.9 Transformation of DBT over 0.5CoMo/Al_2O_3 catalyst.

Figure.4.3.8 shows the transformation of DBT over 0.4CoMo/Al_2O_3 at 350^oC a similar trend was observed as in the case of 0.3CoMo/Al_2O_3 catalysts. The conversion of DBT was 98% and the selectivity of biphenyl was 85%.The DBT conversion over 0.5CoMo/Al_2O_3 was 96% as can be observed from Figure.4.3.9. The same hydrodesulfurization products were formed from DBT that is, biphenyl and cyclohexyl benzene. The selectivity of biphenyl that is direct desulfurization was 82% and the yield of biphenyl after 120 minutes was 78%.

Figure 4.3.10 shows the biphenyl to cyclohexyl benzene ratio plotted against the reaction time. 0.4CoMo/Al_2O_3 catalyst showed higher DDS selectivity as compared to other catalysts. The ratio was initially higher at the start of reaction but as the reaction advanced the ratio decreased which suggest that cyclohexyl benzene concentration increased as the reaction advanced.

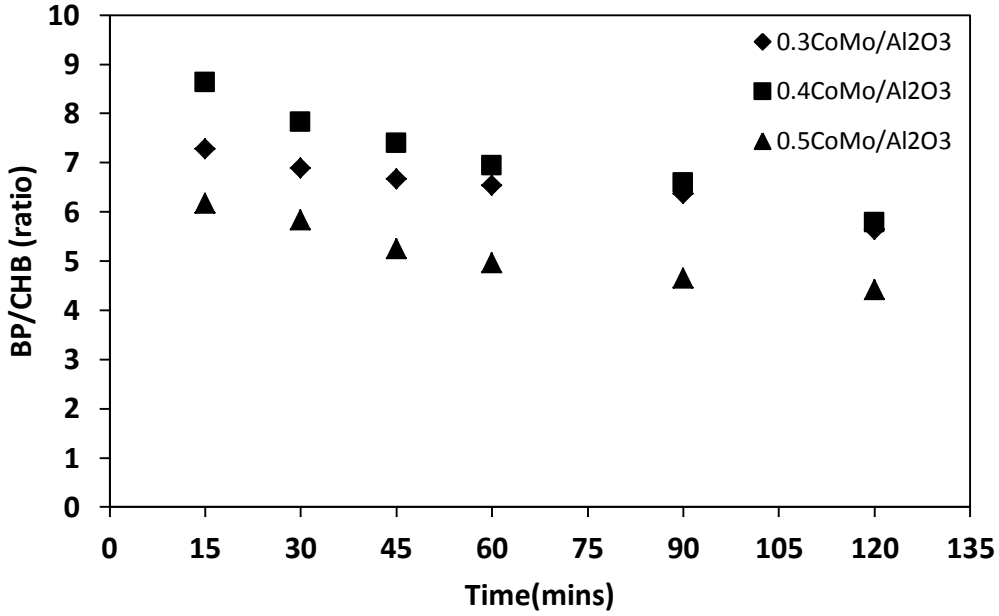

Figure 4.3.10 Biphenyl to Cyclohexyl Benzene ratio over all CoMo/Al$_2$O$_3$ catalysts versus reaction time.

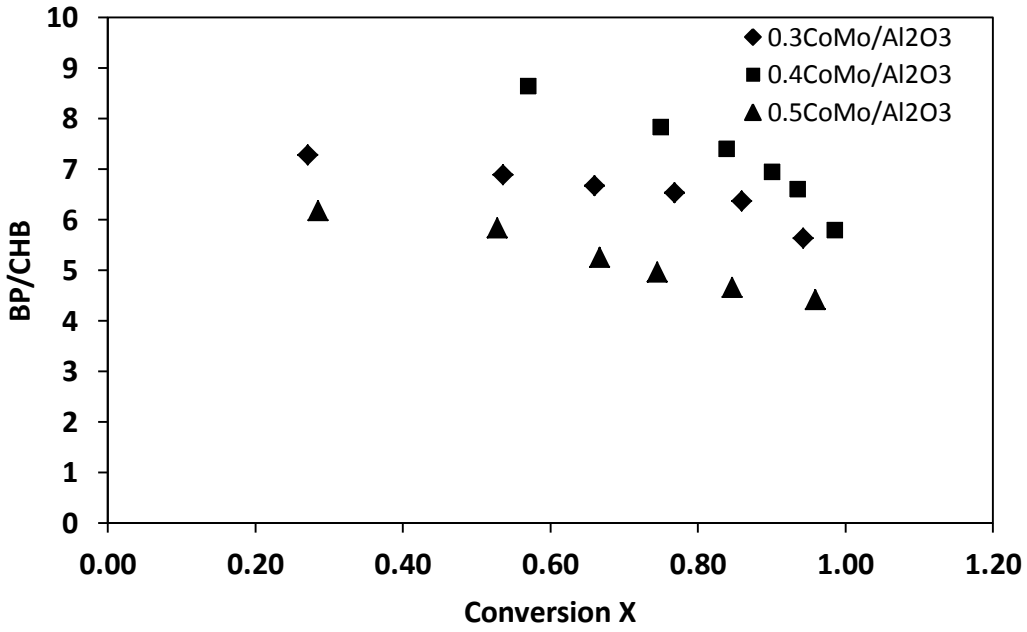

Figure 4.3.11 Biphenyl to Cyclohexyl Benzene ratio over all CoMo/Al$_2$O$_3$ catalysts versus total Conversion.

As DBT desulfurized by two routes which Figure 4.3.12 shows the rate constants calculated from the formation rate of biphenyl and cyclohexyl benzene at 350°C.

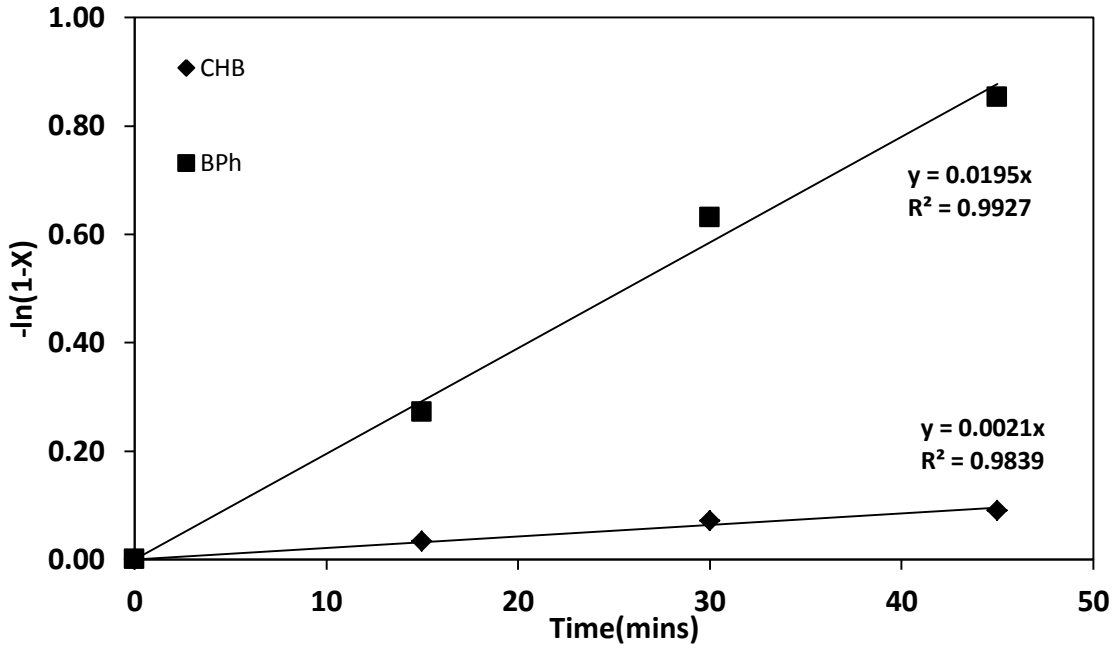

Figure 4.3.12 Formation rates of BP and CHB at 350°C ***over 0.3CoMo/Al$_2$O$_3$ catalyst.***

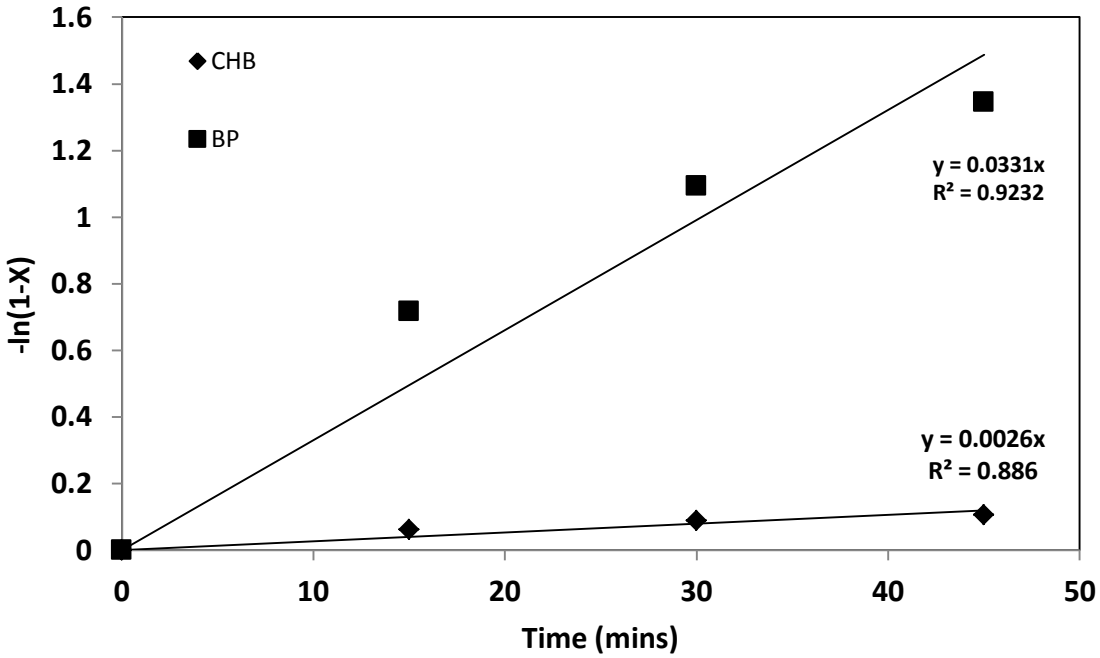

Figure 4.3.13 Formation rates of BP and CHB at 350oC over 0.4CoMo/Al2O3 catalyst.

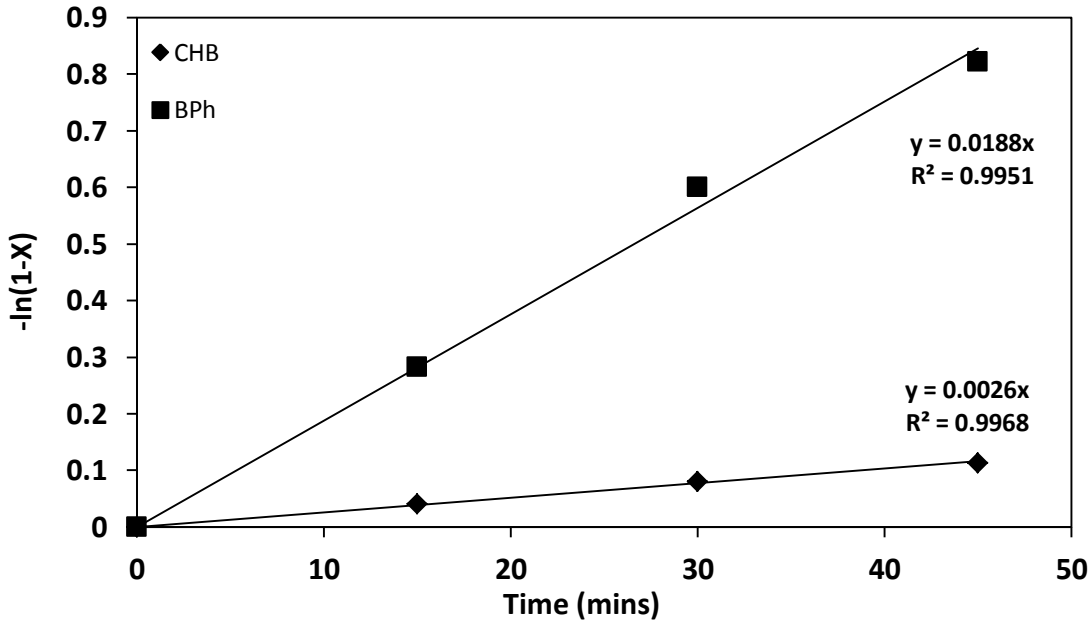

Figure 4.3.14 Formation rates of BP and CHB at 350°C ***over 0.5CoMo/Al$_2$O$_3$ catalyst.***

Table 4.3.4 Rate constants of biphenyl and cyclohexyl benzene obtained from initial transformation of DBT.

Catalysts	Biphenyl (min^{-1})	CHB (min^{-1})	Overall (min^{-1})
0.3CoMo/Al_2O_3	0.019	0.002	0.024
0.4CoMo/Al_2O_3	0.033	0.002	0.048
0.5CoMo/Al_2O_3	0.018	0.002	0.022

By the formation rates of BP and CHB over different CoMo catalysts it was observed that the Co/Co+Mo ratio was found to only affects the DDS pathway because formation rates of CHB was constant 0.002(min^{-1}) over all catalysts but the formation of CHB was not constant and the highest formation rate of BP was 0.033(min^{-1}) over 0.4CoMo/Al_2O_3.

4.3.3 Apparent Activation energy

Activation energies for HDS reaction were calculated from pseudo-first order rate constants at three different temperatures 300,325 and 350°C. Arrhenius plot was plotted between -ln(k) and 1/T (Kelvin).The slope of the line multiplied by gas constant gives the value of Activation energy in KJ/mole. The activation energies of DBT lies in the range of 86-94 KJ/mole these values are in good agreement with literature [52]**.** Activation energies of Benzothiophene were found to be 3 times lower as compared to DBT and were in the range of 24-31 KJ/mole.

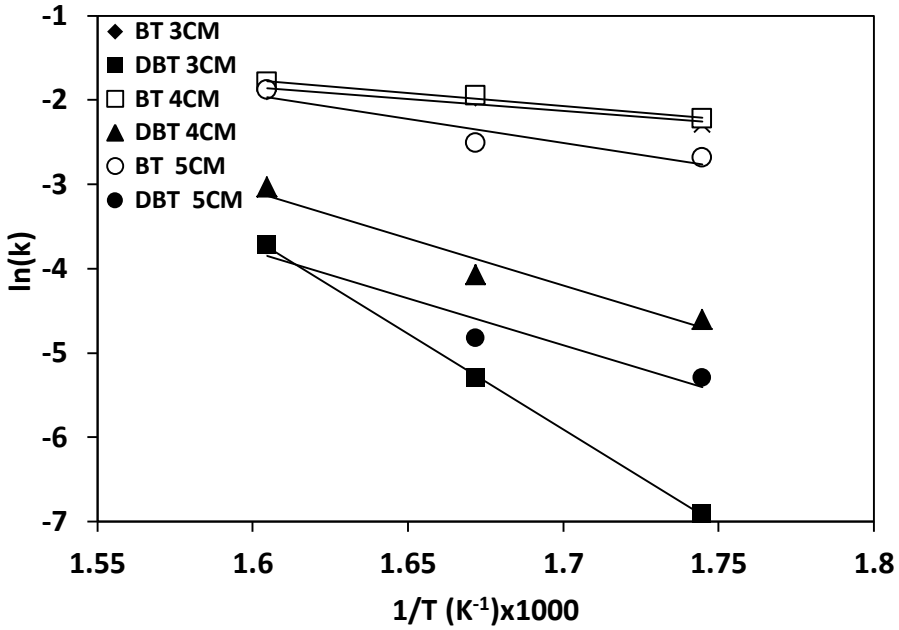

Figure 4.3.15 Arrhenius plot for Benzothiophene and Dibenzothiophene hydrodesulfurization.

Table.4.3.5 Activation energies of Benzothiophene and Dibenzothiophene over $CoMo/Al_2O_3$.

Catalyst	Activation Energy KJ/mole	
	BT	DBT
$0.3CoMo/Al_2O_3$	24	94
$0.4CoMo/Al_2O_3$	25	86
$0.5CoMo/Al_2O_3$	31	94

4.4 Simultaneous HDS of Dibenzothiophene and 4-Methyl Dibenzothiophene over Phosphorus modified CoMoP/Al_2O_3.

Dibenzothiophene (DBT) and 4 methyl dibenzothiophene (4-MDBT) were desulfurized over a series of phosphorus modified CoMoP/Al_2O_3 catalysts Table 4.4.1 shows the compositions of the catalysts. The concentration of DBT and 4-MDBT were 2800 and 3100 ppm respectively and this equals to 500ppm of sulfur contribution from each compound so the total sulfur was 1000ppm.

Table 4.4.1 Composition of Phosphorus modified catalysts.

Catalysts	**MoO(wt %)**	**CoO(wt**	**NiO(wt %)**	**P_2O_5(wt %)**
CoMoP(0)/Al_2O_3	15	4	0	0
CoMoP(0.5)/Al_2O_3	15	4	0	0.5
CoMoP(1)/Al_2O_3	15	4	0	1
CoMoP(1.5)/Al_2O_3	15	4	0	1.5

The hydrodesulfurization of Dibenzothiophene and 4-Methyl Dibenzothiophene were carried out together in a simultaneous HDS reaction over unmodified CoMoP(0)/Al_2O_3. The conversion of DBT was found out to be higher as compared to 4-MDBT at a given temperature. Figure 4.4.1 shows that HDS of DBT and 4-MDBT over three different temperatures 300,325 and 350°C. The maximum conversion of DBT and 4-MDBT after 60 minutes of reaction time was 66% and 39.5% at 350°C respectively.

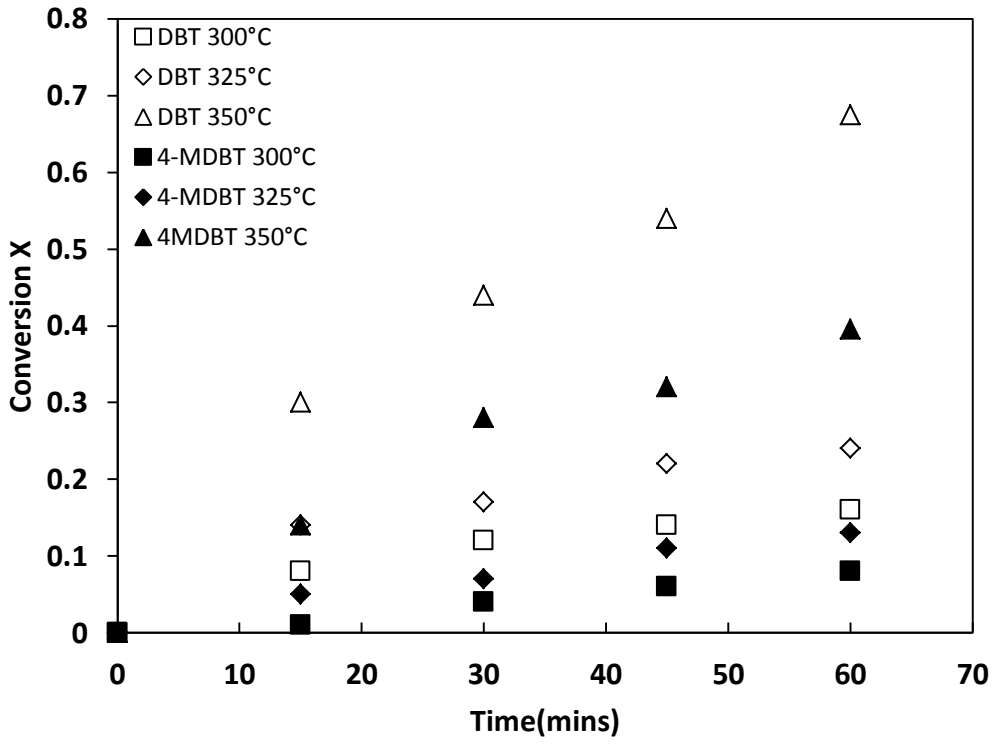

Figure 4.4.1 Conversion of DBT and 4-MDBT in Competitive reaction over CoMoP(0)/Al_2O_3

Table 4.4.2 shows the total sulfur content and the sulfur due to DBT and 4-MDBT. It is clear that DBT desulfurized comparatively faster as compared to 4-MDBT. The highest amount of desulfurization took place at 350°C.

Table 4.4.2 Sulfur (ppm) remaining in the reaction mixture over CoMoP(0) /Al_2O_3 catalyst

	300°C			325°C			350°C		
Time	DBT	4-MDBT	Total Sulfur	DBT	4-MDBT	Total Sulfur	DBT	4-MDBT	Total Sulfur
0	500	500	1000	500	500	1000	500	500	1000
15	460	495	955	430	475	905	350	430	780
30	440	480	920	415	465	880	280	360	640
45	430	470	900	390	445	835	230	340	570
60	420	460	880	380	435	815	163	302	465

Figure 4.4.2 shows the HDS of DBT and 4-MDBT over phosphorus modified CoMoP(0.5)/Al_2O_3 catalyst. Reaction conditions and all other parameters were constant as in the case of unmodified CoMoP(0)/Al_2O_3. The maximum conversion of DBT and 4-MDBT were achieved at 350°C which were 76% and 41% respectively.

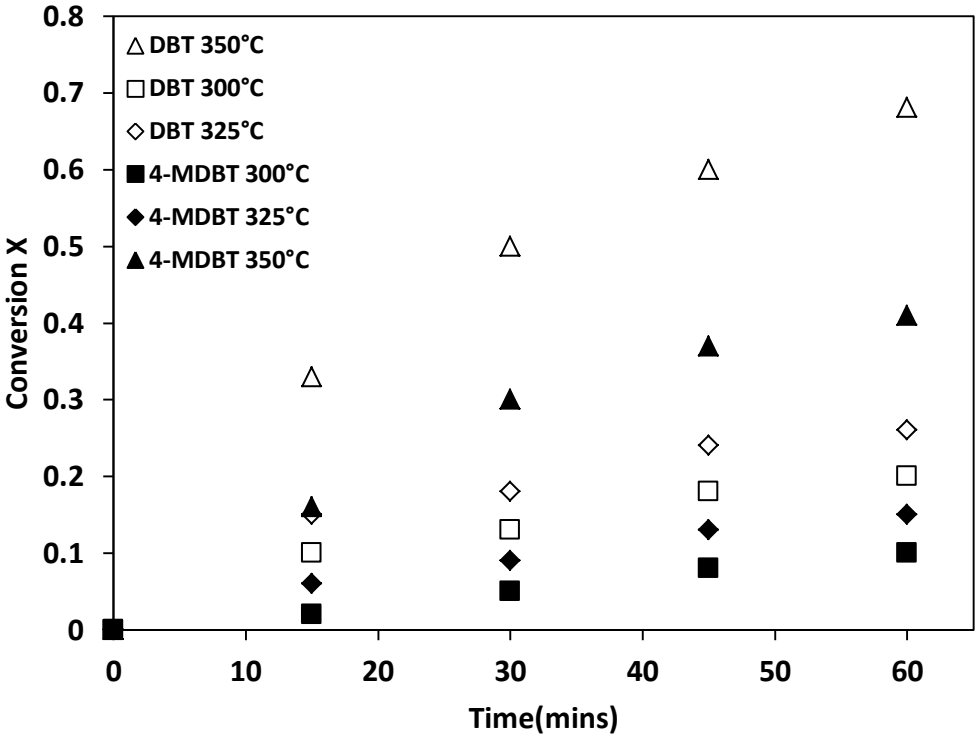

Figure 4.4.2 Conversion of DBT and 4-MDBT in Competitive reaction over CoMoP(0.5)/Al_2O_3

Table 4.4.3 shows the total sulfur content and the sulfur due to DBT and 4-MDBT. The highest amount of desulfurization took place at 350°C.

Table 4.4.3 Sulfur remaining in the reaction mixture over CoMoP(0.5)/Al2O3 catalyst

	300°C			325°C			350°C		
Time	DBT	4-MDBT	Total Sulfur	DBT	4-MDBT	Total Sulfur	DBT	4-MDBT	Total Sulfur
0	500	500	1000	500	500	1000	500	500	1000
15	450	490	940	425	470	895	335	420	755
30	435	475	910	410	455	865	250	350	600
45	410	460	870	380	435	815	200	315	515
60	400	450	850	370	425	795	160	295	455

The HDS of DBT and 4-MDBT over CoMoP(1)/Al_2O_3 was faster as compared to above catalysts discussed. The maximum conversion of DBT and 4-MDBT were achieved at 350°C which were 80% and 47% respectively after 60mins of reaction time. Figure 4.4.3 shows the conversion at different temperatures.

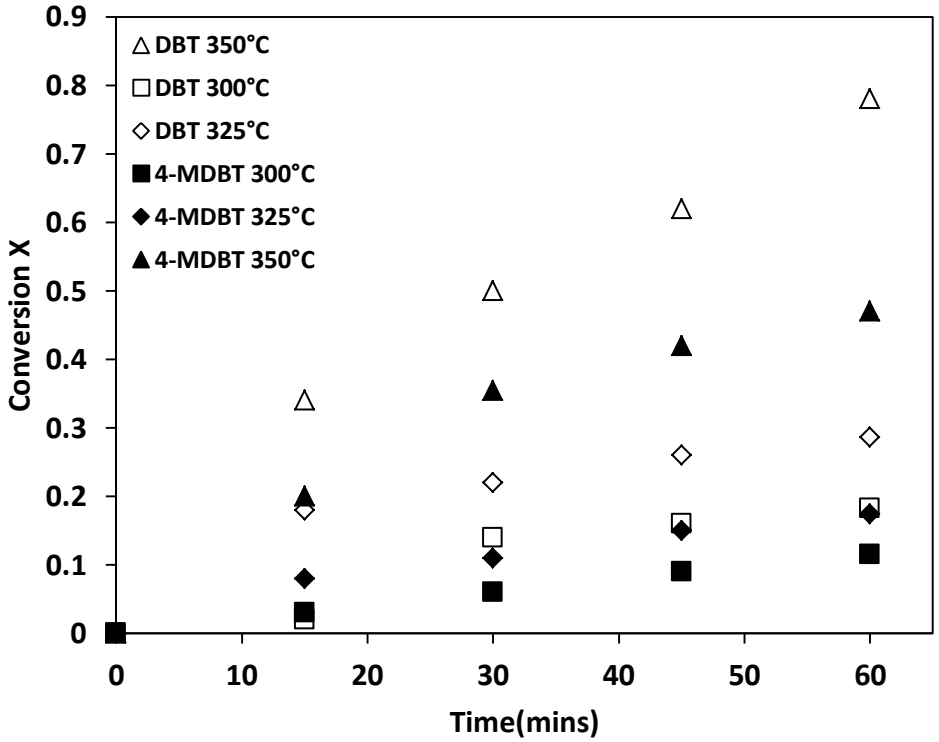

Figure 4.4.3 Conversion of DBT and 4-MDBT in Competitive reaction over CoMoP(1)/Al_2O_3

The sulfur removal over the CoMoP(1)/Al_2O_3 was found out to higher as compared to other catalysts as shown in Table 4.4.4.

Table 4.4.4 Sulfur remaining in the reaction mixture over CoMoP(1)/Al_2O_3 catalyst

	300°C			325°C			350°C		
Time	DBT	4-MDBT	Total Sulfur	DBT	4-MDBT	Total Sulfur	DBT	4-MDBT	Total Sulfur
0	500	500	1000	500	500	1000	500	500	1000
15	490	485	975	410	460	870	330	400	730
30	430	470	900	390	445	835	250	323	573
45	420	455	875	370	425	795	190	290	480
60	409	443	851	357	413	770	110	265	375

The conversion of DBT and 4-MDBT over CoMo(1.5)Al_2O_3 was bit lower as compared to other phosphorus modified catalysts as shown in Figure 4.4.4. However the conversion of both compounds were higher as compared to unmodified CoMoP(0)/Al_2O_3. The maximum conversion for DBT and 4-MDBT at 350°C was 71% and 38% respectively.

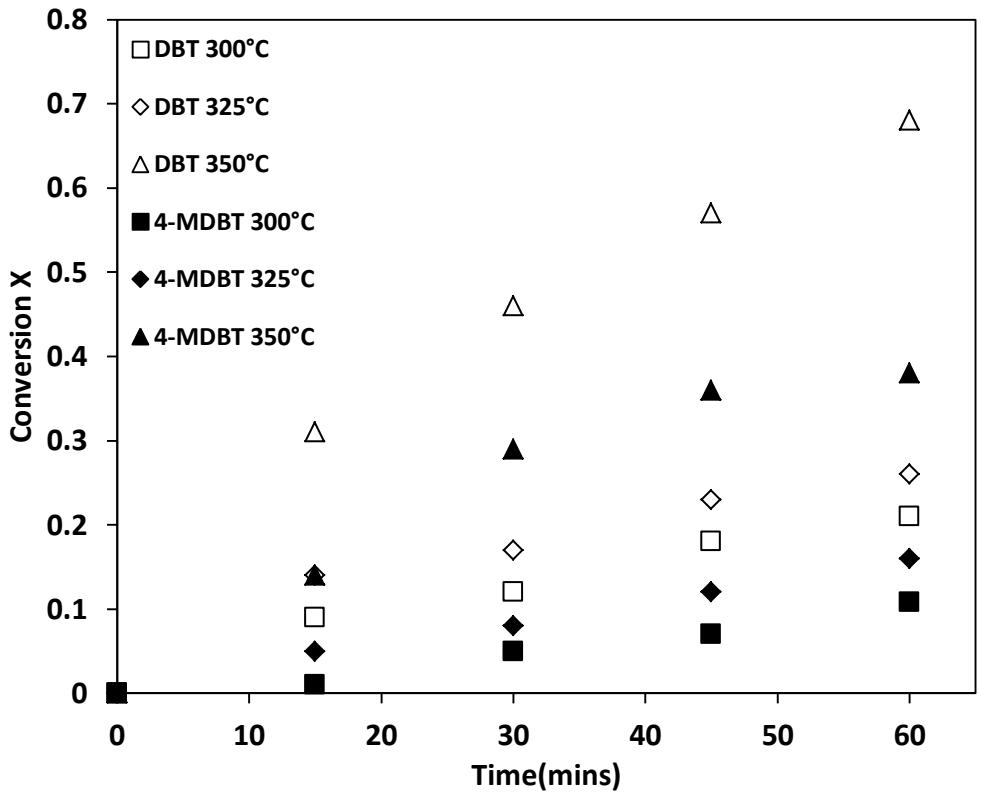

Figure 4.4.4 Conversion of DBT and 4-MDBT in Competitive reaction over CoMoP(1.5)/Al_2O_3.

Table 4.4.5 Sulfur remaining in the reaction mixture over CoMoP(1.5)/Al_2O_3 catalyst.

	300°C			325°C			350°C		
Time	DBT	4-MDBT	Total Sulfur	DBT	4-MDBT	Total Sulfur	DBT	4-MDBT	Total Sulfur
0	500	500	1000	500	500	1000	500	500	1000
15	455	495	950	430	475	905	345	430	775
30	440	475	915	415	460	875	270	355	625
45	410	465	875	385	440	825	215	320	535
60	395	446	841	370	420	790	110	310	470

4.4.1 Reaction Rate constants for Simultaneous HDS of DBT and 4-MDBT over phosphorus modified $CoMo/Al_2O_3$

In order to compare the reactivities of sulfur compound, hydrodesulfurization behavior of dibenzothiophene and 4 methyl dibenzothiophene was analyzed according to the first-order kinetic equation .The integral rate equation is shown below.

$-\ln(1-X) = kt$

Where X is the conversion of benzothiophene and dibenzothiophene and k is the rate constant (min^{-1}). Figure 4.4.5 to Figure 4.4.8 shows the plot of –ln(1-X) versus reaction time. Where X is the conversion of DBT or 4-MDBT. The rate constants for DBT was found out to be higher than 4-MDBT. The rate constant for both compounds was lower at 300°C and becomes higher at 350°C. The rate constant of DBT and 4-MDBT was found out to be lower over unmodified $CoMoP(0)Al_2O_3$ and increase for all phosphorus modified catalyst. The rate constants over all temperature have the trend that they increase over phosphorus modified catalysts up to 1wt.% P_2O_5 and decrease when the phosphorus content of the catalyst was 1.5wt.% P_2O_5. However, at 1.5wt.% P_2O_5 content that is over $CoMoP(1.5)/ Al_2O_3$ catalysts the rate constant was still higher than unmodified $CoMoP(0)/Al_2O_3$. There is an increment of 18%, 18.3% and 7% in the rate constant of DBT for $CoMoP(0.5)/Al_2O_3$, $CoMoP(0.5)Al_2O_3$ and $CoMoP(0.5)/Al_2O_3$ respectively as compared to $CoMoP(0)/Al_2O_3$. The same incremental trend was observed for 4-MDBT as the rate constant was increased to 14%, 38% and 7% in the same order as for the DBT over phosphorus modified catalysts..

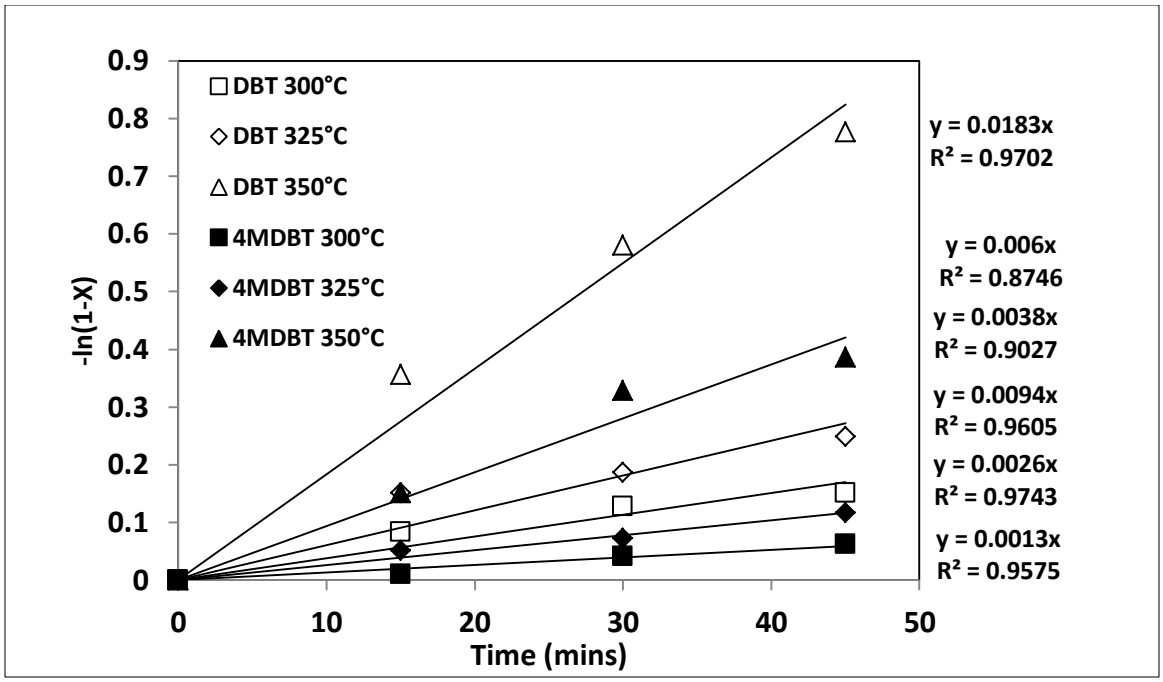

Figure 4.4.5 Rate constant of DBT and 4-MDBT at different temperatures over CoMoP(0)/Al_2O_3.

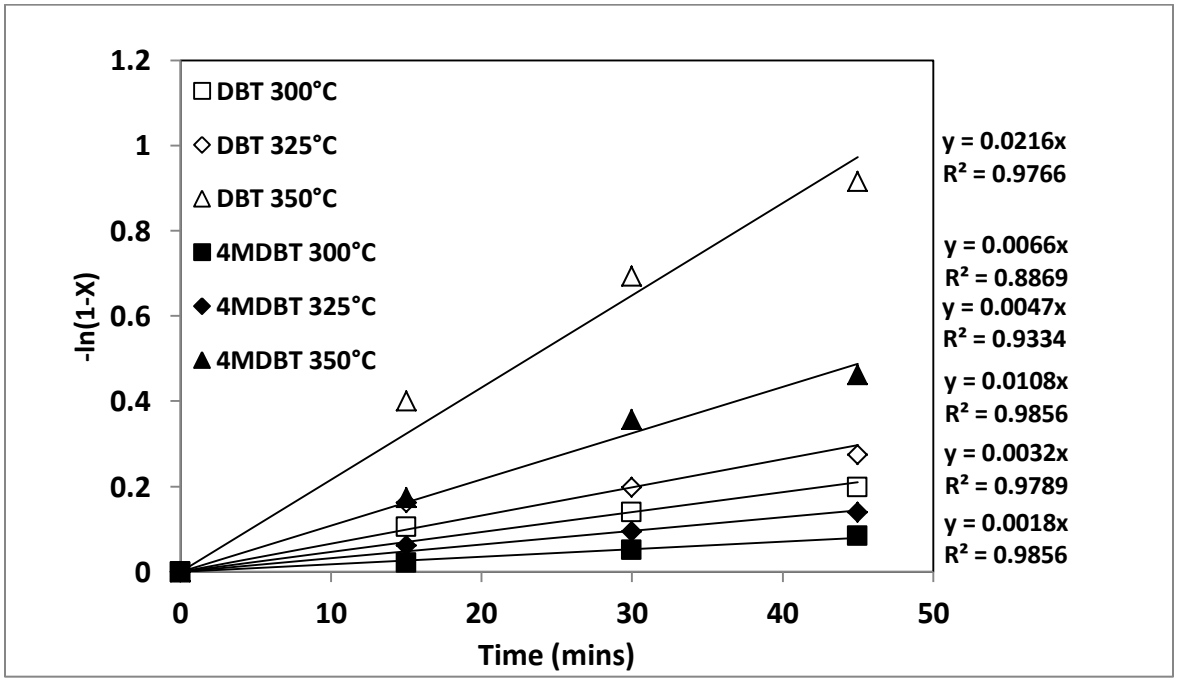

Figure 4.4.6 Rate constant of DBT and 4-MDBT at different temperaturesover CoMoP(0.5)/Al_2O_3.

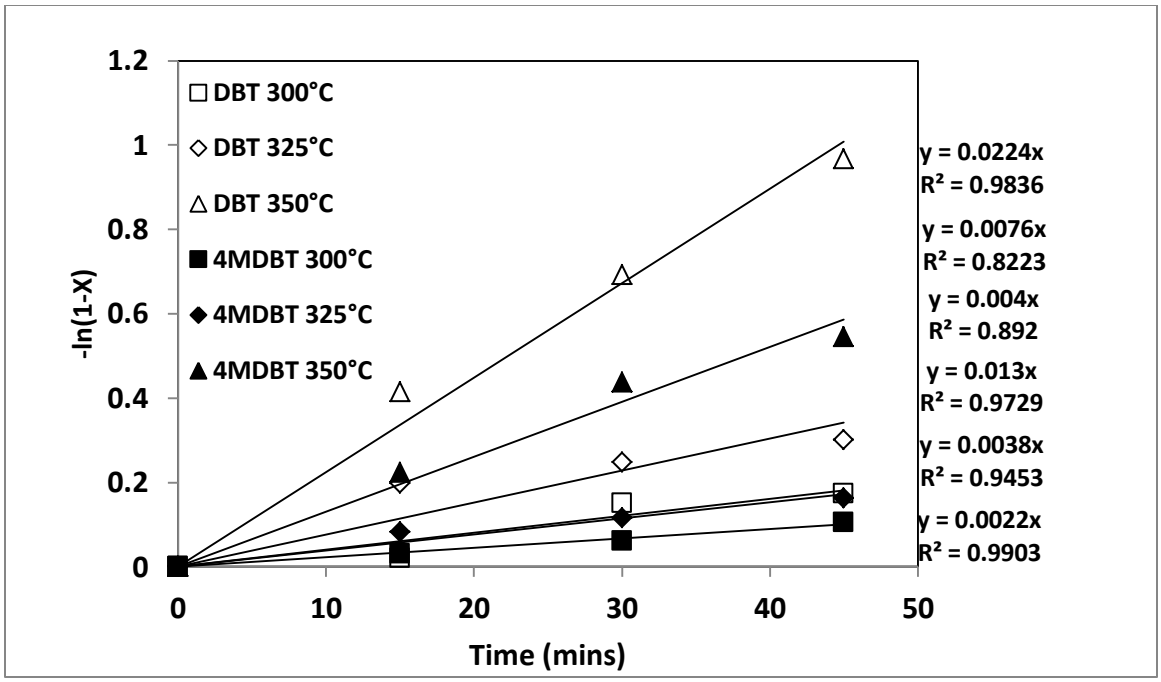

Figure 4.4.7 Rate constant of DBT and 4-MDBT at different temperatures over CoMoP(1)/Al_2O_3.

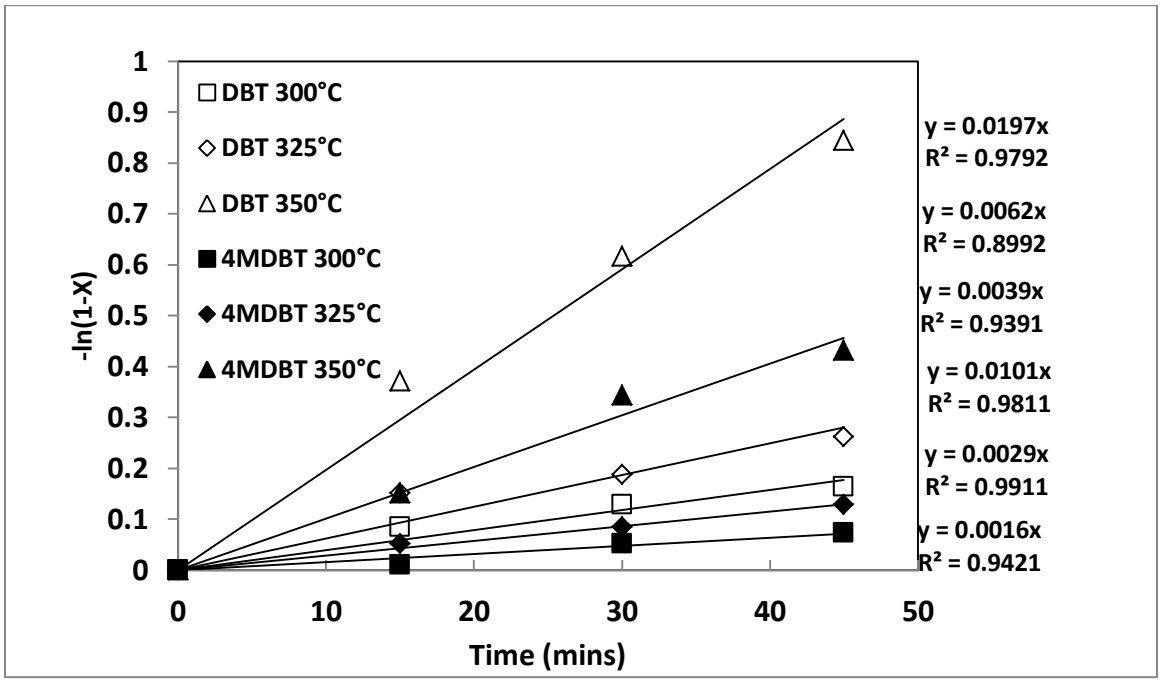

Figure 4.4.8 Rate constant of DBT and 4-MDBT at different temperatures over CoMoP(1.5)/Al_2O_3.

Table 4.4.6 and 4.4.7 gives the rate constant of DBT and 4-MDBT over all the catalyst at different temperatures.

Table 4.4.6 Reaction rate constants kx1000 (min^{-1}) of dibenzothiophene over different catalysts.

Temperature	$CoMoP(0)/Al_2O_3$	$CoMoP(0.5)/Al_2O_3$	$CoMoP(1)/Al_2O_3$	$CoMoP(1.5)/ Al_2O_3$
	k_{DBT}			
300°C	3.8	4.6	5.0	3.9
325°C	6	6.6	7.6	6.2
350°C	18.3	21.6	22.4	19.7

Table 4.4.7 Reaction rate constants kx1000 (min^{-1}) of 4 methyl dibenzothiophene over different catalysts.

Temperature	$CoMoP(0)/Al_2O_3$	$CoMoP(0.5)/Al_2O_3$	$CoMoP(1)/Al_2O_3$	$CoMoP(1.5)/ Al_2O_3$
	$k_{4\text{-}MDBT}$			
300°C	1.3	1.8	1.6	2.4
325°C	2.6	3.2	2.9	4.4
350°C	9.4	10.8	10.1	13.9

Table 4.4.8 shows the ratio of k_{DBT} to $k_{4\text{-}MDBT}$. The $k_{DBT}/k_{4\text{-}MDBT}$ was calculated in order to see the relative reactivity of DBT and 4-MDBT in a competitive reaction. The ratio was found to decrease as the temperature increase suggesting that at higher temperatures the HDS of 4-MDBT was more favored. The ratio was highest over CoMoP (0)/Al_2O_3 at 300°C and decreased to 1.95 over the same catalyst at 350°C. The phosphorus modification also influenced the ratio as $k_{DBT}/k_{4\text{-}MDBT}$ decreased to 1.72 over CoMoP(1)/Al_2O_3 at 350°C but there was not much change for CoMoP(0.5)/Al_2O_3 and CoMoP(1.5)/Al_2O_3 As the ratio was approximately constant over these two catalyst.

At 300°C and 325°C the ratio was found to decrease as we move from right to left column in Table 4.4.8. This shows that the by phosphorus modification the rate of 4-MDBT was enhanced as compared to DBT.

Table 4.4.8 $k_{DBT}/k_{4\text{-}MDBT}$ ratio at two different temperatures

Temperature	CoMoP(0)/Al_2O_3	CoMoP(0.5)/Al_2O_3	CoMoP(1)/Al_2O_3	CoMoP(1.5)/ Al_2O_3
	$k_{DBT}/k_{4\text{-}MDBT}$			
300°C	2.92	2.56	2.27	2.44
325°C	2.31	2.06	2.00	2.14
350°C	1.95	2.00	1.72	1.95

4.4.2 Reaction pathways for DBT and 4-MDBT

Analyses of DBT HDS products by GC-MS indicated the presence of both BPh and CHB in all samples. This result indicates that DBT HDS has occurred through both direct desulfurization (DDS) and hydrogenation (HYD) pathways. Figure 4.4.9 presents the product distribution during HDS of DBT over CoMoP (0)/Al_2O_3 catalyst at 350^oC. With the increase in reaction time, DBT content reduced while BPh (product of hydrogenolysis) and CHB (product of hydrogenation) contents increased. After a reaction time of 120 minutes, DBT conversion was 83.75%. The maximum conversion of Biphenyl and Cyclohexyl benzene (CHB) was 74% and 9.3% respectively. The expected intermediates of the HYD route (THDBT and HHDBT) were observed in trace amounts. This result indicates that DDS route is predominant over HYD route under these conditions.

The HDS of 4-MDBT results in two main products methyl biphenyl (MBP) which is the product of DDS and methyl cyclohexyl benzene by HYD pathway. Figure 4.4.10 shows the product distribution over CoMoP (0)/Al_2O_3 at 350^oC. The maximum conversion of 4-MDBT achieved was 46.8% and the conversion of 4-MDBT into methyl biphenyl (MBP) and methyl cyclohexyl benzene (MCHB) were 37.8% and 9% respectively. This shows that the HDS of 4-MDBT also takes place predominantly by DDS to yield methyl biphenyl.

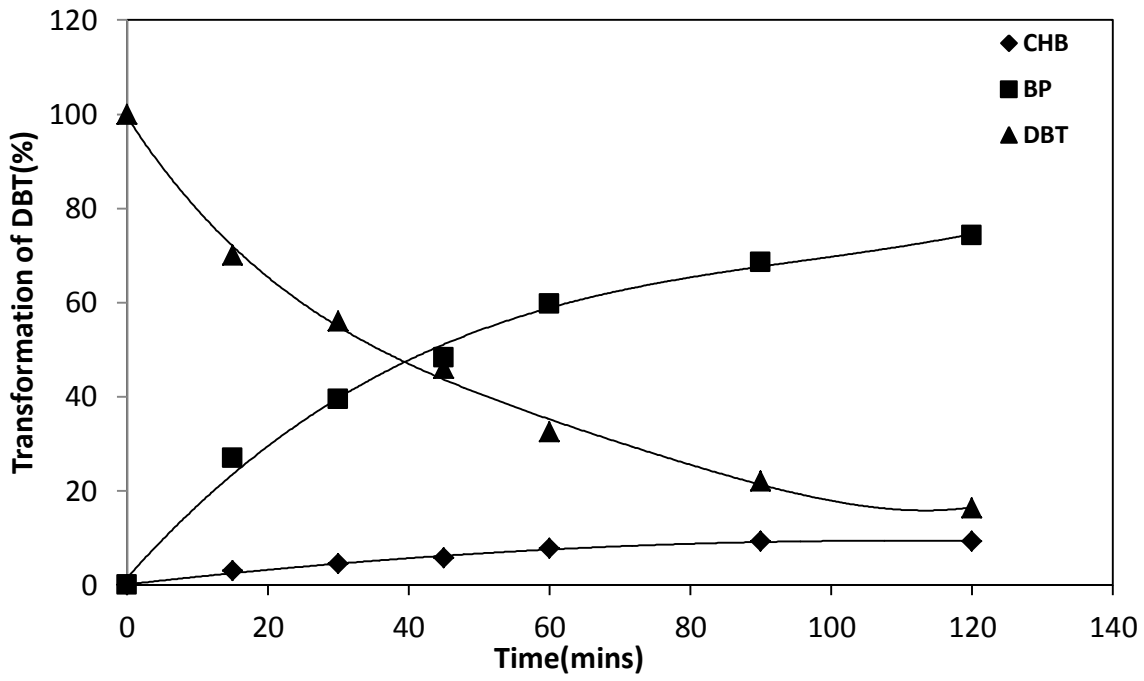

Figure 4.4.9 Transformation of DBT over CoMoP(0)/Al_2O_3 catalyst.

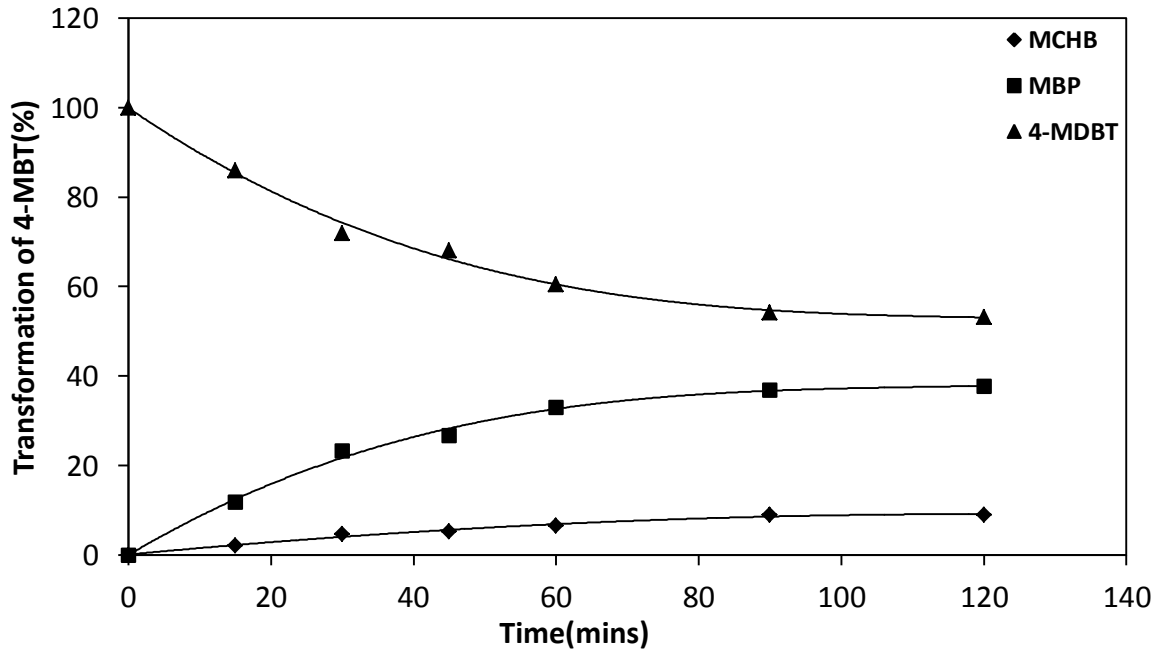

Figure 4.4.10 Transformation of 4-MDBT over CoMoP(0)/Al_2O_3 catalyst.

Figure 4.4.11 shows the transformation of DBT over CoMoP(0.5)/Al_2O_3 at 350^oC a similar trend was observed as in the case of CoMoP(0)/Al_2O_3 catalysts. The conversion of DBT after 120 minutes was 85.7% and the conversion of biphenyl and Cyclohexyl benzene were 75.8% and 9.91% respectively. In case of 4-MDBT over the same catalyst the maximum conversion was 51.3% and the conversion of 4-MDBT into (MBP) and MCHB were 42.7% and 8.7% respectively. Figure 4.4.12 shows the transformation of 4-MDBT over CoMoP(0.5)/Al_2O_3. The product distribution over phosphorus modified catalyst was found out to be similar as in the case of unmodified catalyst the difference was increase of conversion of both refractory sulfur compounds DBT and 4-MDBT.

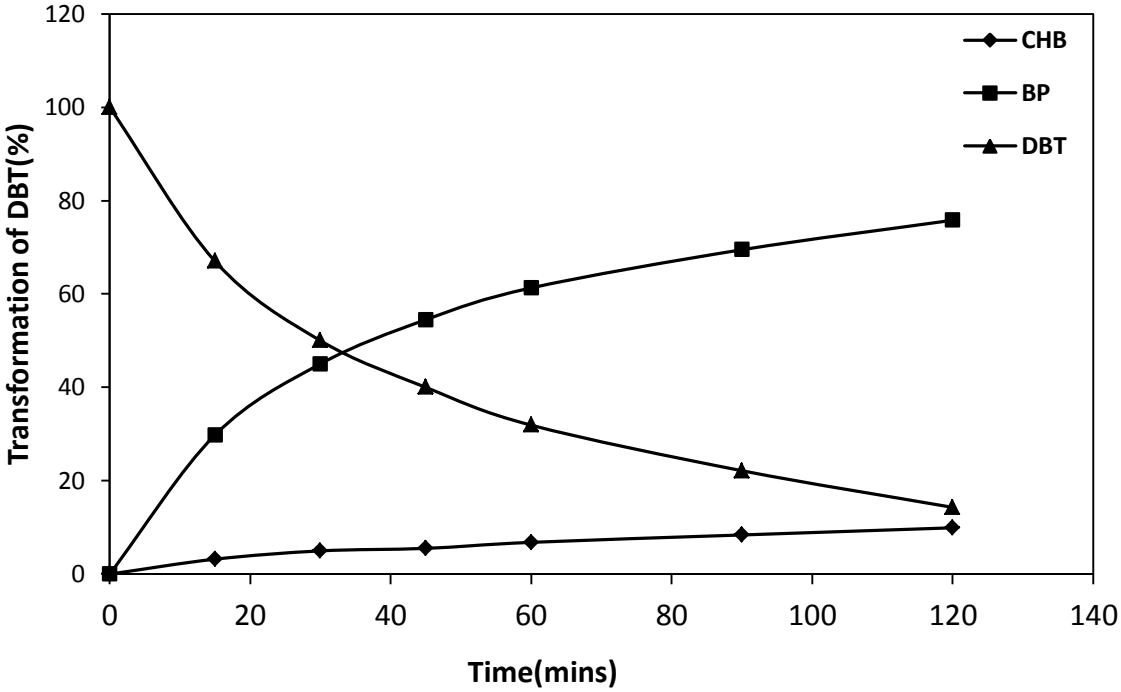

Figure 4.4.11 Transformation of DBT over CoMoP(0.5)/Al_2O_3

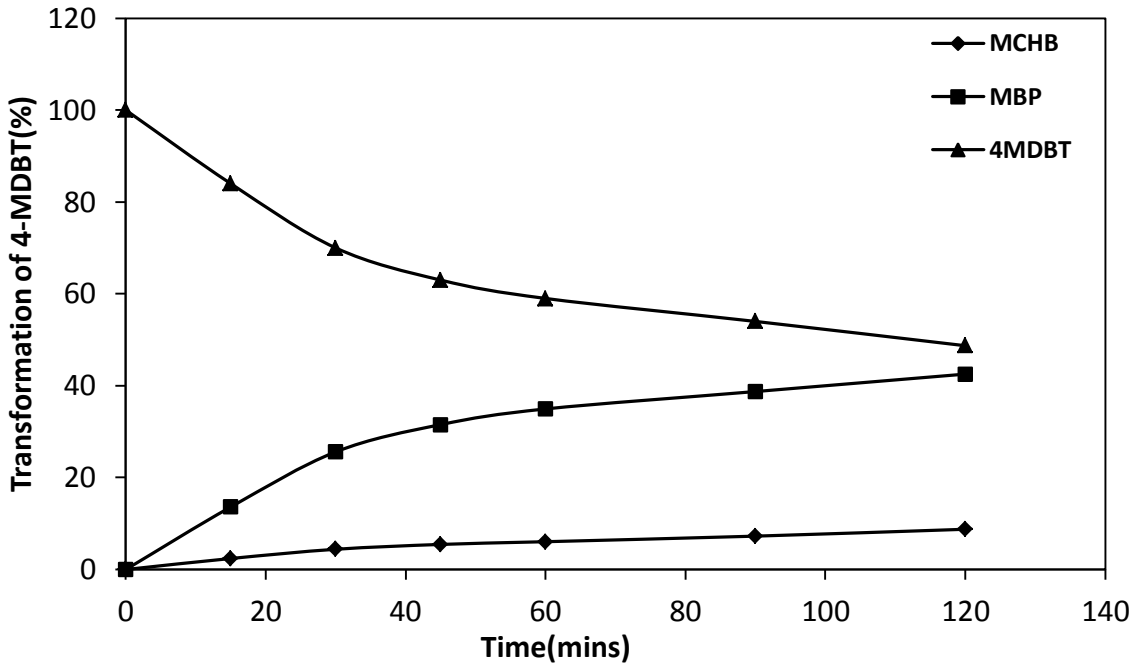

Figure 4.4.12 Transformation of 4-MDBT over CoMoP (0.5)/Al_2O_3 catalyst.

Figure 4.4.13 shows the transformation of DBT over CoMoP(1)/Al_2O_3 catalyst. The conversion of DBT was higher as compared to unmodified catalyst and and phosphorus modified catalyst with P_2O_5 content of 0.5wt.%. The maximum conversion of DBT was 87.5% and the conversion of DBT into biphenyl was 76.7% and into cyclohexyl benzene were 10.9%.

The transformation of 4-MDBT into MBP and MCHB was also found to be higher as compared to other two catalysts discussed. Figure 4.4.14 shows the transformation of 4-MDBT over CoMoP(1)/Al_2O_3. The maximum conversion of 4-MDBT were 58.7% and into MBP and MCHB were 47.8% and 11.8% respectively.

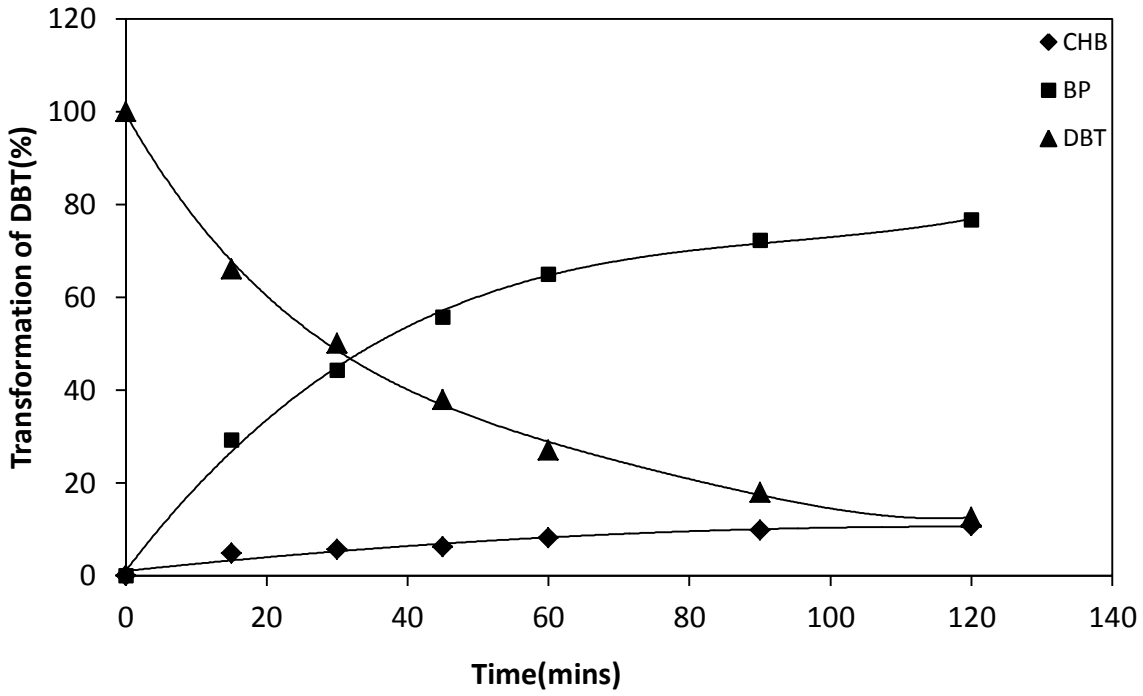

Figure 4.4.13 Transformation of DBT over CoMoP(1)/Al_2O_3 catalyst.

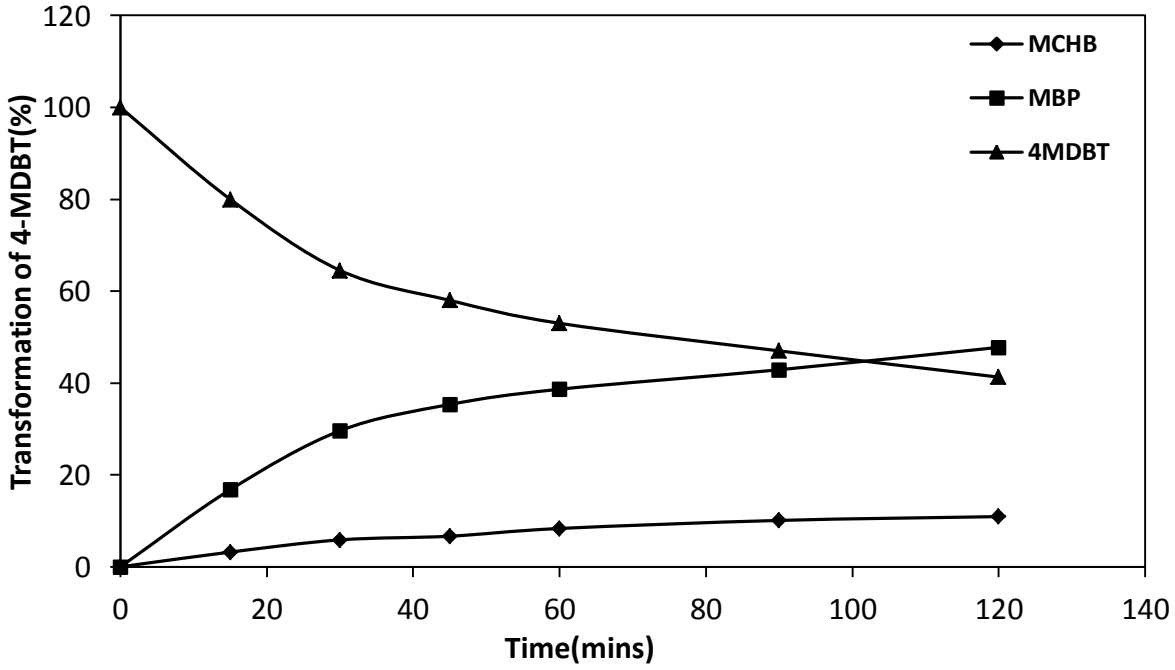

Figure 4.4.14 Transformation of 4-MDBT over CoMoP(1)/Al_2O_3 catalyst.

The coversion of DBT was found to bit lower over CoMoP(1.5)/Al_2O_3 as compared to CoMo/Al_2O_3 catalyst with 0.5 and 1 wt.% P_2O_5. Figure 4.4.15 shows the transformation of DBT over CoMoP(1.5)/Al_2O_3. The maximum conversion was 86% and conversion into biphenyl and cyclohexyl benzene were 75.8% and 10.18%. These conversion were comparatively low whene compared with other phosphorus modified catalyst.

Figure 4.4.16 shows the same trend as the phosphours content of the catalyst increased to 1.5wt.% the conversion of 4-MDBT were 43.5% which is comparatively low. However the conversion is still higher than unmodified CoMo(1.5)/Al_2O_3 catalyst. The maximum conversion of 4-MDBT into MBP and MCHB were 36.8% and 6.7% respectively.

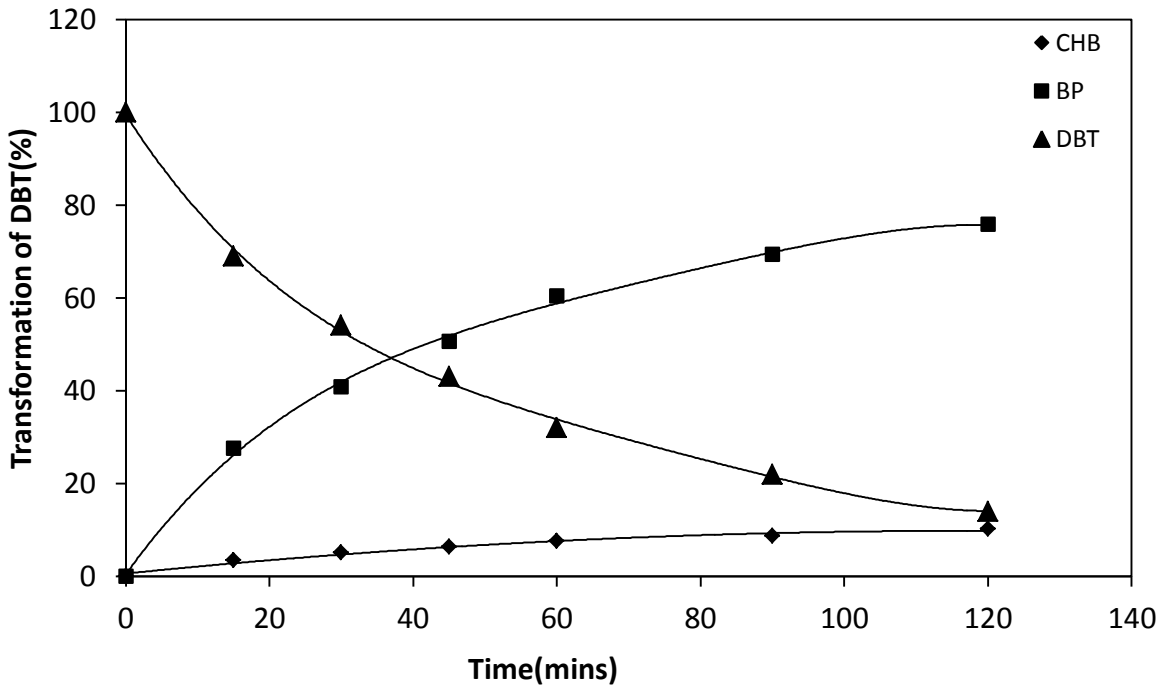

Figure 4.4.15 Transformation of DBT) over CoMoP(1.5)/Al_2O_3 catalyst.

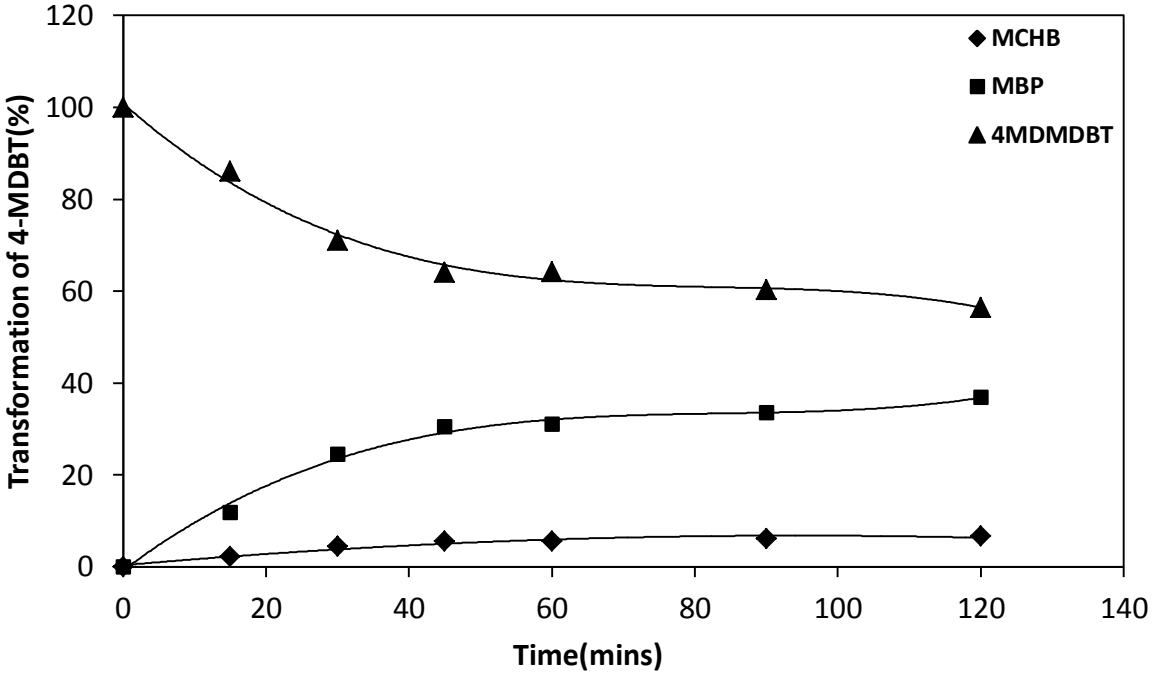

Figure 4.4.16 Transformation of 4-MDBT over CoMoP(1.5)/Al_2O_3 catalyst.

4.4.3 Rate of Formation for HDS product of DBT and 4-MDBT

In order to investigate the reaction pathways individual rate constant were calculated from the plot of –ln(1-X) versus time. Where X is the conversion of DBT or 4-MDBT into biphenyl, cyclohexyl benzene, methyl cyclohexyl benzene and methyl biphenyl. Figure 4.4.17 to 4.24 shows the rate constants of individual products obtained during the HDS reaction.

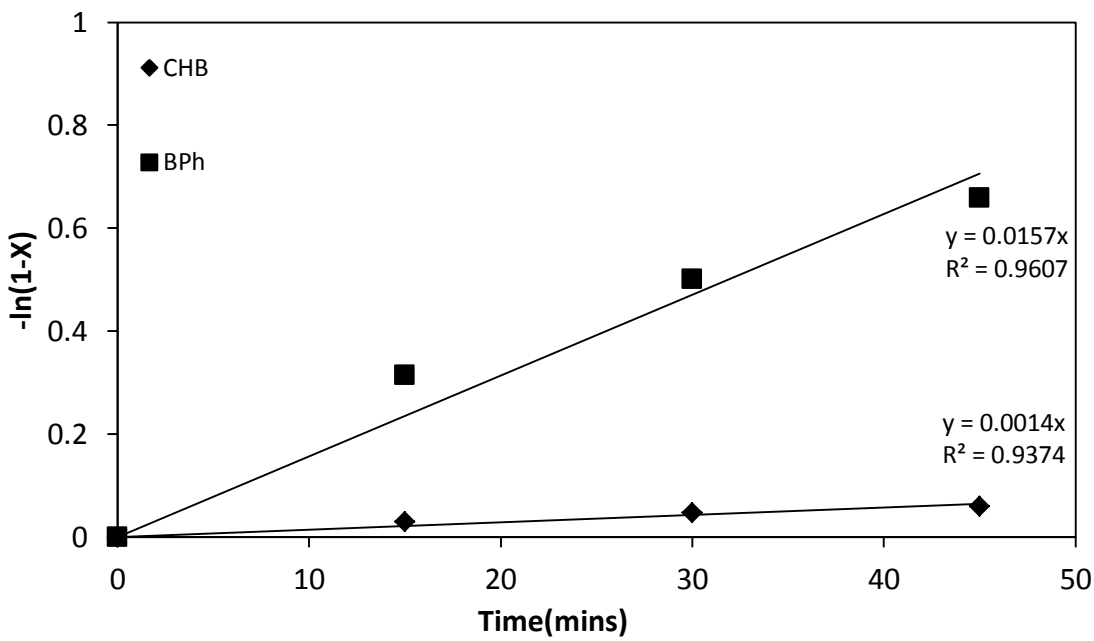

Figure 4.4.17 Formation rates of BP and CHB over CoMoP (0)/Al_2O_3 catalyst.

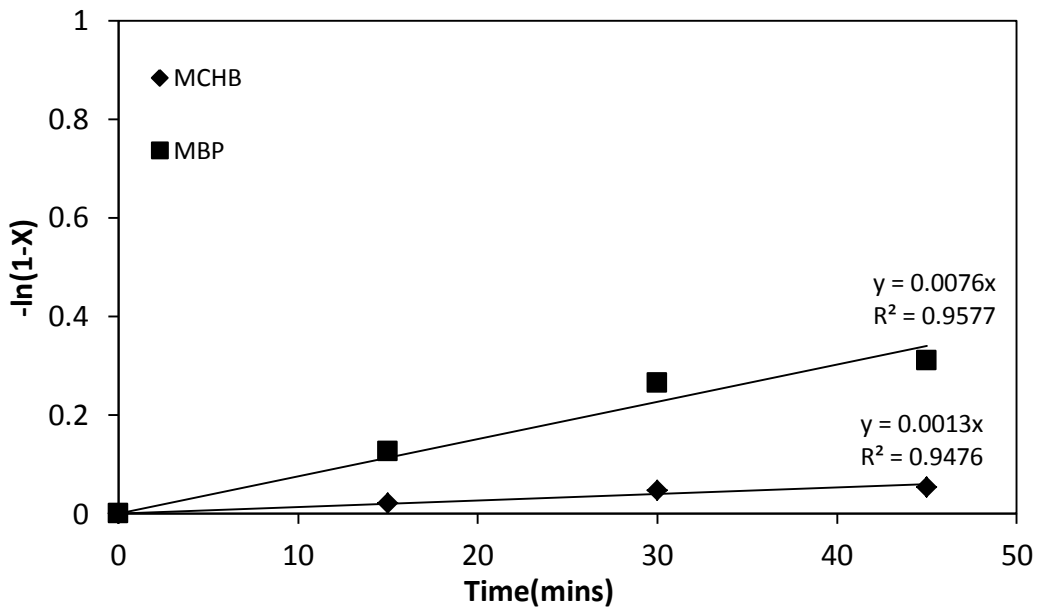

Figure 4.4.18 Formation rates of MBP and MCHB over CoMoP(0)/Al_2O_3 catalyst.

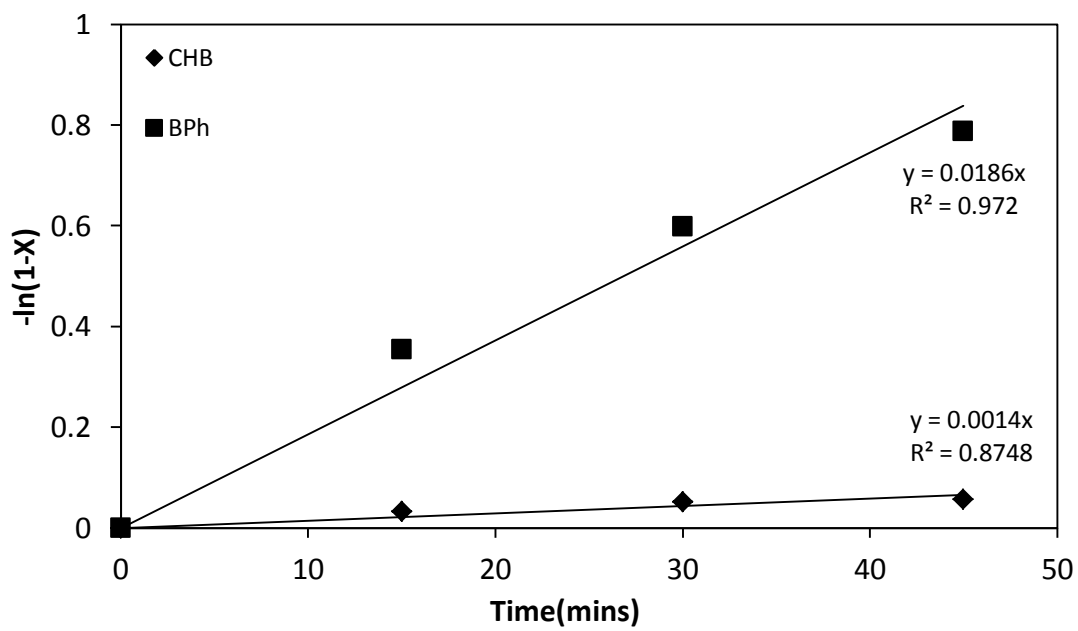

Figure 4.4.19 Formation rates of BP and CHB over CoMoP (0.5)/Al_2O_3 catalyst.

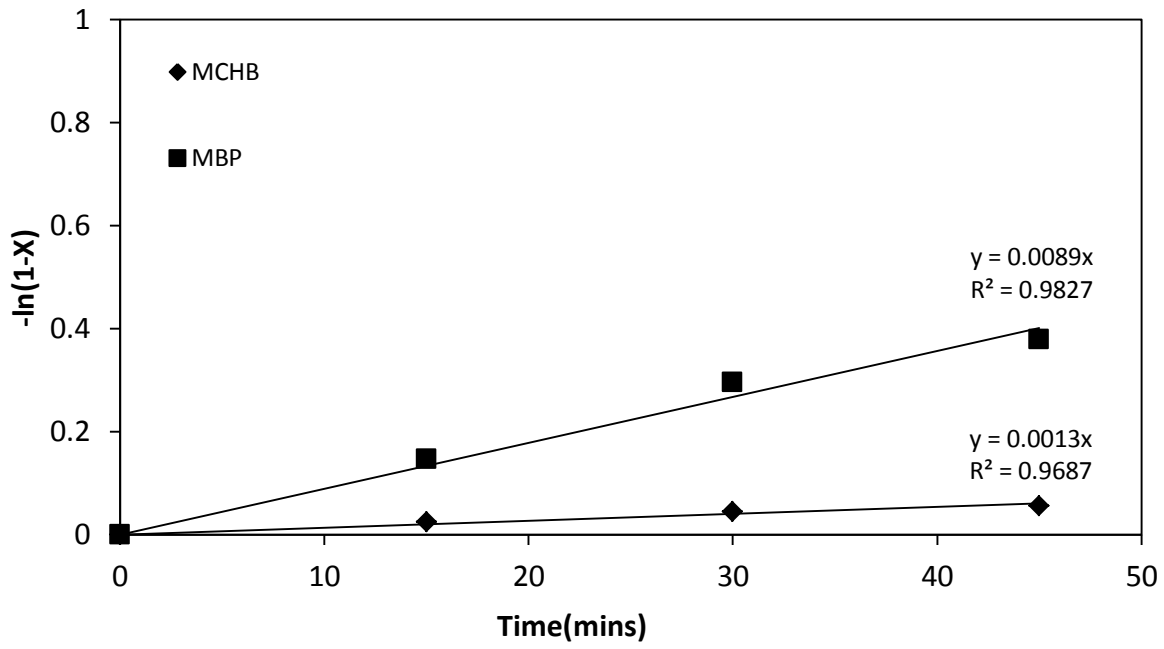

Figure 4.4.20 Formation rates of MBP and MCHB over CoMoP(0.5)/Al_2O_3 catalyst.

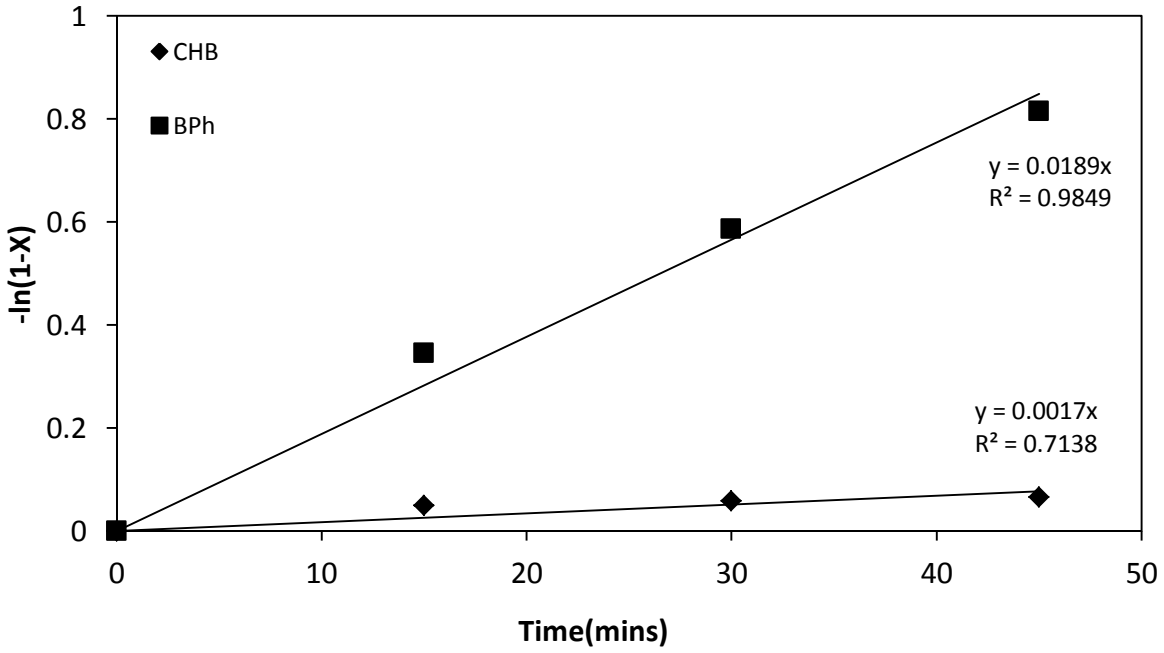

Figure 4.4.21 Formation rates of BP and CHB over CoMoP(1)/Al_2O_3 catalyst.

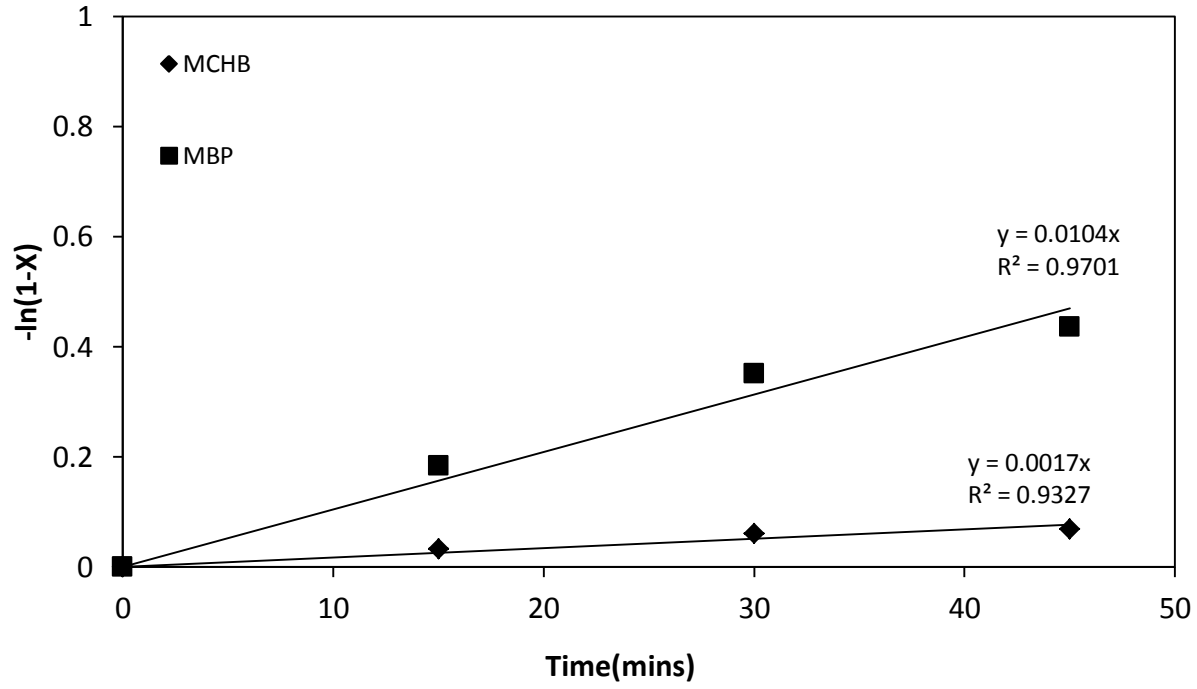

Figure 4.4.22 Formation rates of MBP and MCHB over CoMoP(1)/Al_2O_3 catalyst.

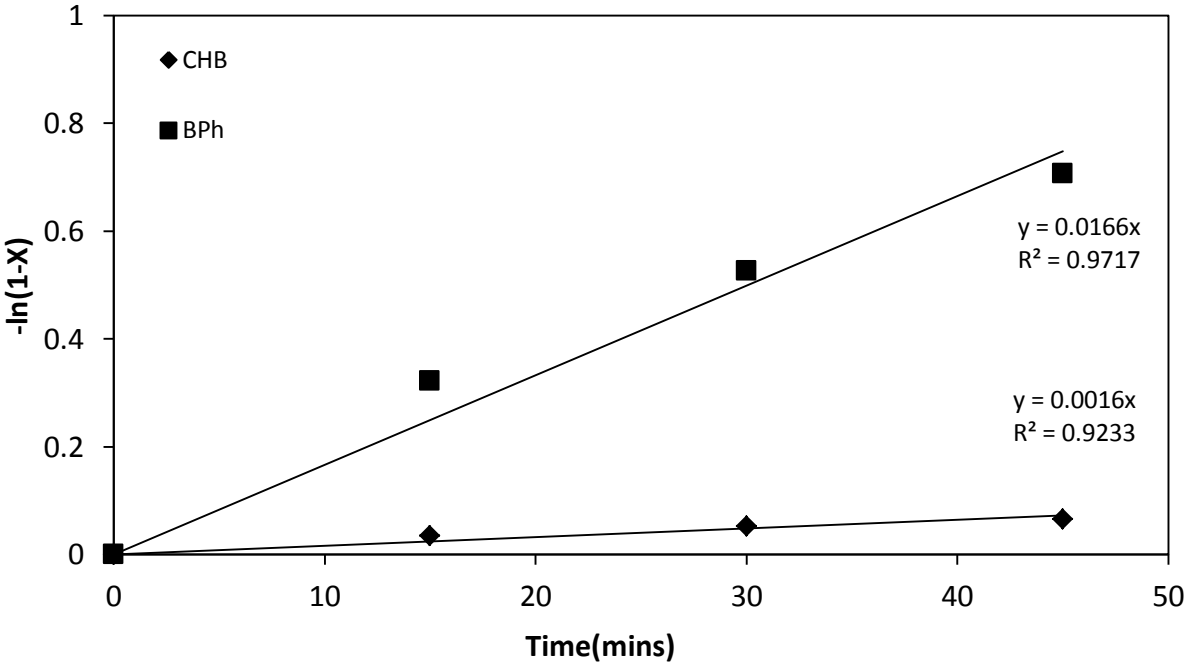

Figure 4.4.23 Formation rates of BP and CHB over CoMoP (1.5)/Al_2O_3 catalyst.

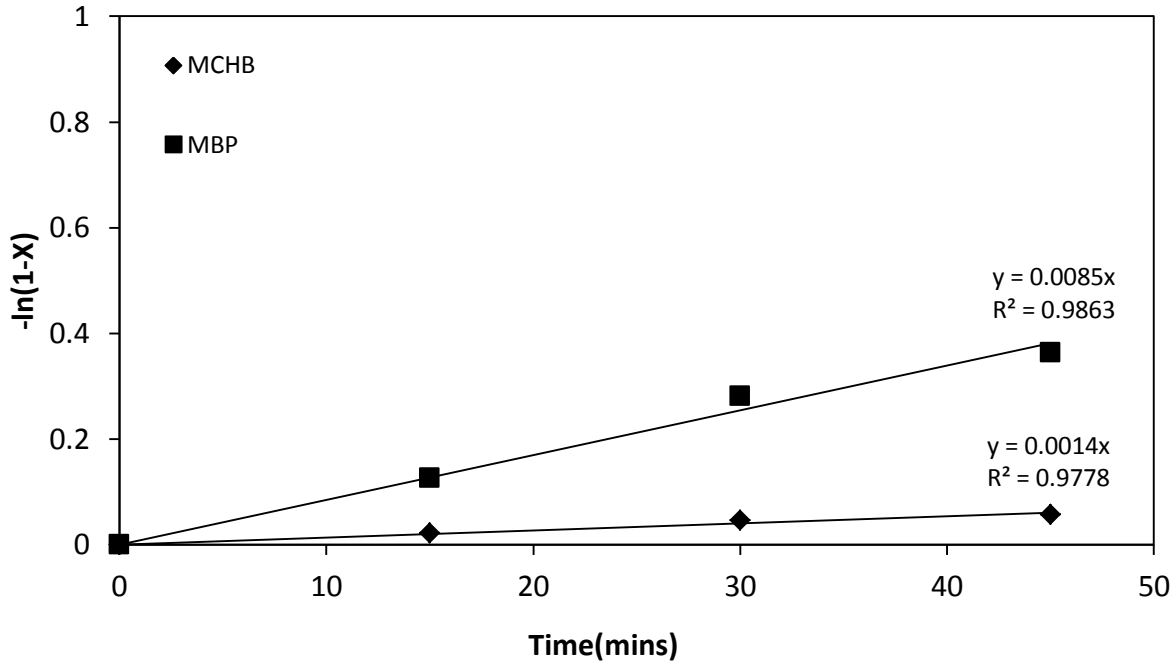

Figure 4.4.24 Formation rates of MBP and MCHB over CoMoP(1.5)/Al_2O_3 catalyst.

The rate constants of formation of biphenyl are shown in Table 4.4.9. The rate of formation of BP was found to be influenced by the temperature over all catalysts. The rate increases with the increase in the temperature. The rate constant increases 3 to 4 time as the reaction was performed from 300°C to 350°C. At each temperature the rate constant was found to increase as we move from left to right in a row in Table 4.4.9. This means that phosphorus modification increased the rate of biphenyl formation. However the rate constant increases and reach to its maximum value over CoMoP(1)/Al_2O_3 catalyst and with further increase in P_2O_5 content to 1.5wt.% the rate constant starts to decrease. Compared to the unmodified catalyst the rate constant over CoMoP (1.5)/Al_2O_3 was still higher. These results show that phosphorus modification increases the rate of formation of biphenyl.

Table.4.4.9 Formation rate constant kx1000 (min^{-1}) of biphenyl at different temperatures.

Temperature	$CoMoP(0)/Al_2O_3$	$CoMoP(0.5)/Al_2O_3$	$CoMoP(1)/Al_2O_3$	$CoMoP(1.5)/ Al_2O_3$
	k_{BP}			
300°C	3.4	4.4	4.4	3.9
325°C	5.5	6	6.6	5.4
350°C	15.7	18.6	18.9	16.6

Table 4.4.10 shows the formation rate constant of cyclohexyl benzene formed during HDS of DBT. The rate of formation of CHB was also influenced by the temperature and it increased to 3 to 4 times at 350°C. A similar trend was observed as in the case of biphenyl that the rate constant increases as we move from left to right in a row in Table 4.4.10. As in the previous section it was found out that the main reaction products of DBT desulfurization is biphenyl that's why the rate constant of biphenyl were higher than cyclohexyl benzene at all temperatures and over all catalysts.

Table.4.4.10 Formation rate constant of kx1000 (min^{-1}) Cyclohexyl benzene at different temperatures.

Temperature	$CoMoP(0)/Al_2O_3$	$CoMoP(0.5)/Al_2O_3$	$CoMoP(1)/Al_2O_3$	$CoMoP(1.5)/ Al_2O_3$
	k_{CHB}			
300°C	0.3	0.4	0.5	0.5
325°C	0.5	0.5	0.8	0.7
350°C	1.4	1.4	1.7	1.6

Table 4.4.11 shows the k_{BP}/k_{CHB}. The ratio was found to initially increase from 11.21 for $CoMoP(0)/Al_2O_3$ to 13.29 which means that by phosphorus modification of 0.5wt.% P_2O_5 the influence was only on DDS pathway. When the phosphorus content increased to 1wt.% P_2O_5 the ratio decreased to 11.12 which suggest that over $CoMoP(1)/Al_2O_3$ catalyst the rate of CHB formation was enhanced as compared to unmodified $CoMoP(0)/Al_2O_3$ catalyst. After further increase in P_2O_5 content to 1.5wt.% the ratio

further decreased to 10.37 which means that phosphorus modification increase the rate of formation of CHB. The ratio was even low for NiMoP (0.5)/Al_2O_3 at which the ratio was 7.8. This is the clear indication that NiMoP (0.5)/Al_2O_3 catalyst were relatively higher in hydrogenation activity.

Table.4.4.11 k_{BP}/k_{CHB} ratio at two different temperatures

Temperature	CoMoP(0)/Al_2O_3	CoMoP(0.5)/Al_2O_3	CoMoP(1)/Al_2O_3	CoMoP(1.5)/ Al_2O_3
	k_{BP}/k_{CHB}			
325°C	11.0	12.0	8.25	7.71
350°C	11.21	13.29	11.12	10.3

The HDS of 4-MDBT results in MBP and MCHB the formation rate constant are presented in Table 4.4.12. As in the previous section it was found out that the main product from the HDS of 4-MDBT was MBP which is formed by direct desulfurization route. The formation rate constant increased with temperature and MBP also follows the same trend that the rate increase from 0.0076 $min^{-}1$ for CoMoP(0)/Al_2O_3 to 0.0104 min^{-1} for CoMoP(1)/Al_2O_3 and it decreases to 0.0084 $min^{-}1$ over CoMoP(1.5)/Al_2O_3 at 350°C.

Table.4.4.12 Formation rate constant of kx1000 (min^{-1}) methyl biphenyl benzene at different temperatures.

Temperature	CoMoP(0)/Al_2O_3	CoMoP(0.5)/Al_2O_3	CoMoP(1)/Al_2O_3	CoMoP(1.5)/ Al_2O_3
	k_{MBP}			
300°C	3.8	4.6	5.0	3.9
325°C	6	6.6	7.6	6.2
350°C	18.3	21.6	22.4	19.7

Table 4.4.13 presented the rate of formation of MCHB. The rate of MCHB also increased with temperature increase and the rate of formation of MCHB was lower as compared to MBP as the main route for 4-MDBT was DDS which results in mainly MBP. The rate constant increase from 0.00013 $min^{-}1$ for $CoMoP(0)/Al_2O_3$ to 0.00017 min^{-1} for $CoMoP(1)/Al_2O_3$.

Table.4.4.13 Formation rate constant of kx1000 (min^{-1}) methyl cyclohexyl benzene at different temperatures.

Temperature	$CoMoP(0)/Al_2O_3$	$CoMoP(0.5)/Al_2O_3$	$CoMoP(1)/Al_2O_3$	$CoMoP(1.5)/ Al_2O_3$
	k_{MCHB}			
300°C	0.2	0.2	0.4	0.19
325°C	0.5	0.5	0.7	0.4
350°C	1.3	1.3	1.7	1.4

Table.4.4.14 k_{MBP}/k_{MCHB} ratio at two different temperatures

Temperature	$CoMoP(0)/Al_2O_3$	$CoMoP(0.5)/Al_2O_3$	$CoMoP(1)/Al_2O_3$	$CoMoP(1.5)/ Al_2O_3$
	k_{MBP}/k_{MCHB}			
325°C	4.40	5.20	4.43	6.25
350°C	5.85	6.85	6.12	6.07

The k_{MBP}/k_{CHB} ratio for HDS of 4-MDBT was in the range of 5.8-6.0. The DDS to HYD ratio for HDS of 4-MDBT were less as compared to HDS of DBT. The reason for the decrease in DDS route was due to the presence of one methyl substituent which gives steric hindrance in the sulfur removal by DDS pathway [53].

4.4.4 Apparent Activation energy for DBT and 4-MDBT.

Activation energies for HDS reaction were calculated from pseudo-first order rate constants at three different temperatures 300, 325 and 350°C. Arrhenius plot was plotted between -ln(k) and 1/T (Kelvin).Where k is the rate constant. The slope of the line multiplied by gas constant gives the value of Activation energy in KJ/mole. The activation energies of DBT lies in the range of 87-95 KJ/mole these values are in good agreement with literature**.** Activation energies of 4-MDBT were found to be in the range of 103 to 117 KJ/mole.

Table 4.4.15 Activation Energies (KJ/mole).

Catalysts	DBT	4-MDBT	BP	CHB	MBP	MCHB
CoMoP(0)/Al_2O_3	92.75	117	91.01	90.33	114.49	113.07
CoMoP(0.5)/Al_2O_3	91.45	105.82	87.68	73.66	101.24	112.90
CoMoP(1)/Al_2O_3	88.46	104.87	85.61	72.33	106.42	86.96
CoMoP(1.5)/Al_2O_3	95.56	108.76	85.31	90.10	108.08	106.49
NiMoP(0.5)/Al_2O_3	87.72	103.76	83.14	75.39	105.92	75.09

4.5 Simultaneous HDS of Dibenzothiophene and 4,6-dimethyl dibenzothiophene over Phosphorus modified $CoMoP/Al_2O_3$.

Dibenzothiophene (DBT) and 4,6 dimethyl dibenzothiophene (4,6-DMDBT) were desulfurized over a series of phosphorus modified catalysts Table 4.4.1 shows the compositions of the catalysts. The concentration of DBT and 4,6-DMDBT were 2800 and 3320 ppm respectively and this equals to 500ppm of sulfur contribution from each compound so the total sulfur was 1000ppm in the reaction mixture.

The hydrodesulfurization of dibenzothiophene and 4,6 dimethyl dibenzothiophene were carried out together in a competitive reaction over unmodified $CoMoP(0)/Al_2O_3$ at 350°C. The conversion of DBT was found out to be higher as compared to 4,6-DMDBT. Figure 4.5.1 shows that HDS of DBT and 4,6-DMDBT at 350°C. The maximum conversion of DBT and 4,6-DMDBT after 120 minutes of reaction time was 90% and 26.6% at 350°C respectively.

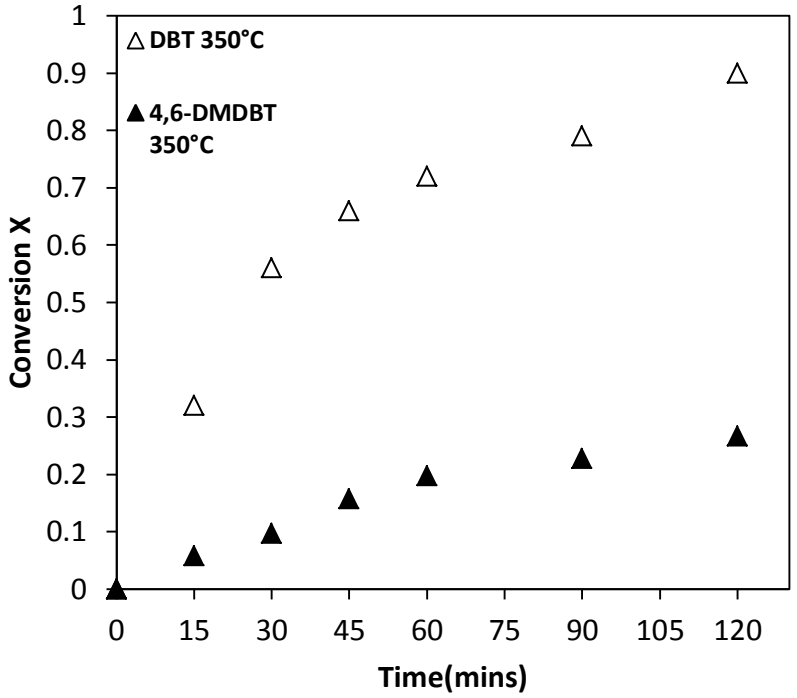

Figure 4.5.1 Conversion of DBT and 4,6-DMDBT in Competitive reaction over CoMoP(0)/Al_2O_3.

Table 4.5.1 shows the total sulfur content and the sulfur due to DBT and 4,6-DMDBT. 4,6-DMDBT was found to be comparatively less reactive than DBT. The total sulfur left after 120 mins was 408ppm it is interesting to note that the sulfur due to DBT left was only 50ppm and sulfur due to 4,6-DMDBT was 367ppm which means that 4,6-DMDBT is very unreactive in nature and desulfurization is quite difficult as compared to DBT.

Table 4.5.1 Sulfur (ppm) remaining in the reaction mixture over CoMoP(0)/Al_2O_3 catalyst.

Time(mins)	DBT	4,6-DMDBT	Total Sulfur
0	500	500	1000
15	340	471	811
30	220	452	672
45	170	421	591
60	140	409	549
90	105	388	493
120	50	367	417

The phosphorus modified CoMoP(0.5)/Al_2O_3 shows higher conversion as compared to unmodified CoMoP (0)/Al_2O_3 as shown in Figure 4.5.2. DBT conversion increased to 94% and 4,6-DMDBT conversion to 30%.

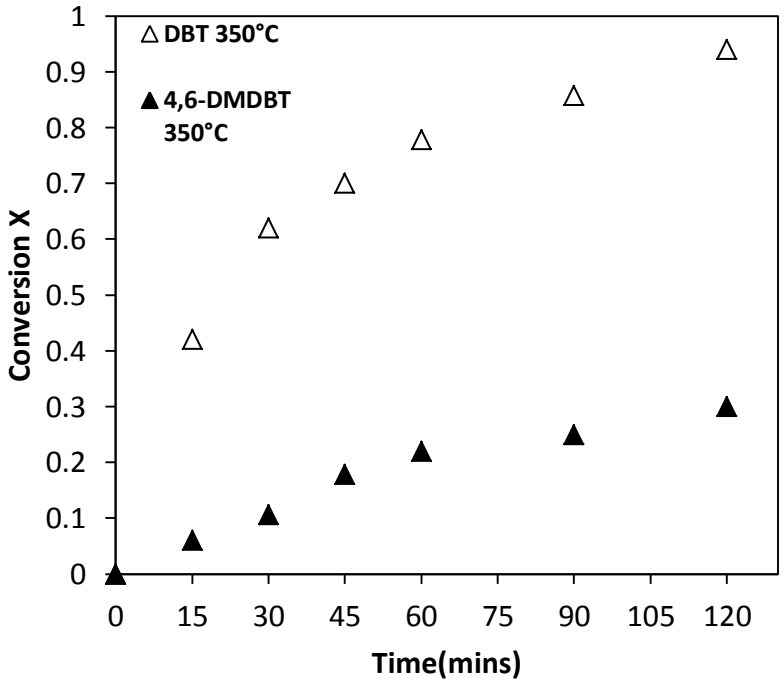

Figure 4.5.2 Conversion of DBT and 4,6-DMDBT in Competitive reaction over CoMoP(0.5)/Al_2O_3.

Table 4.5.2 shows the sulfur content over CoMoP(0.5)/Al_2O_3 . The total sulfur after 120 mins in the reaction mixture was 380ppm. 4,6-DMDBT has the same trend as a refractory sulfur compound and it desulfurized to 350ppm sulfur level.

Table 4.5.2 Sulfur (ppm) remaining in the reaction mixture over CoMoP (0.5)/Al_2O_3 catalyst.

Time(mins)	DBT	4,6-DMDBT	Total Sulfur
0	500	500	1000
15	290	470	760
30	190	447	637
45	150	411	561
60	111	390	501
90	71	388	459
120	30	350	380

By increasing the phosphorus content to 1wt. % P_2O_5 there is increase in HDS activity. The conversion of DBT and 4,6-DMDBT increased to 97% and 36% respectively.

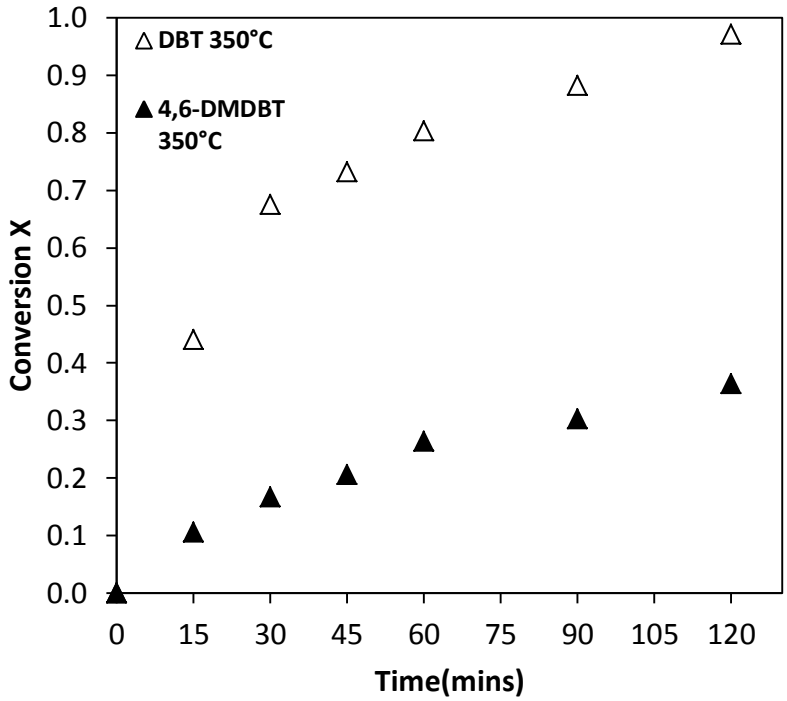

Figure 4.5.3 Conversion of DBT and 4,6-DMDBT in Competitive reaction over CoMoP(1)/Al_2O_3.

Considerable difference was observed in HDS activity over CoMoP (1)/Al_2O_3 for both DBT and 4,6-DMDBT. Table 4.5.3 shows the sulfur due to DBT, which reduced to 14ppm and there is also some improvement in desulfurization of 4,6-DMDBT as the sulfur content reduced to 318ppm. Nearly all sulfur left after the reaction was due to 4,6-DMDBT.

Table 4.5.3 Sulfur (ppm) remaining in the reaction mixture over CoMoP(1)/Al_2O_3 catalyst.

Time(mins)	DBT	4,6-DMDBT	Total Sulfur
0	500	500	1000
15	280	447	727
30	163	417	579
45	134	397	531
60	98	368	466
90	59	349	407
120	14	318	332

By increasing the phosphorus content to 1.5wt.% P_2O_5 the HDS activity decrease for both DBT and 4,6-DMDBT as compared to other phosphorus modified catalyst. The conversion of DBT and 4,6-DMDBT was 92% and 28.8% respectively.

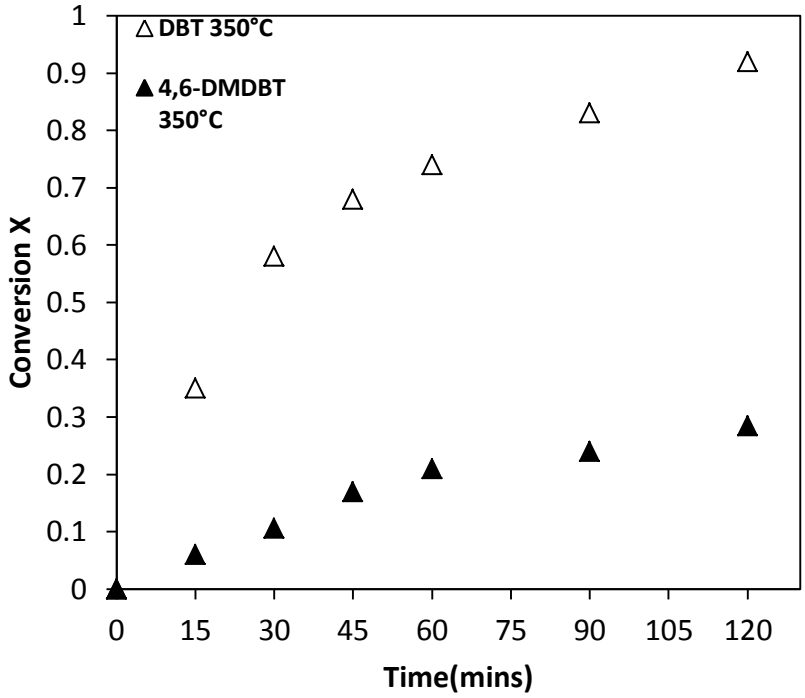

Figure 4.5.4 Conversion of DBT and 4,6-DMDBT in Competitive reaction over CoMoP(1.5)/Al_2O_3.

The conversion of DBT and 4-MDBT both reduced over CoMoP(1.5)/Al_2O_3. The total sulfur reduced to 398ppm.

Table 4.5.4 Sulfur (ppm) remaining in the reaction mixture over CoMoP(1.5)/Al_2O_3 catalyst.

Time(mins)	DBT	4,6-DMDBT	Total Sulfur
0	500	500	1000
15	325	470	795
30	210	447	657
45	160	415	575
60	130	402	532
90	85	386	471
120	40	358	398

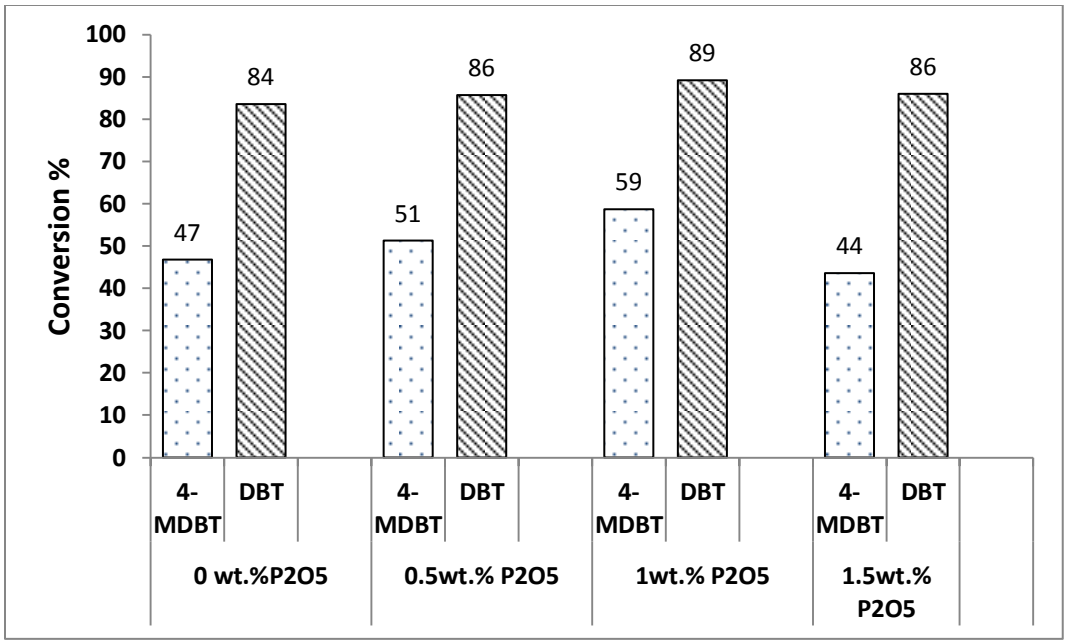

Figure 4.5.5 Promotional effect of phosphorus with increasing P_2O_5 content for HDS of DBT and 4-MDBT at 350°C.

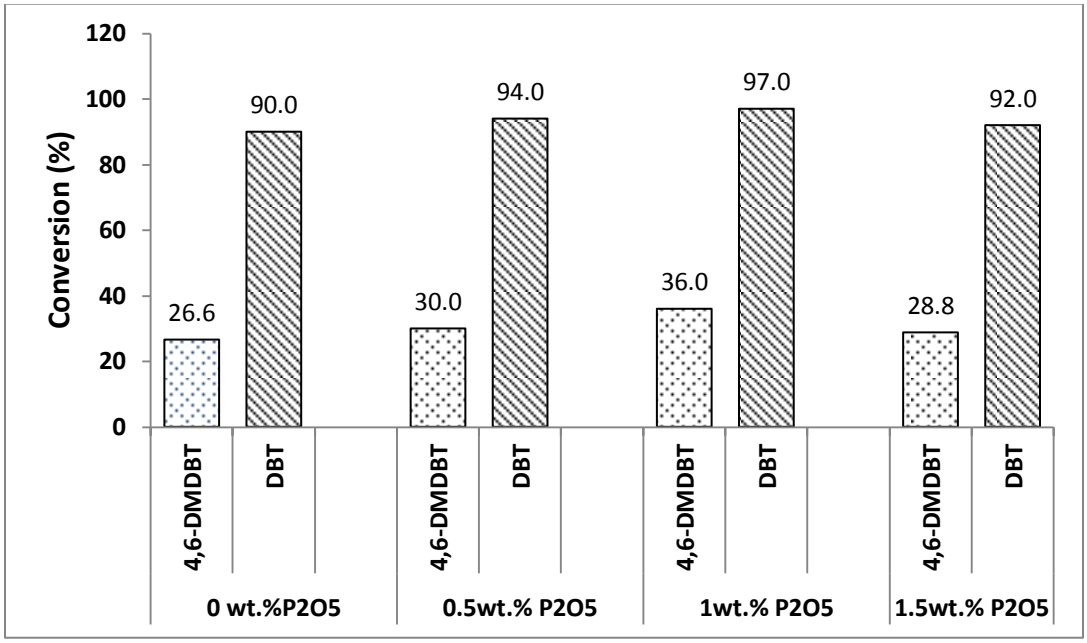

Figure 4.5.6 Promotional effect of phosphorus with increasing P2O5 content for HDS of DBT and 4,6-DMDBT at 350°C.

Figure 4.5.5 shows the promotional effect of phosphorus for simultaneous HDS of DBT and 4-MDBT over the final conversion at 350°C after the reaction time of 120 minutes. The coversion increased with the phosphorus content upto 1wt% P_2O_5 and then decreased at 1.5wt.%. The surface area of CoMoP/Al_2O_3 decrease significantly at 1.5wt.% P_2O_5. The decrease in the activity with increasing the phosphorus content can be explained by the fact that, with increase in phosphorus content the substantial amount of MoS_2 nanoparticles stacks up and the size of crystalline nanoparticles increased that leads to the poor dispersion of Mo [45]. This results in decrease of conversion at higher loadings.

Figure 4.5.6 shows the effect of phosphorus promotion over the HDS conversion of DBT and 4,6-DMDBT. Maximum conversion for both model compounds was achieved at 1wt% of P_2O_5. The conversion of DBT was higher when desulfurized with 4,6-DMDBT as compared to when DBT is desulfurized simultaneously with 4-MDBT under the same reaction conditions. This might be due to the fact that both DBT and 4-MDBT were predominantly desulfurized via DDS route and there exists some competition for DDS sites. As many studies showed that the DDS and HYD sites are different [54,55] and also the mode of adsorption of Dibenzothiophenes molecules in case of DDS is by σ-bonds which is the perpendicular adsorption by the sulfur atoms and in case of HYD the adsorption is by the aromatic ring[54].

4.5.1 Reaction Rate constants for Simultaneous HDS of DBT and 4,6-DMDBT over phosphorus modified $CoMo/Al_2O_3$

Figure 4.5.7 to 4.5.10 shows the plot of –ln(1-X) versus reaction time. Where X is the conversion of DBT or 4,6-DMDBT. The rate constants for DBT was found out to be higher than 4,6-DMDBT. The rate constant of DBT and 4,6-DMDBT was found out to be lower over unmodified $CoMoP(0)Al_2O_3$ and increase over all phosphorus modified catalysts.

The same trend was observed as in the case of competitive reaction of DBT and 4-MDBT. In case of competitve reaction between DBT and 4,6-DMDBT.The rate constants increased over phosphorus modified catalysts upto 1wt.% P_2O_5 and decrease when the phosphours content of the catalyst was 1.5wt.% P_2O_5. Howerver, at 1.5wt.% P_2O_5 content that is over $CoMoP(1.5)/Al_2O_3$ catalysts the rate constant was still higher than unmodified $CoMoP(0)/Al_2O_3$. There is an increment of 15.9% ,26.3% and 6% in the rate constant of DBT for $CoMoP(0.5)/Al_2O_3$, $CoMoP(1)/Al_2O_3$ and $CoMoP(1.5)/Al_2O_3$ respectively as compared to $CoMoP(0)/Al_2O_3$. The same incremental trend was observer for 4,6-DMDBT as the rate constant was increased to 13.5%, 51.3% and 8% in the same order as for the DBT over phosphorus modified catalysts. Table 4.5.5 gives the rate constant of DBT and 4,6-DMDBT over all the catalyst at 350^oC.

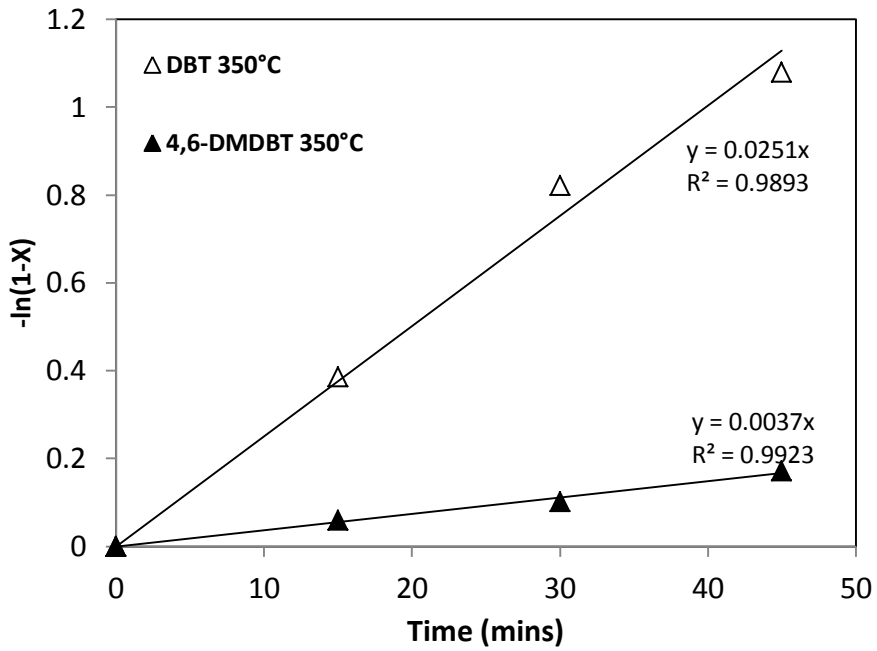

Figure 4.5.7 Rate constant of DBT and 4,6-DMDBT over CoMoP (0)/Al_2O_3.

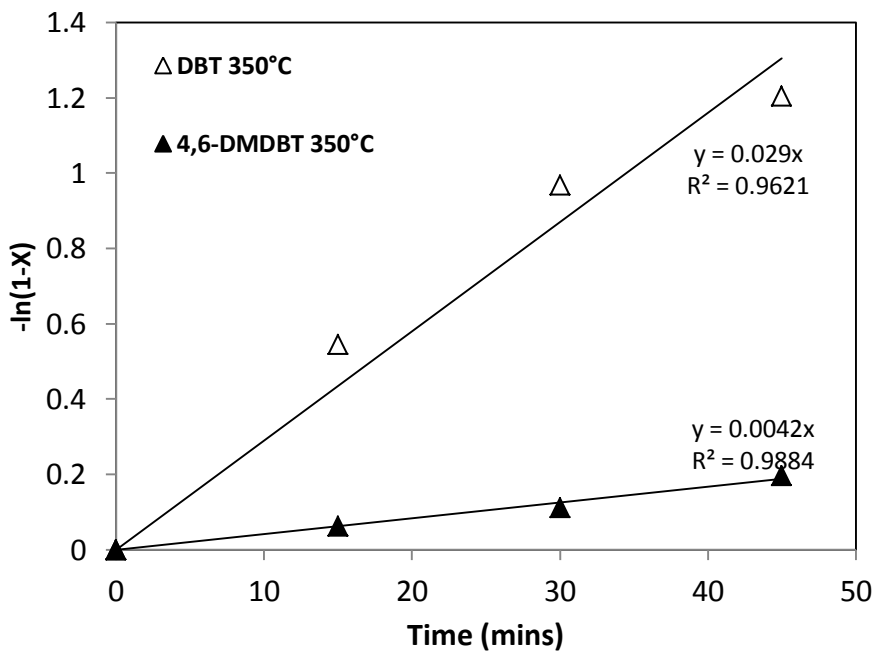

Figure 4.5.8 Rate constant of DBT and 4,6-DMDBT over CoMoP (0.5)/Al_2O_3.

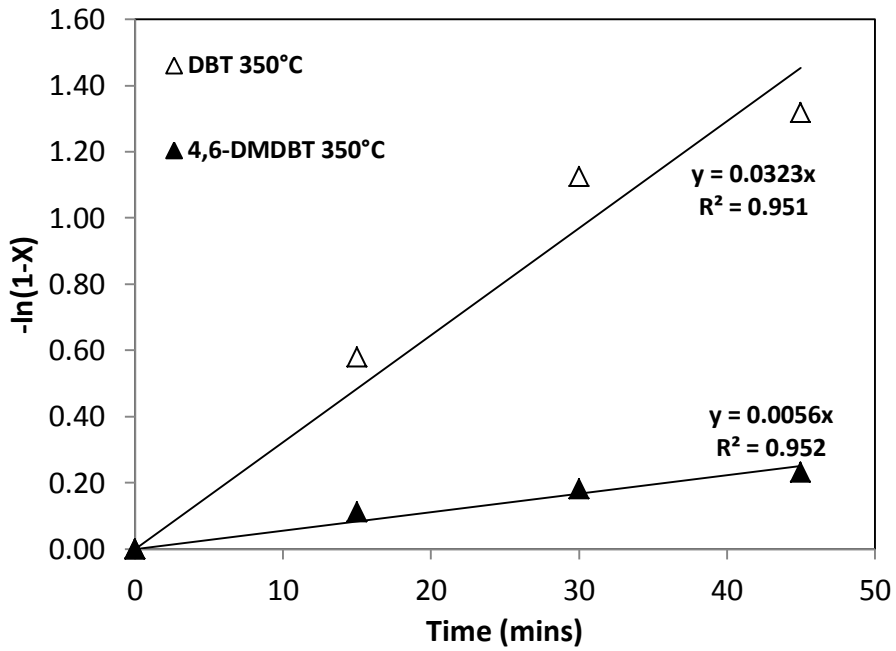

Figure 4.5.9 Rate constant of DBT and 4,6-DMDBT over CoMoP(1)/Al_2O_3.

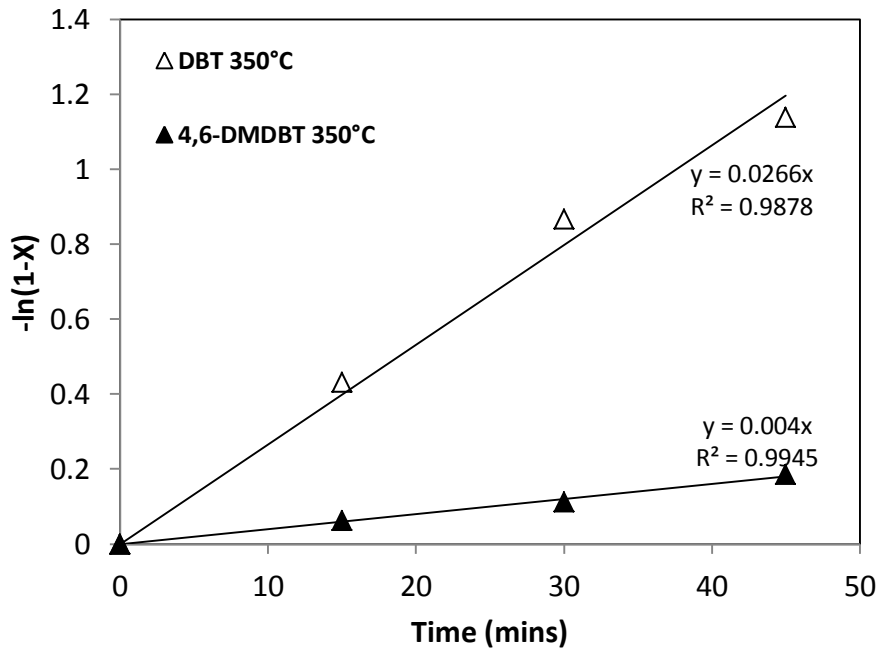

Figure 4.5.10 Rate constant of DBT and 4,6-DMDBT over CoMoP(1.5)/Al_2O_3.

Table 4.5.5 shows the ratio of k_{DBT} to $k_{4,6\text{-}DMDBT}$. The $k_{DBT}/k_{4,6\text{-}DMDBT}$ shows the relative reactivity of DBT and 4,6-DMDBT in a competitive reaction. The ratio ranges from 5.76 over CoMoP(1)/(Al_2O_3) to 6.90 over CoMoP(0.5)/Al_2O_3. The lowest ratio over phosphorus modified series was obtained over CoMoP (1)/Al_2O_3 which was 5.76 suggesting that the rate of 4,6-DMDBT was enhanced at P_2O_5 content of 1wt. %.

Table 4.5.5 rate constants kx1000 of DBT and 4,6-DMDBT over different catalysts at 350°C.

Catalysts	DBT	4,6-DMDBT	$k_{DBT}/k_{4,6\text{-}DMDBT}$
CoMoP(0)/Al_2O_3	25.1	3.7	6.78
CoMoP(0.5)/Al_2O_3	29	4.5	6.90
CoMoP(1)/Al_2O_3	32.3	5.6	5.76
CoMoP(1.5)/Al_2O_3	26.6	4	6.65

4.5.2 Reaction Pathways for DBT and 4,6-DMDBT

The HDS of DBT results in two main product biphenyl and cyclohexyl benzene. This result indicates that DBT HDS has occurred through both direct desulfurization (DDS) and hydrogenation (HYD) pathways. The HDS of 4,6-DMDBT also results in two main products dimethyl biphenyl (DMBP) which is formed by direct desulfurization route and methyl cyclohexyl toluene (MCHT) obtained from hydrogenation pathway route. Figure 4.5.11 to Figure 4.5.18 presents the product distribution during HDS of DBT and 4,6-DMDBT over a series of catalyst at 350°C. With the increase in reaction time, DBT and 4,6-DMDBT concentration reduced while BPs (product of hydrogenolysis) and CHBs (product of hydrogenation) contents increased.

Analyses of DBT HDS products by GC-MS indicated the presence of both BPh and CHB in all samples. This result indicates that DBT HDS has occurred through both direct desulfurization (DDS) and hydrogenation (HYD) pathways. Figure 4.5.11 presents the product distribution during HDS of DBT over CoMoP(0)/Al_2O_3 catalyst at 350°C. With the increase in reaction time, DBT content reduced while BPh (product of hydrogenolysis) and CHB (product of hydrogenation) contents increased. After a reaction time of 120 minutes, DBT conversion was 90%. The maximum conversion of Biphenyl and Cyclohexyl benzene (CHB) was 80% and 10% respectively. The expected intermediates of the HYD route (THDBT and HHDBT) were observed in trace amounts. This result indicates that DDS route is predominant over HYD route under these conditions.

The HDS of 4,6-DMDBT results in two main products methyl biphenyl (DMBP) which is the product of DDS and methyl cyclohexyl toluene by HYD pathway. Figure 4.5.12 shows the product distribution over CoMoP(0)/Al_2O_3 at 350^oC. The maximum conversion of 4,6-DMDBT achieved was 26.6% and the conversion of 4,6-DMDBT into dimethyl biphenyl (DMBP) and methyl cyclohexyl toluene (MCHB) were 12.4% and 14.2% respectively. The HDS of 4,6-DMDBT was mainly took place by HYD route and DDS was no more the predominant route. This is due to the presence of two methyl substituted to DBT which give rise to steric hindrance and also results in lower reactivity of 4,6-DMDBT [54,56,57].

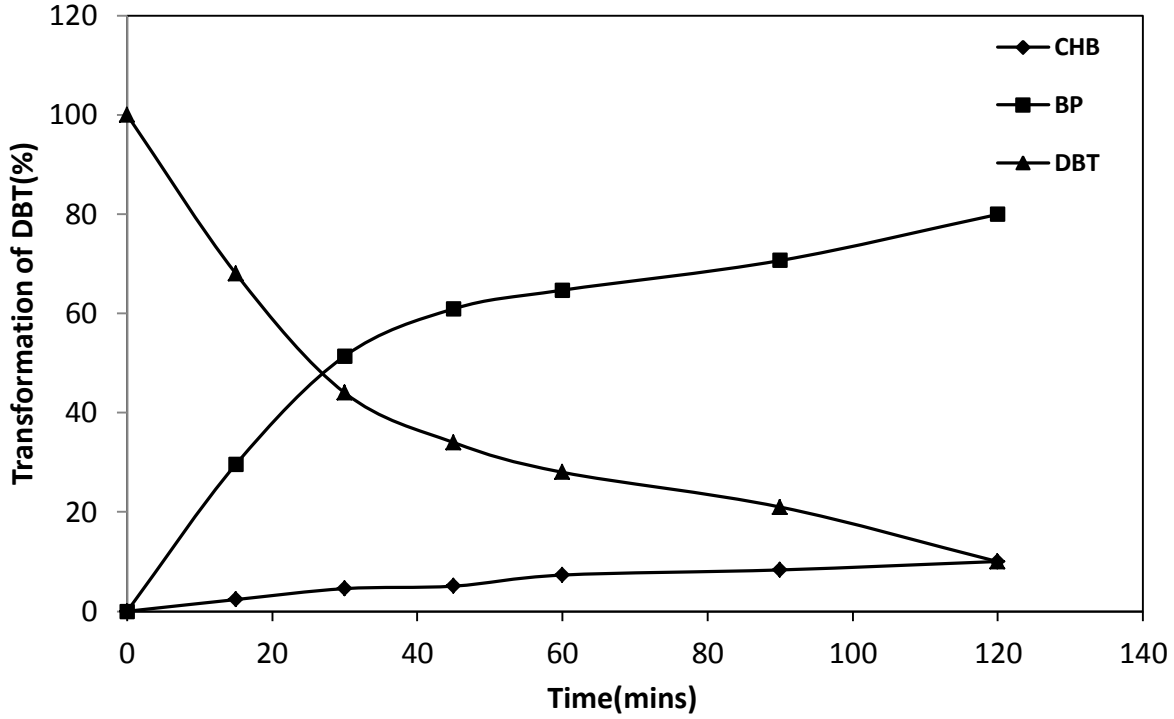

Figure 4.5.11 Transformation of DBT over CoMoP(0)/Al_2O_3 catalyst.

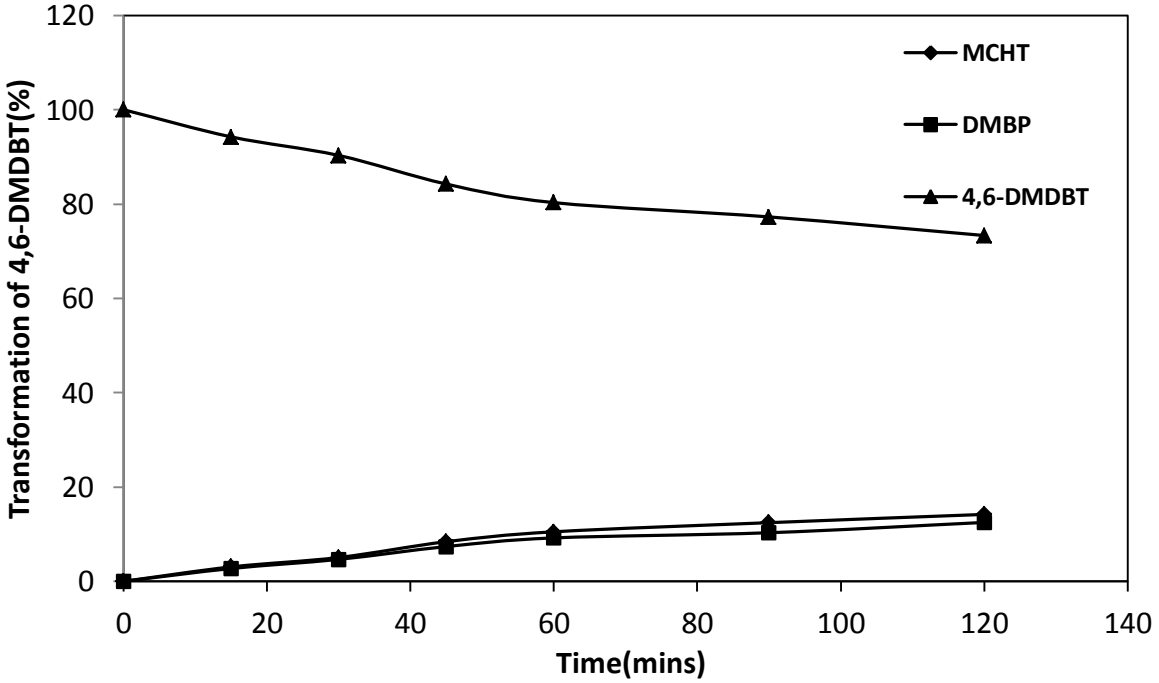

Figure 4.5.12 Transformation of 4,6-DMDBT over CoMoP (0)/Al_2O_3 catalyst.

Figure 4.5.13 shows the transformation of DBT over CoMoP(0.5)/Al_2O_3 at 350^oC a similar trend was observed as in the case of CoMoP(0)/Al_2O_3 catalysts. The conversion of DBT after 120 minutes was 94% and the conversion of biphenyl and Cyclohexyl benzene were 84.6% and 9.4% respectively. In case of 4,6-DMDBT over the same catalyst the maximum conversion was 30% and the conversion of 4,6-DMDBT into (MBP) and MCHB were 14% and 16% respectively. Figure 4.5.14 shows the transformation of 4-MDBT over CoMoP(0.5)/Al_2O_3. The product distribution over phosphorus modified catalyst was found out to be similar as in the case of unmodified catalyst the difference was increase of conversion of both refractory sulfur compounds DBT and 4-MDBT.

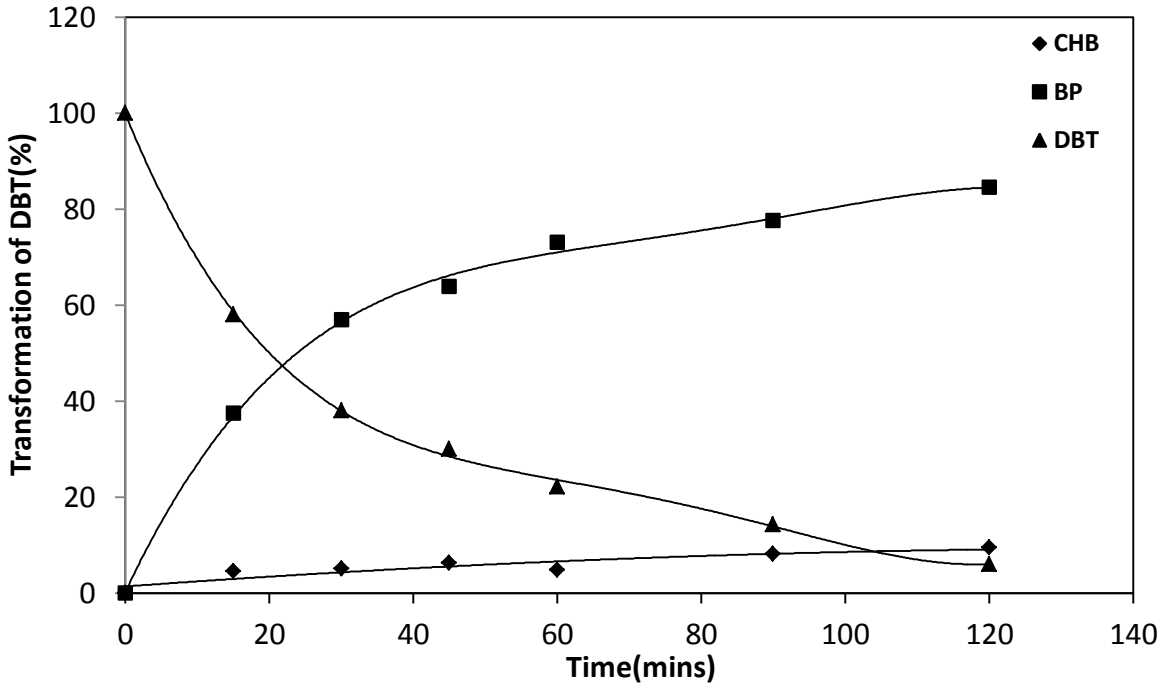

Figure 4.5.13 Transformation of DBT over CoMoP (0.5)/Al_2O_3 catalyst.

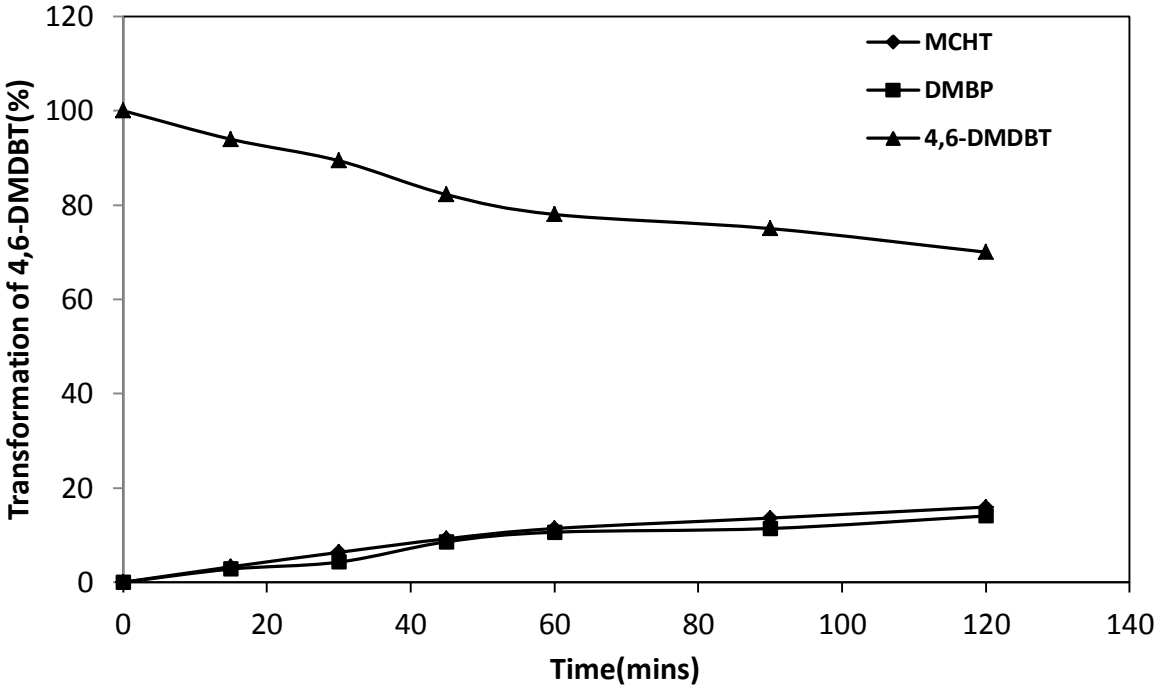

Figure 4.5.14 Transformation of 4,6-DMDBT over CoMoP (0.5)/Al_2O_3 catalyst.

Figure 4.5.15 shows the transformation of DBT over CoMoP(1)/Al_2O_3 catalyst. The conversion of DBT was higher as compared to unmodified catalyst and and phosphorus modified catalyst with P_2O_5 content of 0.5wt.%. The maximum conversion of DBT was 97.2% and the conversion of DBT into biphenyl was 85.5% and into cyclohexyl benzene were 11.3%.

The transformation of 4-MDBT into DMBP and MCHT was also found to be higher as compared to other two catalysts discussed. Figure 4.5.16 shows the transformation of 4,6DMDBT over CoMoP(1)/Al_2O_3. The maximum conversion of 4,6DMDBT were 36.4% and into DMBP and MCHT were 17% and 19.2% respectively.

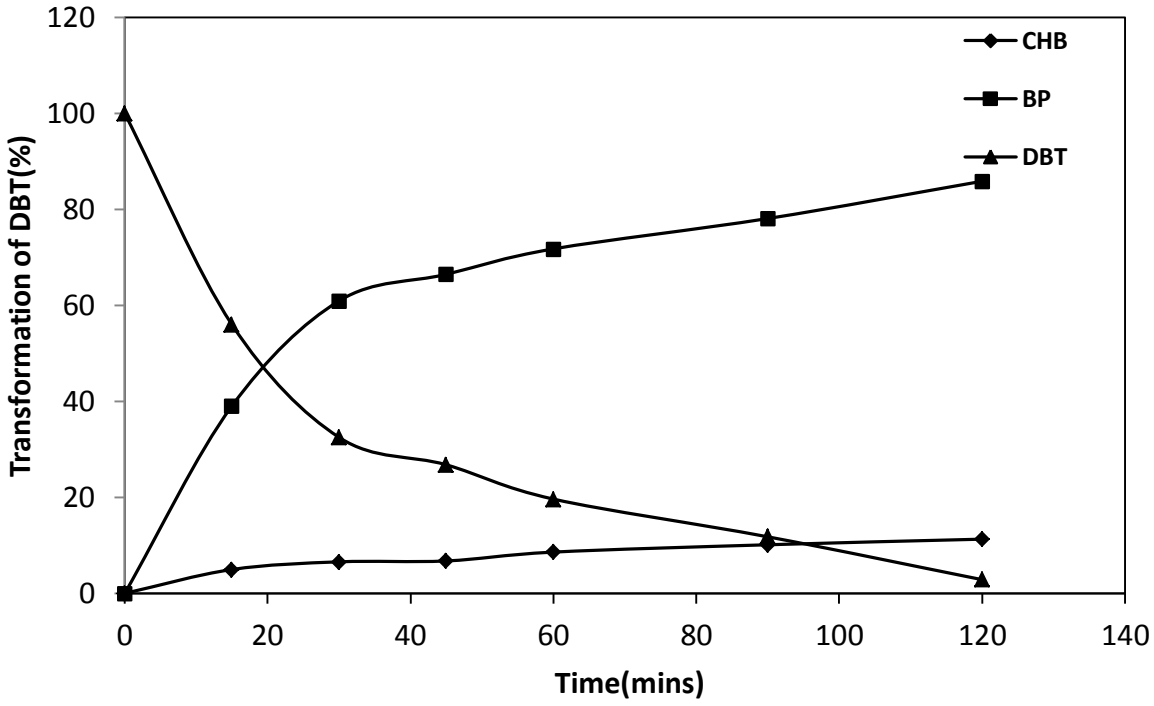

Figure 4.5.15 Transformation of DBT over CoMoP(1)/Al_2O_3 catalyst.

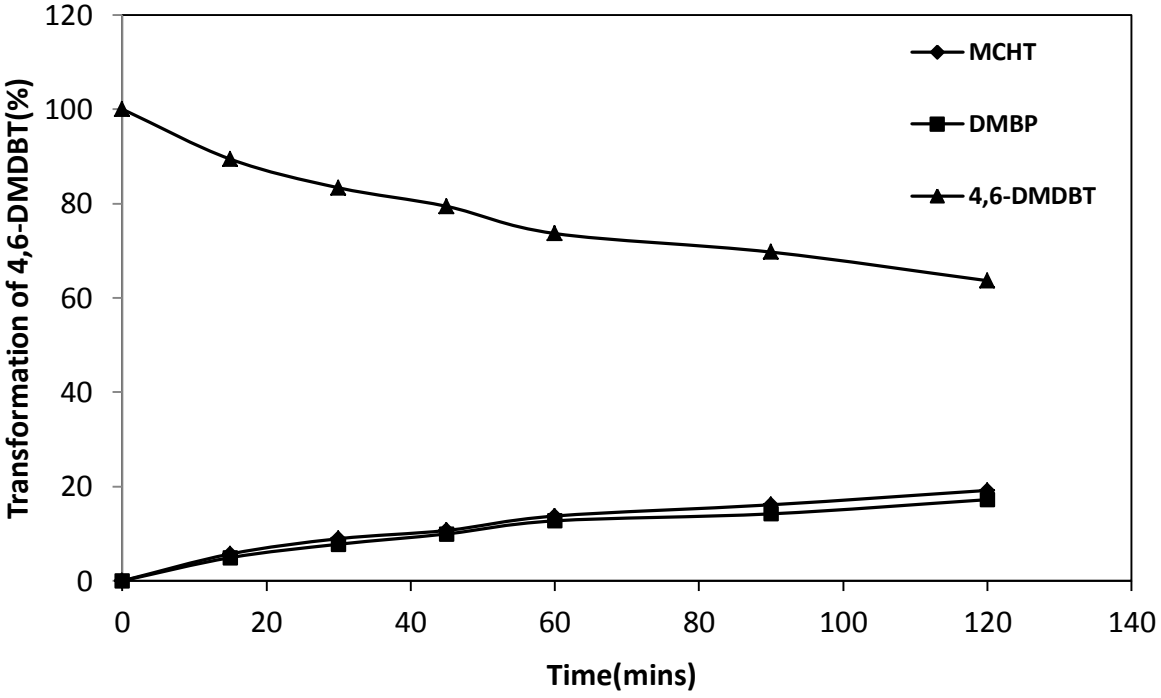

Figure 4.5.16 Transformation of 4,6-DMDBT over CoMoP(1)/Al_2O_3 catalyst.

The coversion of DBT was found to bit lower over CoMoP(1.5)/Al_2O_3 as compared to CoMo/Al_2O_3 catalyst with 0.5 and 1 wt.% P_2O_5. Figure 4.5.17 shows the transformation of DBT over CoMoP(1.5)/Al_2O_3. The maximum conversion was 86% and conversion into biphenyl and cyclohexyl benzene were 75.8% and 10.18%. These conversion were comparatively low whene compared with other phosphorus modified catalyst.

Figure 4.5.18 shows the same trend as the phosphours content of the catalyst increased to 1.5wt.% the conversion of 4,6DMDBT were 28.5% which is comparatively low. However the conversion is still higher than unmodified CoMo(1.5)/Al_2O_3 catalyst. The maximum conversion of 4,6DMDBT into DMBP and MCHT were 12.8% and 15.6% respectively.

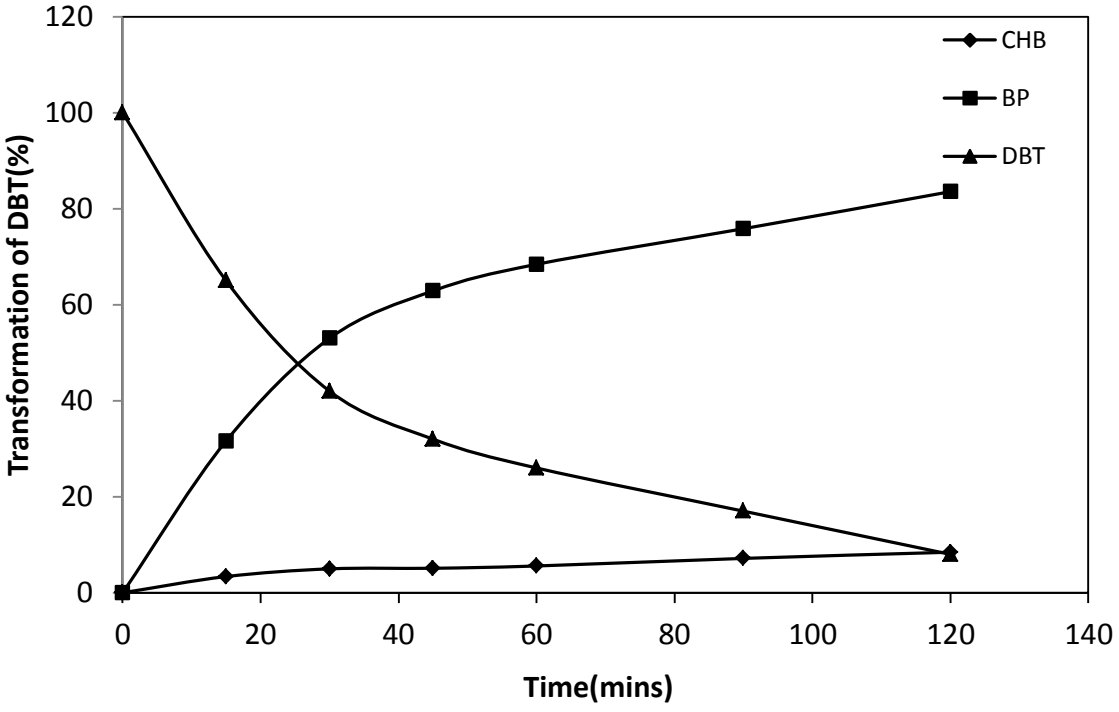

Figure 4.5.17 Transformation of DBT over CoMoP(1.5)/Al_2O_3 catalyst.

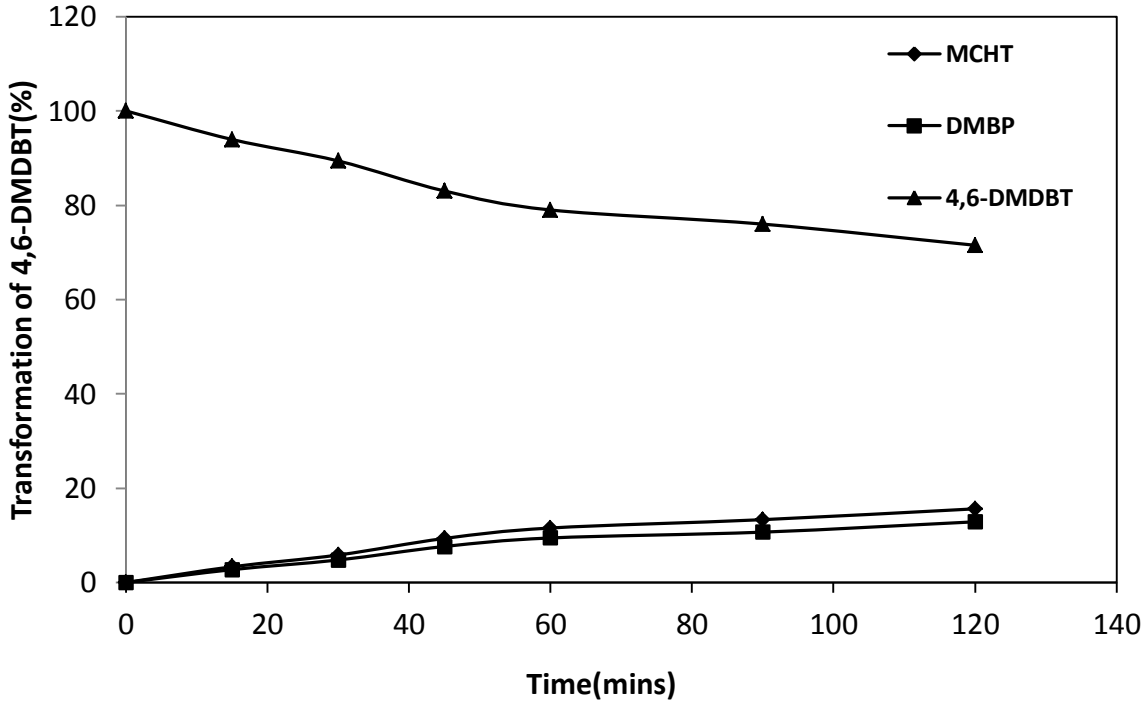

Figure 4.5.18 Transformation of 4,6-DMDBT over CoMoP(1.5)/Al_2O_3 catalyst.

4.5.3 Rate of Formation for HDS product of DBT and 4,6-DMDBT

In order to investigate the reaction pathways individual rate constant were calculated from the plot of –ln(1-X) versus time. Where X is the conversion of DBT or 4,6MDBT into biphenyl, cyclohexyl benzene, methyl cyclohexyl benzene and methyl biphenyl. Figure 4.5.19 to 4.5.26 shows the rate constants of individual products obtained during the HDS reaction.

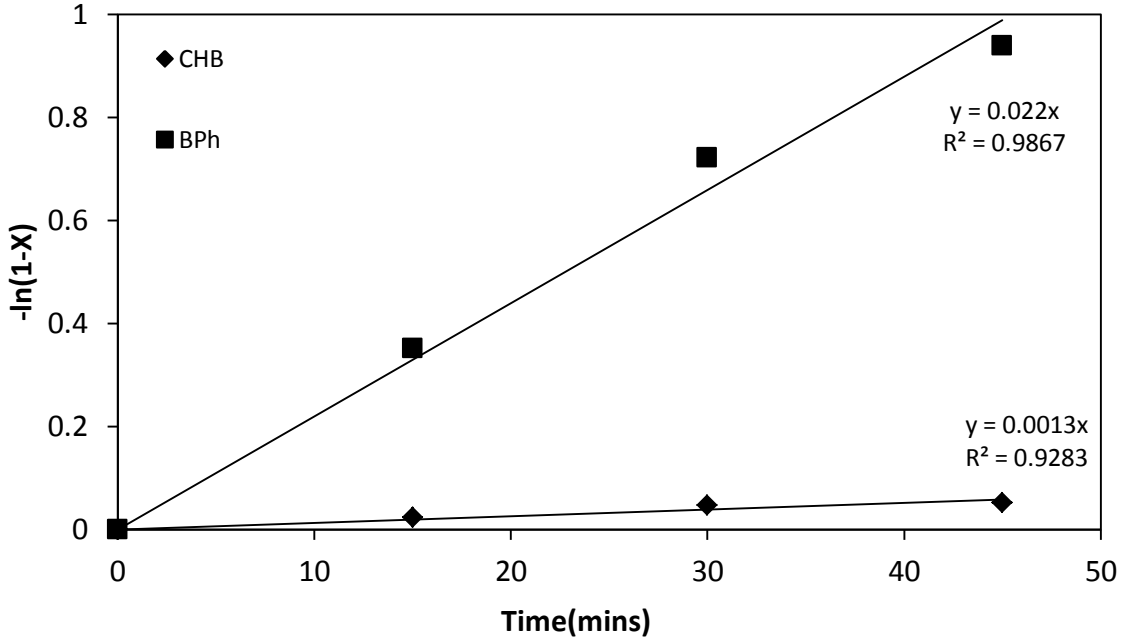

Figure 4.5.19 Formation rates of BP and CHB over CoMoP (0)/Al_2O_3 catalyst.

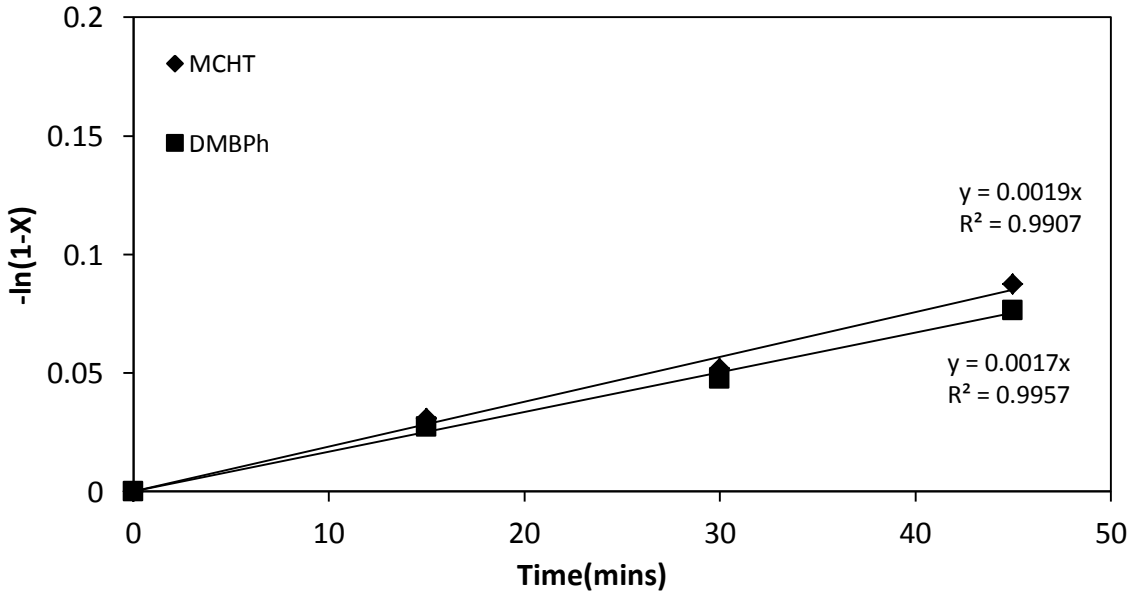

Figure 4.5.20 Formation rates of DMBP and MCHT over CoMoP(0)/Al_2O_3 catalyst.

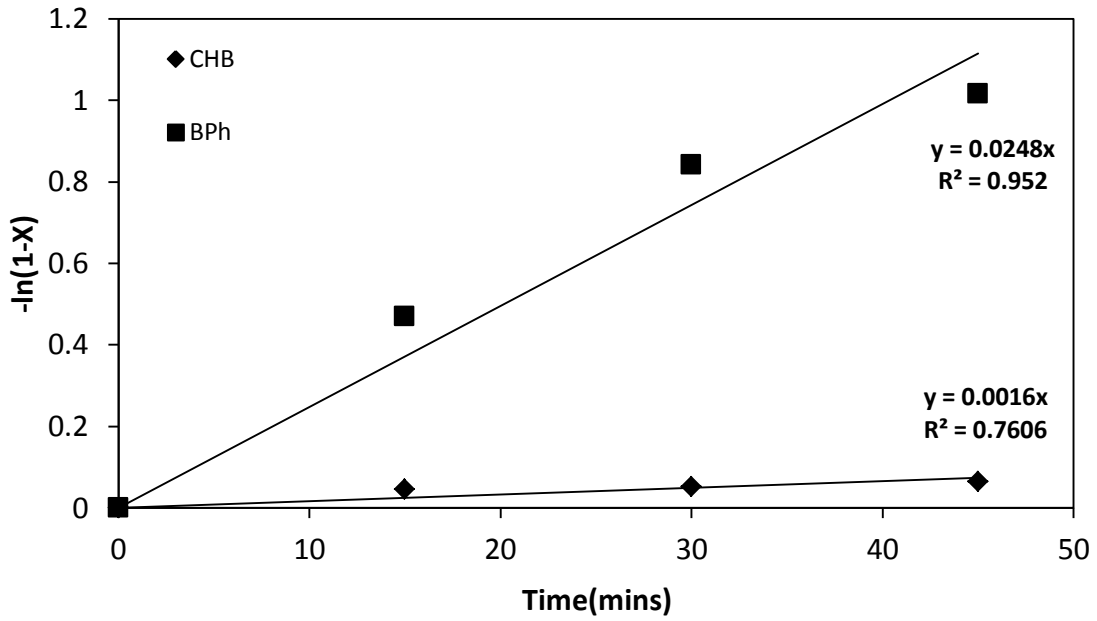

Figure 4.5.21 Formation rates of BP and CHB over CoMoP (0.5)/Al_2O_3 catalyst.

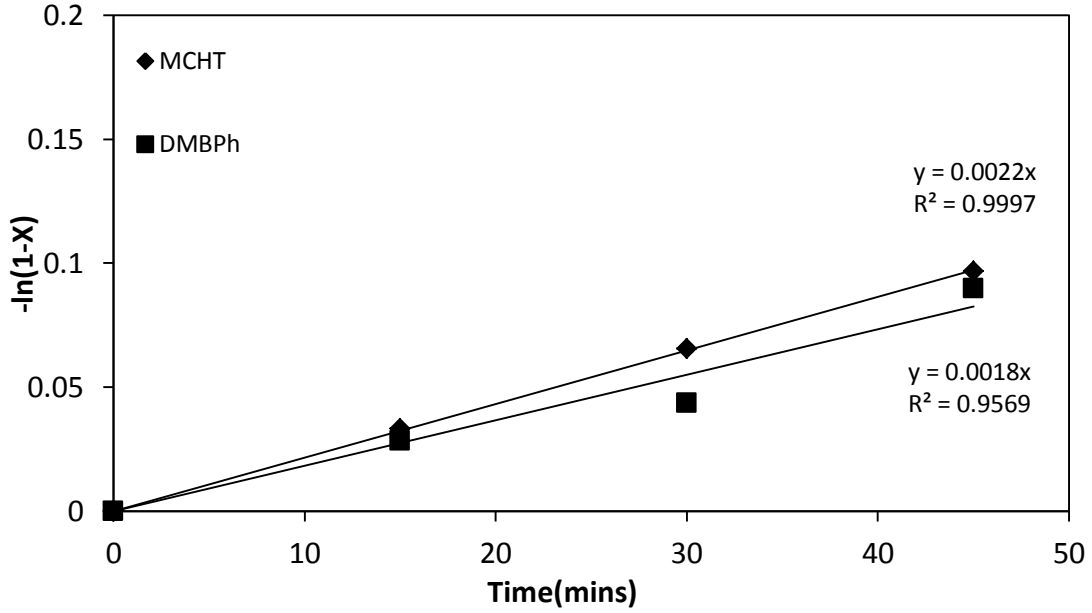

Figure 4.5.22 Formation rates of DMBP and MCHT over CoMoP(0.5)/Al_2O_3 catalyst.

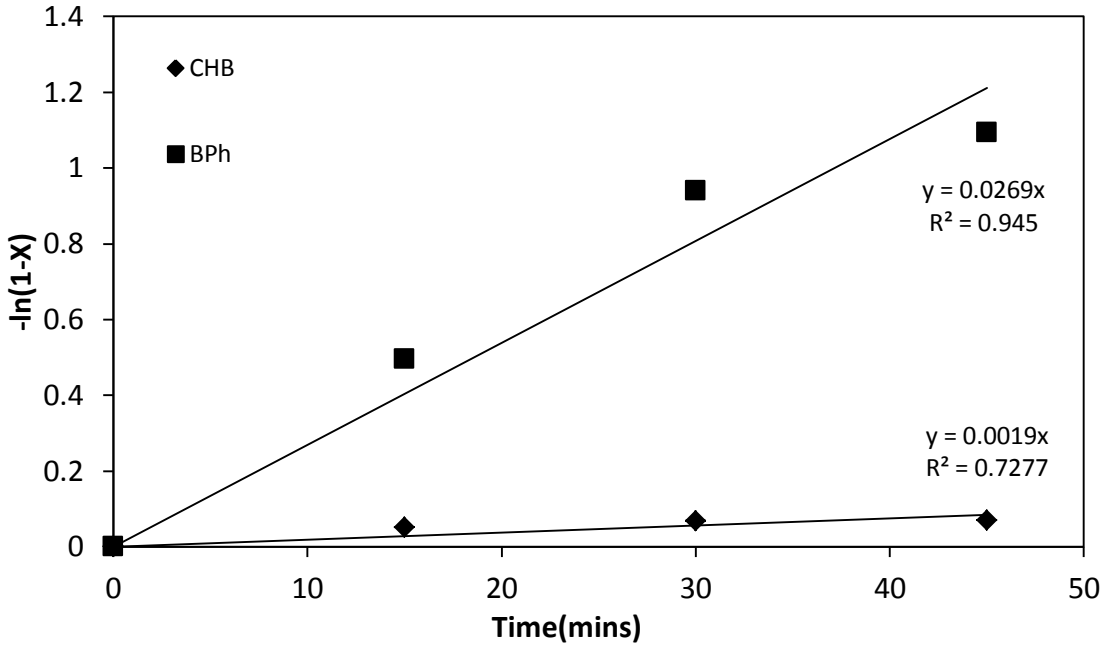

Figure 4.5.23 Formation rates of BP and CHB over CoMoP (1)/Al_2O_3 catalyst.

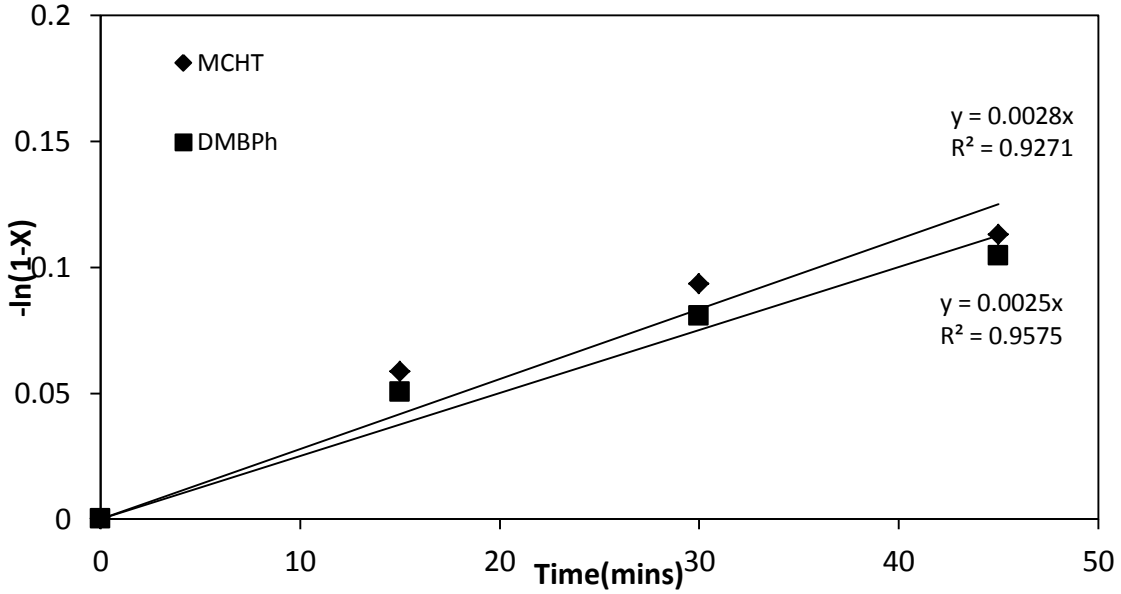

Figure 4.5.24 Formation rates of DMBP and MCHT over CoMoP(1)/Al_2O_3 catalyst.

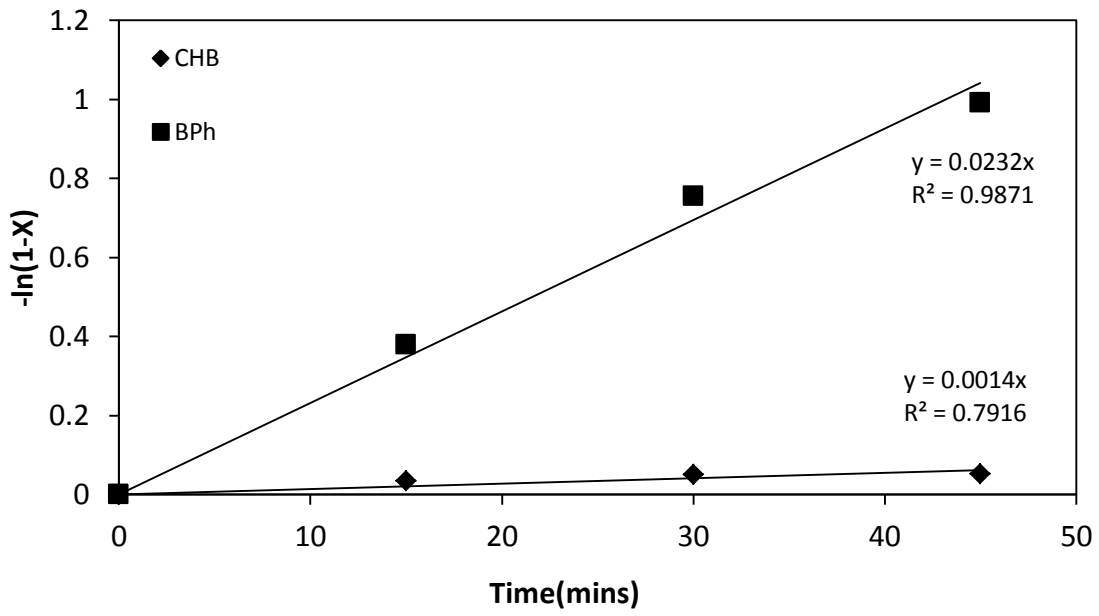

Figure 4.5.25 Formation rates of BP and CHB over CoMoP (1.5)/Al_2O_3 catalyst.

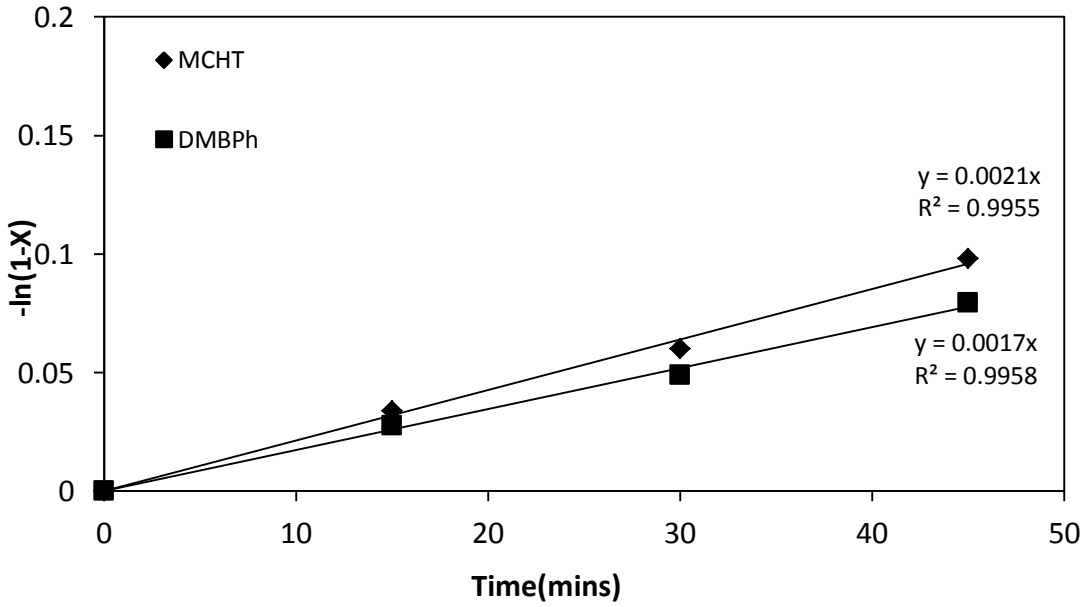

Figure 4.5.26 Formation rates of DMBP and MCHT over CoMoP (1.5)/Al_2O_3 catalyst.

The rate constants of formation of biphenyl and cyclohexyl benzene are shown in Table 4.5.6. The rate of biphenyl was increased over all phosphorus modified catalysts. This

means that phosphorus modification increased the rate of biphenyl formation. However the rate constant increases and reach to its maximum value over CoMoP(1)/Al_2O_3 catalyst and with further increase in P_2O_5 content to 1.5wt.% the rate constant start to decrease. Compared to the unmodified catalyst the rate constant over CoMoP (1.5)/Al_2O_3 was still higher. These results show that phosphorus modification increases the rate of formation of biphenyl. The formation rate constant of cyclohexyl benzene, formed during HDS of DBT. A similar trend was observed as in the case of biphenyl that the rate constant increases over all phosphorus modified catalysts. As DBT desulfurized mainly by direct desulfurization route the rate constant of cyclohexyl benzene were lower as compared to biphenyl.

Table 4.5.6 shows the k_{BP}/k_{CHB}. The ratio was found to decrease over all phosphorus modified catalysts. The k_{BP}/k_{CHB} was 16.9 over unmodified CoMoP(0)/Al_2O_3 catalyst as the P_2O_5 content increased the ratio was stating to decrease and decreased to 14.55 over CoMoP(1)/Al_2O_3 which is the minimum ratio obtained over phosphorus modified catalysts.. The trend obtained suggest that the increase in the rate of CHB is more

Table 4.5.6 Foramtion rate constants kx1000 of Biphenyl and Cyclohexyl benzene and the ratio of formation rate constants at 350°C.

Catalysts	k_{BP}	k_{CHB}	k_{BP}/k_{CHB}
CoMoP(0)/Al_2O_3	22	1.3	16.9
CoMoP(0.5)/Al_2O_3	24.8	1.6	15.5
CoMoP(1)/Al_2O_3	26.9	1.9	14.55
CoMoP(1.5)/Al_2O_3	23.2	1.4	16.5

Table 4.5.7 shows the relative rate constants with respect to CoMoP(0)/Al_2O_3. It is clear that the rate of CHB is more influenced by the phosphorus as the relative k_{BP} was found out to be lower as compared to relative k_{CHB}.

Table 4.5.7 Rate constant kx1000 and Relative rate of formation of Biphenyl and Cyclohexyl benzene.

Catalysts	k_{BP}(relative k_{BP})	k_{CHB}(relative k_{CHB})
CoMoP(0)/Al_2O_3	22(1)	1.3(1)
CoMoP(0.5)/Al_2O_3	24.8(1.127)	1.6(1.23)
CoMoP(1)/Al_2O_3	26.9(1.22)	1.9(1.46)
CoMoP(1.5)/Al_2O_3	23.2(1.054)	1.4(1.076)

The rate constants of formation of dimethyl biphenyl and methyl cyclohexyl toluene are shown in Table 4.5.8. The rate of MCHT was increased over all phosphorus modified catalysts. This means that phosphorus modification increased the rate of MCHT formation for HDS of 4,6-DMDBT. However the rate constant increases and reach to its maximum value over CoMoP(1)/Al_2O_3 catalyst and with further increase in P_2O_5 content to 1.5wt.% the rate constant start to decrease. Compared to the unmodified catalyst the rate constant over CoMoP (1.5)/Al_2O_3 was still higher. The rate of formation of DMBP was lower than MCHT over all catalysts as the HDS of 4,6-DMDBT desulfurized predominantly by hydrogenation route to yield MCHT.

Table 4.5.8 Foramtion rate constants kx1000 of Dimethyl biphenyl and Cyclohexyl benzene and the ratio of formation rate constants at 350°C.

Catalysts	k_{DMBP}	k_{MCHT}	k_{DMBP}/k_{MCHT}
CoMoP(0)/Al_2O_3	1.7	1.9	0.86
CoMoP(0.5)/Al_2O_3	1.8	2.2	0.86
CoMoP(1)/Al_2O_3	2.5	2.8	0.89
CoMoP(1.5)/Al_2O_3	1.7	2.1	0.80

4.6 Comparison of CoMoP(0.5)/Al_2O_3 and NiMo(0.5)/Al_2O_3 in simultaneous HDS of DBT and 4-MDBT.

In this section CoMoP(0.5)/Al_2O_3 and NiMoP(0.5)/Al_2O_3 catalysts will be compared. Both catalysts have the same metal oxide MoO_3 concentration of 15wt.% and the promoter content of 4wt.% and the phosphorus content in both catalyst were 0.5wt.% P_2O_5 Table 4.6.1 shows the composition of both catalysts. The kinetics of DBT + 4-MDBT and DBT + 4,6-DMDBT over CoMoP(0.5)/Al_2O_3 have already been discussed in previous sections 4.4 and 4.5.

In this section Kinetics for simultaneous HDS of DBT + 4-MDBT and DBT + 4,6-DMDBT over NiMoP(0.5)Al_2O_3 will be discussed and compared with its counterpart CoMoP(0.5)/Al_2O_3 catalyst.

Table 4.6.1 Composition of Catalysts.

Catalysts	MoO(wt.%)	CoO(wt %)	NiO(wt %)	P_2O_5(wt %)
CoMoP(0.5)/Al_2O_3	15	4	0	0.5
NiMoP(0.5)/Al_2O_3	15	0	4	0.5

Figure 4.6.1 shows the HDS of DBT and 4-MDBT over NiMoP(0.5)/Al_2O_3 at three different temperatures 300°C, 325°C and 350°C. The maximum conversion at 350°C for DBT and 4- MDBT was 79% and 48% respectively. On other hand at these same reaction conditions the conversion of DBT and 4-MDBT were 76% and 41% respectively.

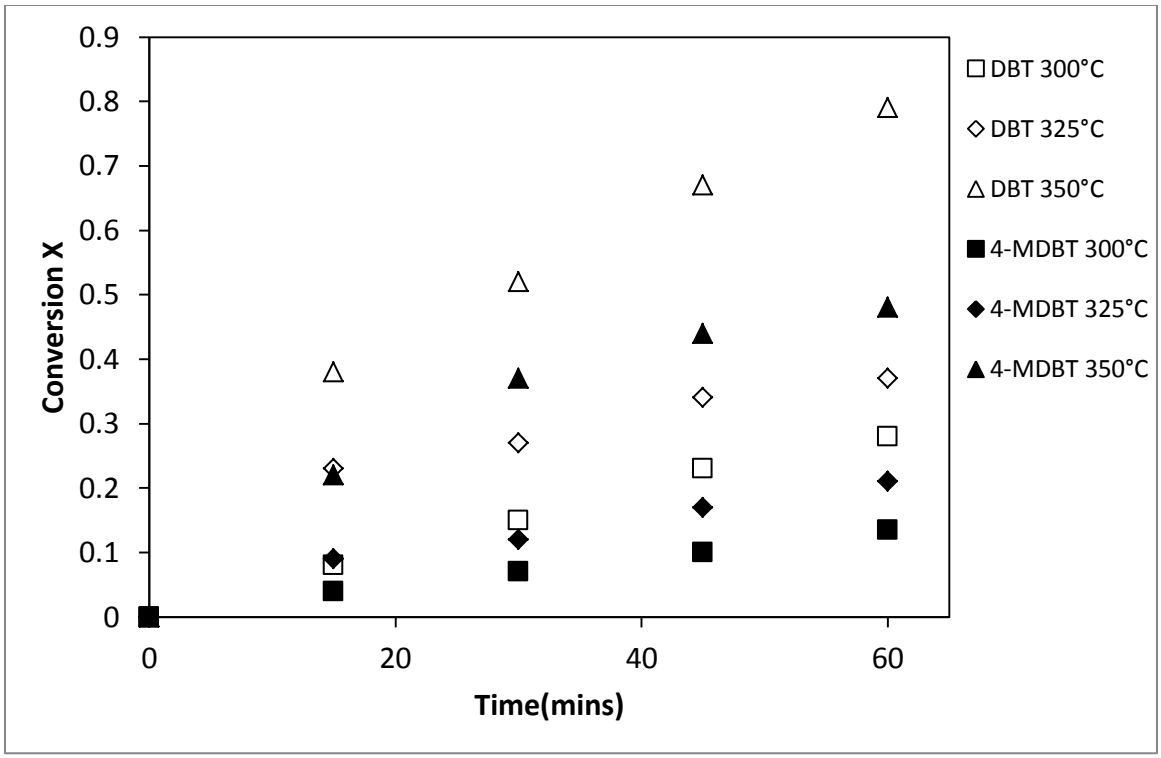

Figure 4.6.1 Conversion of DBT and 4-MDBT in Competitive reaction over NiMoP(0.5)/Al_2O_3.

Table 4.6.2 shows the sulfur content remaining in the reaction mixture at different temperatures. In 60 minutes at 350°C DBT was almost desulfurized and only 85ppm of sulfur corresponding to DBT left in the reaction mixture whereas the desulfurization of 4-MDBT was also higher compared to other catalysts.

Table 4.6.2 Sulfur remaining in the reaction mixture over NiMoP(0.5)/Al_2O_3 catalyst.

	300°C			325°C			350°C		
Time	DBT	4-MDBT	Total Sulfur	DBT	4-MDBT	Total Sulfur	DBT	4-MDBT	Total Sulfur
0	500	500	1000	500	500	1000	500	500	1000
15	460	480	940	385	455	840	310	390	700
30	425	465	890	365	440	805	240	315	555
45	385	450	835	330	415	745	165	280	445
60	360	433	933	315	395	710	85	260	345

The rate constant of for the desulfruization of DBT and 4-MDBT were calculated by first order plot. Figure 4.6.2 shows the plot of –ln(1-X) vs the reaction time.

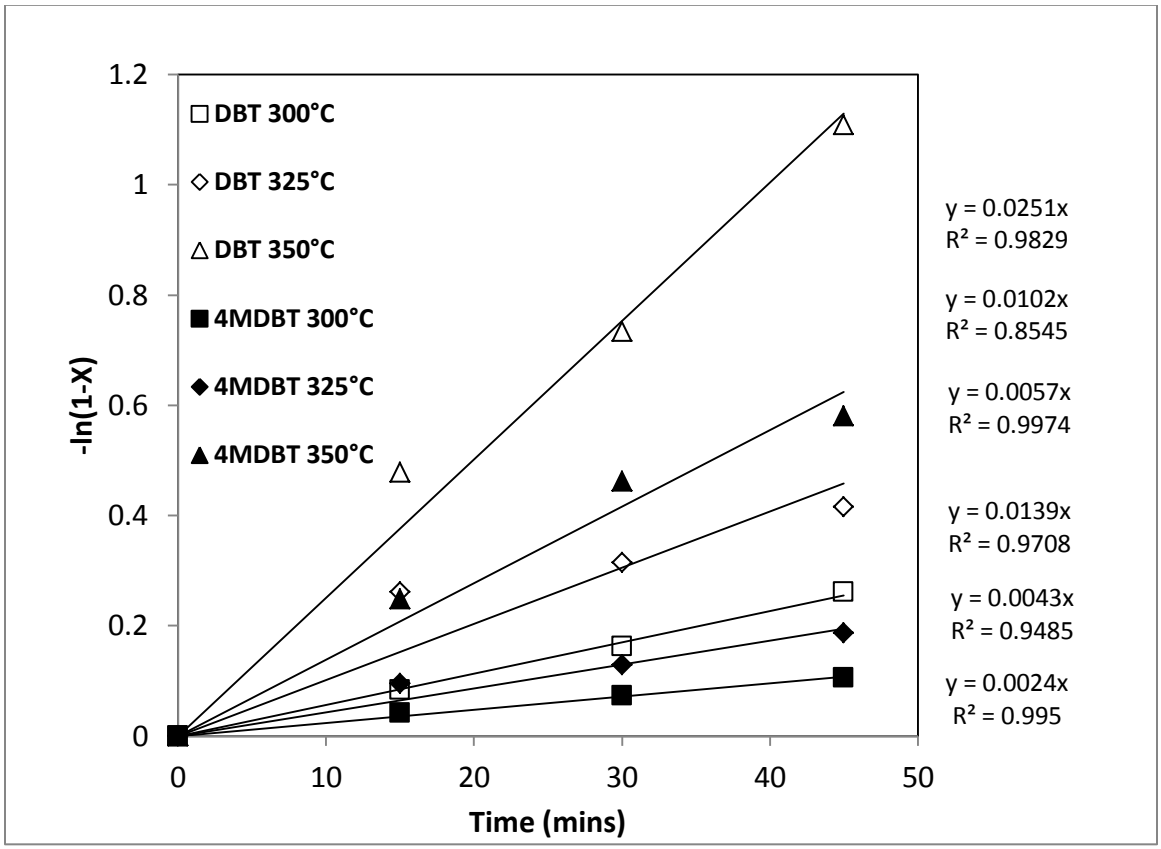

Figure 4.6.2 Rate constant of DBT and 4-MDBT at different temperature sover NiMoP(0.5)/Al_2O_3.

The rate constant at various temperatures are presented in Table 4.6.3. and 4.6.4 and the rate constants over CoMoP(0)/Al_2O_3 were also presented to compare both catalysts.

Table 4.6.3 Reaction rate constants kx1000 (min^{-1}) of dibenzothiophene over different catalysts.

Temperature	CoMoP(0)/Al_2O_3	CoMoP(0.5)/Al_2O_3	NiMoP(0.5)/Al_2O_3
	k_{DBT} x 1000		
300°C	3.8	4.6	5.7
325°C	6	6.6	10.2
350°C	18.3	21.6	25.1

Table 4.6.4 Reaction rate constants kx1000 (min^{-1}) of 4 methyl dibenzothiophene over different catalysts.

Temperature	$CoMoP(0)/Al_2O_3$	$CoMoP(0.5)/Al_2O_3$	$NiMoP(0.5)/Al_2O_3$
	$k_{4\text{-}MDBT}$		
300°C	1.3	1.8	2.4
325°C	2.6	3.2	4.4
350°C	9.4	10.8	13.9

Both catalyst showed higher rate constant as compared to unmodified $CoMoP(0)/Al_2O_3$ catalyst. However the rate constants for DBT and 4-MDBT were higher over $NiMoP(0.5)/Al_2O_3$ catalyst. The rate constant of DBT over $NiMoP(0.5)/Al_2O_3$ was 16.2% higher and for 4-MDBT it was 28.7% higher.

Table 4.6.5 shows the ratio of k_{DBT} to $k_{4\text{-}MDBT}$. The ratio of rate constant of DBT and 4-MDBT were calculated to see the competition in HDS. The ratio was found to decrease as the temperature increase suggesting that at higher temperatures the HDS of 4-MDBT was more favored. The ratio at 350°C over $NiMoP(0.5)/Al_2O_3$ was 1.81 and for $CoMo(0.5)/Al_2O_3$ it was 2 from this it can be infer that the HDS of 4-MDBT were higher over $NiMoP(0.5)/Al_2O_3$ as compared to $CoMo(0.5)/Al_2O_3$. These results also shows that the desulfurization rate of 4-MDBT were 2 times slower than DBT.

Table 4.6.5 $k_{DBT}/k_{4\text{-}MDBT}$ ratio at two different temperatures.

Temperature	$CoMoP(0)/Al_2O_3$	$CoMoP(0.5)/Al_2O_3$	$NiMoP(0.5)/Al_2O_3$
	$k_{DBT}/k_{4\text{-}MDBT}$		
300°C	2.92	2.56	2.38
325°C	2.31	2.06	2.37
350°C	1.95	2.0	1.81

4.6.1 Reaction pathways of DBT and 4-MDBT over NiMoP (0.5)/Al_2O_3

As discussed in the previous sections 4.4 and 4.5, that DBTs desulfurized via two parallel pathways yielding Biphenyls and cyclohexyl benzene. In case of NiMo/Al_2O_3 the two desulfurization products also formed but the conversion of DBTs into Cyclohexyl benzenes were higher as compared to unmodified and modified CoMo/Al_2O_3 catalysts.

The conversion of DBT over NiMoP(0.5)/Al_2O_3 were 96% at 350°C and the conversion into biphenyl and cyclohexyl benzene were 74.2% and 20.4% respectively as shown in Figure 4.6.3. At these same conditions the conversion for DBT over CoMoP(0.5)/Al_2O_3 were 85.7% and biphenyl and cyclohexyl benzene formation was 75.8% and 9.9%. The formation of CHB over NiMoP(0.5)/Al_2O_3 was more than 2 times higher as compared to CoMoP(0.5)/Al_2O_3.This means that NiMoP(0.5)/Al_2O_3 has higher capability of hydrogenation.

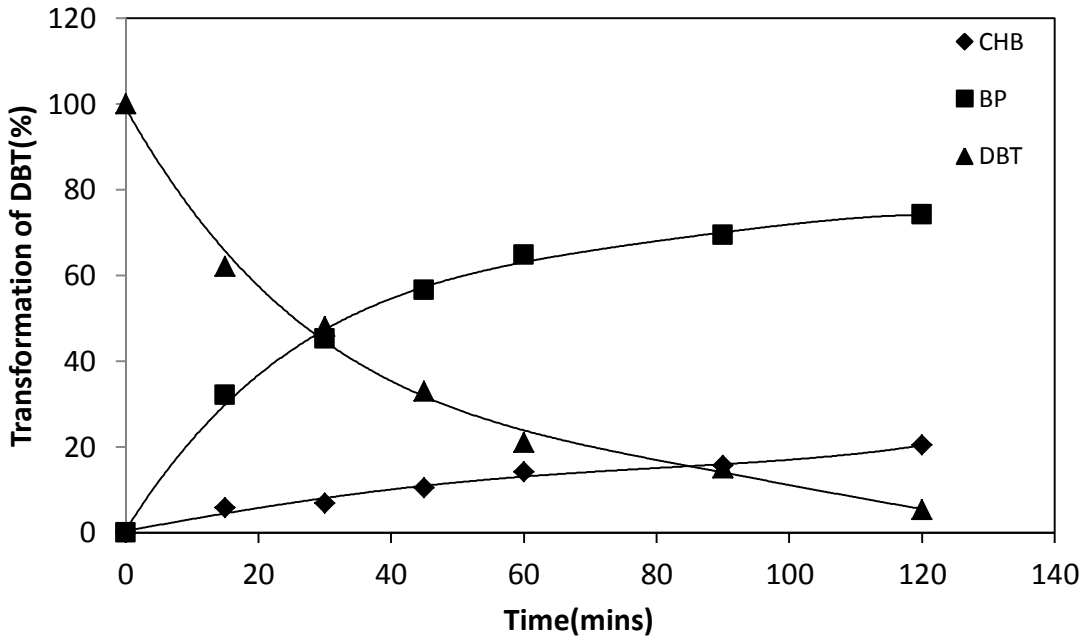

Figure 4.6.3 Transformation of DBT over NiMoP (0.5)/Al_2O_3 catalyst.

The HDS of 4-MDBT over NiMoP(0.5)/Al_2O_3 results in methyl biphenyl and methyl cyclohexyl benzene product of direct desulfurization and hydrogenation respectively. The maximum conversion of 4-MDBT was 63% and into MBP and MCHB were 37.2% and 20.9% as shown in Figure 4.6.4. Over these same reaction conditions the conversion for 4-MDBT over CoMoP(0.5)/Al_2O_3 were 51.3% and biphenyl and cyclohexyl benzene formation was 42.7% and 8.7%. This is the similar result as we get in HDS of DBT as the production of MCHB over NiMoP(0.5)/Al_2O_3 was about more than 2 times as compared to MCHB formation over CoMo(0)/Al_2O_3.

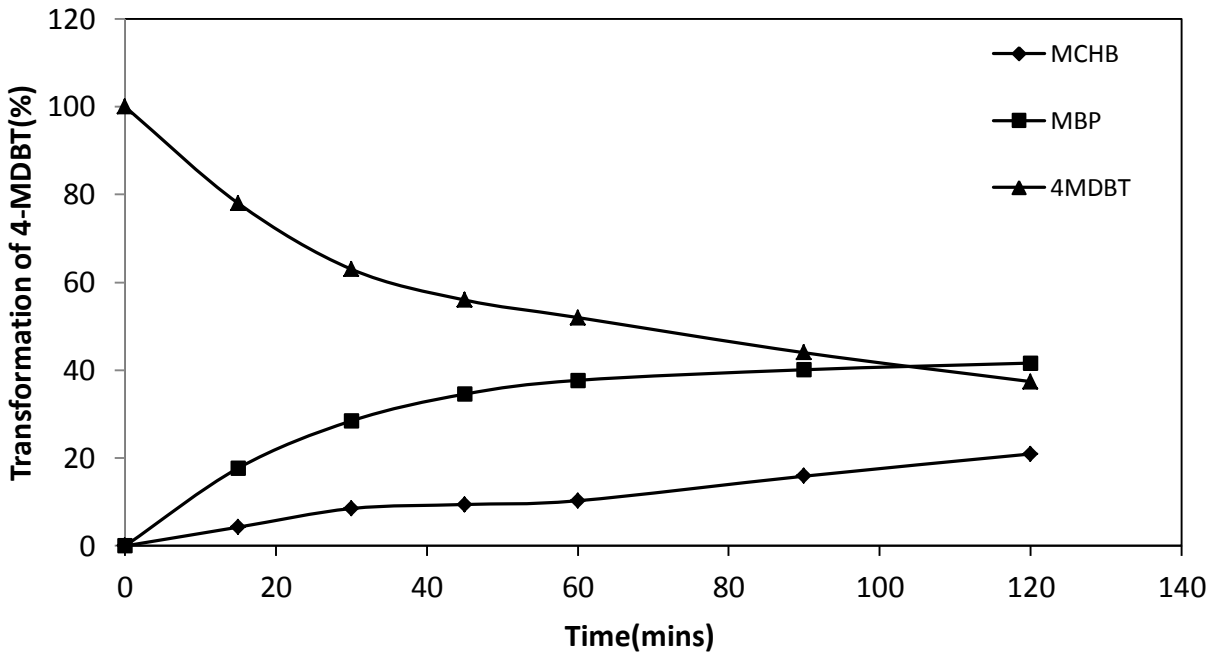

Figure 4.6.4 Transformation of 4-MDBT over NiMoP(0.5)/Al_2O_3 catalyst.

4.6.2 Rate of Formation for HDS product of DBT and 4-MDBT

In order to investigate the reaction pathways individual rate constant were calculated from the plot of –ln(1-X) versus time. Where X is the conversion of DBT or 4-MDBT into biphenyl, cyclohexyl benzene, methyl cyclohexyl benzene and methyl biphenyl. Figure 4.6.5 and Figure 4.6.6 shows the rate constants of individual products obtained during the HDS reaction.

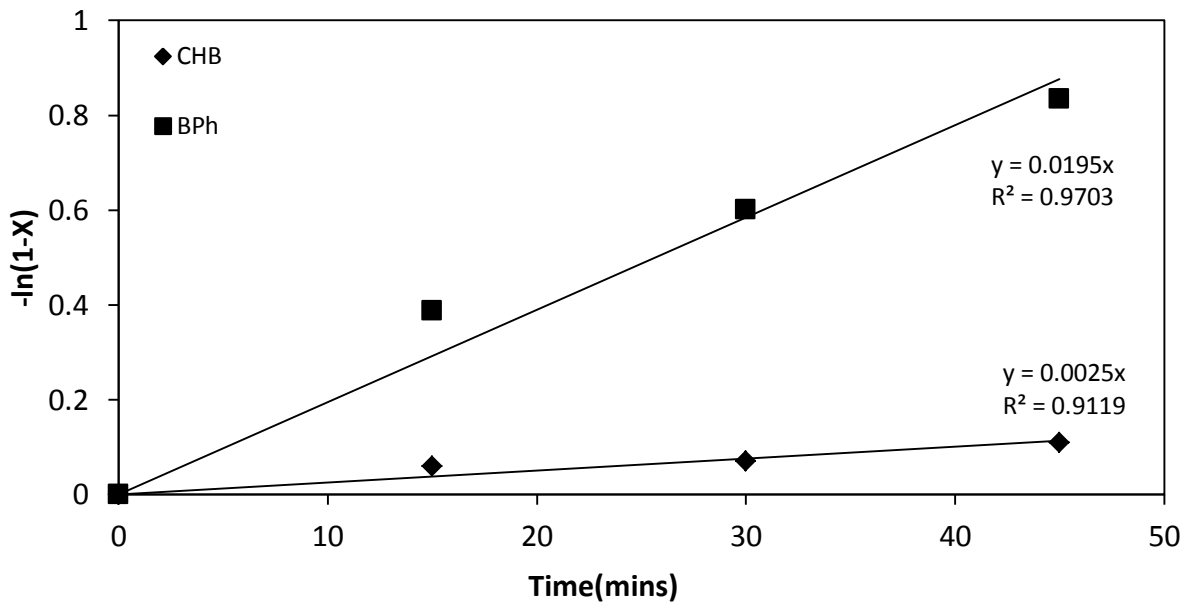

Figure 4.6.5 Formation rates of BP and CHB over NiMoP (0.5)/Al_2O_3 catalyst

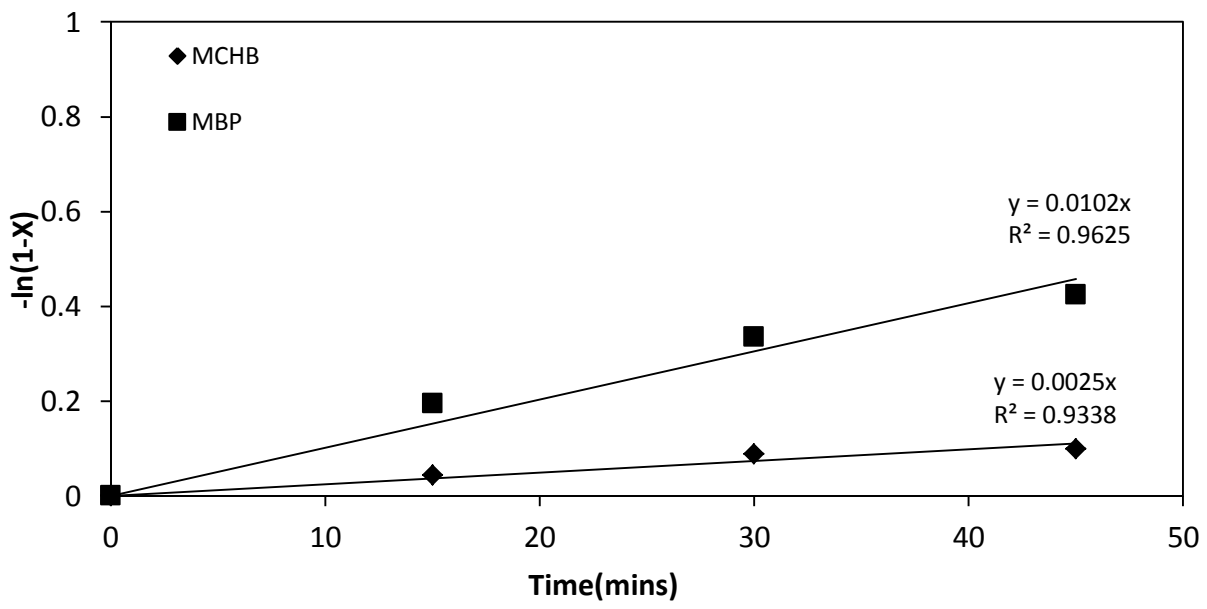

Figure 4.6.6 Formation rates of BP and CHB over NiMoP (0.5)/Al_2O_3 catalyst

The rate constants of formation of biphenyl are shown in table 4.6.6. The rate of formation of BP was found to be influenced by the temperature over all catalysts. The

rate increases with the increase in the temperature. The rate constant increases 3 to 4 time as the reaction was performed from 300°C to 350°C. The rate of formation of biphenyl over NiMoP(0.5)/Al_2O_3 was found to be higher over, all temperature as compared to CoMoP(0.5)/Al_2O_3.

Table.4.6.6 Formation rate constant kx1000 (min^{-1}) of biphenyl at different temperatures.

Temperature	CoMoP(0)/Al_2O_3	CoMoP(0.5)/Al_2O_3	NiMoP(0.5)/Al_2O_3
	k_{BP} x 1000		
300°C	3.4	4.4	4.8
325°C	5.5	6	8.5
350°C	15.7	18.6	19.5

Table 4.6.7 shows the formation rate constant of cyclohexyl benzene formed during HDS of DBT. The rate of formation of CHB was also influenced by the temperature and it increased to 3 to 4 times at 350°C. The rate of formation of CHB over NiMoP(0.5)/Al_2O_3 was found out to be 1.8 times higher than the rate of CHB over CoMoP(0.5)/Al_2O_3.

Table.4.6.7 Formation rate constant of kx1000 (min^{-1}) Cyclohexyl benzene at different temperatures.

Temperature	CoMoP(0)/Al_2O_3	CoMoP(0.5)/Al_2O_3	NiMoP(0.5)/Al_2O_3
	k_{CHB}		
300°C	0.3	0.4	0.7
325°C	0.5	0.5	1.2
350°C	1.4	1.4	2.5

Table 4.6.8 shows the k_{BP}/k_{CHB}. The ratio of k_{BP}/k_{CHB} for NiMoP (0.5)/Al_2O_3 was found to be lower as compared to CoMoP(0.5)/Al_2O_3 this shows that the hydrogenation activity over was higher for the former catalyst.

Table.4.6.8 k_{BP}/k_{CHB} ratio at two different temperatures

Temperature	CoMoP(0)/Al_2O_3	CoMoP(0.5)/Al_2O_3	NiMoP(0.5)/Al_2O_3
	k_{BP}/k_{CHB}		
325°C	11.0	12.0	7.08
350°C	11.21	13.29	7.8

The HDS of 4-MDBT results in MBP and MCHB, the formation rate constant are presented in Table 4.6.9 and 4.6.10. The rate of formation of MBP and MCHB was higher over NiMoP(0.5)/Al_2O_3 as compared to CoMo(0.5)/Al_2O_3. The rate of MCHB over NiMoP(0.5)/Al_2O_3 was 92% higher as compared to CoMoP(0.5)/Al_2O_3.

Table.4.6.9 Formation rate constant of kx1000 (min^{-1}) methyl biphenyl benzene at different temperatures.

Temperature	CoMoP(0)/Al_2O_3	CoMoP(0.5)/Al_2O_3	NiMoP(0.5)/Al_2O_3
	k_{MBP}		
300°C	1.1	1.6	1.7
325°C	2.1	2.6	3.2
350°C	7.6	8.9	10.2

Table.4.6.10 Formation rate constant of kx1000 (min^{-1}) methyl cyclohexyl benzene at different temperatures.

Temperature	CoMoP(0)/Al_2O_3	CoMoP(0.5)/Al_2O_3	NiMoP(0.5)/Al_2O_3
	k_{MCHT}		
300°C	0.2	0.2	0.7
325°C	0.5	0.5	1
350°C	1.3	1.3	2.5

The ratio of rate of formation of MBP to rate of MCHB is summarized in Table 4.6.11. The ratio was lower over NiMoP(0.5)/Al_2O_3 as compared to CoMoP(0.5)/Al_2O_3. This means that for 4-MDBT HDS over NiMoP(0.5)/Al_2O_3 the hydrogenation pathway is higher as compared to CoMoP(0.5)/Al_2O_3.

Table.4.6.11 k_{MBP}/k_{MCHB} ratio at two different temperatures.

Temperature	CoMoP(0)/Al_2O_3	CoMoP(0.5)/Al_2O_3	NiMoP(0.5)/Al_2O_3
	k_{MBP}/k_{MCHB}		
325°C	4.4	5.2	3.2
350°C	5.85	6.85	4.08

4.7 Comparison of CoMoP (0.5)/Al_2O_3 and NiMo (0.5)/Al_2O_3 in simultaneous HDS of DBT and 4,6-DMDBT

Figure 4.7.1 shows the HDS of DBT and 4-MDBT in a competitive reaction over Phosphorus modified NiMoP(0.5)/Al_2O_3. The conversion of DBT and 4,6-DMDBT was 98% and 41.2% respectively at 350°C after the reaction time of 120mins. At these same conditions the conversion of DBT and 4,6-DMDBT were 94% and 30% respectively for CoMoP(0.5)/Al_2O_3. For DBT there was not much difference in conversion but for 4,6-DMDBT NiMoP(0.5)/Al_2O_3 showed higher activity.

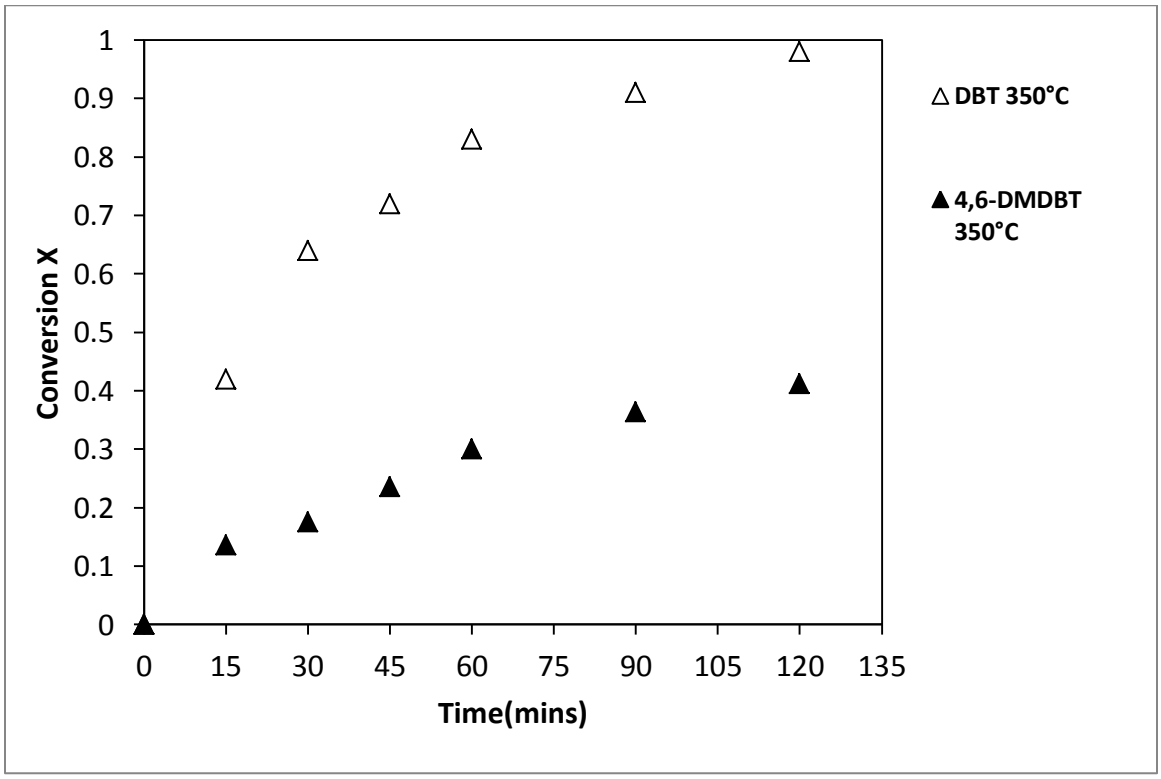

Figure 4.7.1 Conversion of DBT and 4,6-DMDBT in Competitive reaction over NiMoP(0.5)/Al_2O_3.

Table 4.7.1 Sulfur (ppm) remaining in the reaction mixture over NiMoP(0.5)/Al_2O_3 catalyst.

Time(mins)	DBT	4,6-DMDBT	Total Sulfur
0	500	500	1000
15	290	432	722
30	180	412	592
45	140	382	522
60	85	350	435
90	45	318	363
120	10	294	304

As NiMoP(0.5)/Al_2O_3 shows the maximum conversion the sulfur content due to 4,6-DMDBT reduced to 294ppm which means that NiMoP(0.5)/Al_2O_3 showed higher activity as compared to all CoMo/Al_2O_3 catalysts.

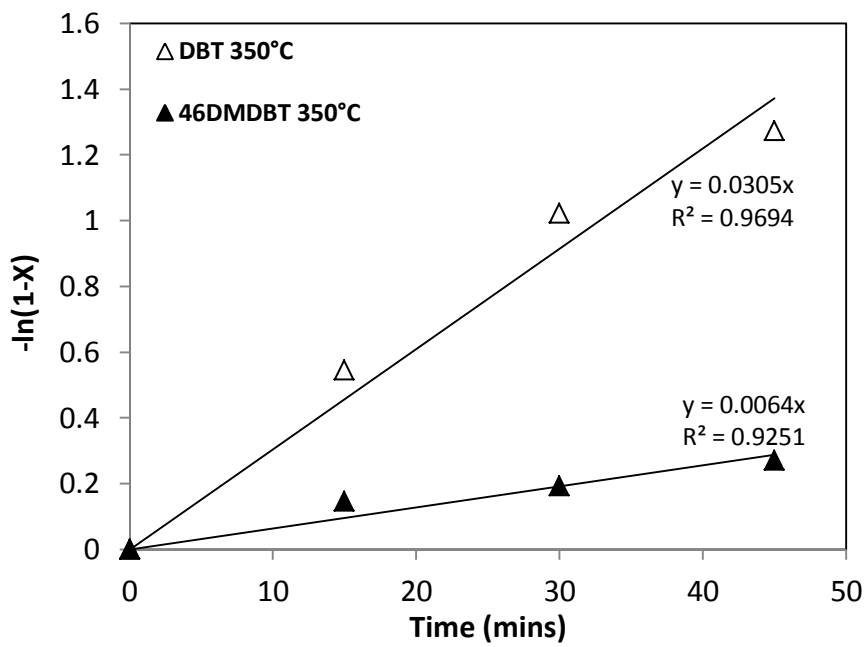

Figure 4.7.2 Rate constant of DBT and 4,6-DMDBT over NiMoP(0.5)/Al_2O_3.

The rate constant of for the desulfruization of DBT and 4,6-MDBT were calculated by first order plot. Figure 4.7.2 shows the plot of –ln(1-X) vs reaction time for HDS reaction at 350°C over NiMoP(0.5)/Al_2O_3. The rate constants are presented in Table 4.7.2 along with the rate constants of HDS of DBT and 4,6-DMDBT over CoMo(0.5)/Al_2O_3 . Table 4.7.2 shows the ratio of k_{DBT} to $k_{4,6\text{-}DMDBT}$. The $k_{DBT}/k_{4,6\text{-}DMDBT}$ shows the relative reactivity of DBT and 4,6-DMDBT in a competitive reaction. There was not much difference for the rate constant of DBT over these catalyst but for 4,6-DMDBT the difference was quite obvious. The ratio of rate constant of DBT to rate constant of 4,6-DMDBT over CoMoP(0.5)/Al_2O_3 and NiMoP(0.5)/Al_2O_3 were 6.90 and 4.76 respectively which means that the rate of HDS of 4,6-DMDBT over CoMoP(0.5)/Al_2O_3 were about 7 times lower and on NiMoP(0.5)/Al_2O_3 it was about 5 times lower.

Table 4.7.2 rate constants kx1000 of DBT and 4-MDBT over different catalysts at 350°C.

Catalysts	DBT	4,6-DMDBT	$k_{DBT}/k_{4,6\text{-}DMDBT}$
CoMoP(0)/Al_2O_3	25.1	3.7	6.78
CoMoP(0.5)/Al_2O_3	29	4.5	6.90
NiMoP(0.5)/Al_2O_3	30.5	6.4	4.76

4.7.1 Reaction Pathways for DBT and 4,6-DMDBT over NiMoP(0.5)/Al_2O_3.

The HDS of DBT results in two main products biphenyl and cyclohexyl benzene. This result indicates that DBT HDS has occurred through both direct desulfurization (DDS) and hydrogenation (HYD) pathways. The HDS of 4,6-DMDBT results also results in two main products dimethyl biphenyl (DMBP) which is formed by direct desulfurization route and methyl cyclohexyl toluene (MCHT) obtained from hydrogenation pathway

route. Figure 4.7.3 and Figure 4.7.4 presents the product distribution during HDS of DBT and 4,6-DMDBT over a series of catalyst at 350°C. With the increase in reaction time, DBT and 4,6-DMDBT concentration reduced while BPs (product of hydrogenolysis) and CHBs (product of hydrogenation) contents increased.

Figure 4.7.3 presents the product distribution of HDS of DBT over NiMoP(0.5)/Al_2O_3 at 350°C for the reaction time of 120mins. The conversion of DBT was 98% and the conversion of DBT into biphenyl and cyclohexyl benzene were 81.8% and 16.17% respecively. Where as the conversion of DBT, biphenyl and cyclohexyl benzene were 94%. 84.5% and 9.4% respectively over CoMoP(0.5)/Al_2O_3. If we compare both catalysts the formation of biphenyl was lesser for NiMoP(0.5)/Al_2O_3 but the cyclohexyl benzene formation i.e hydrogenation pathway is higher than CoMoP(0.5)/Al_2O_3.

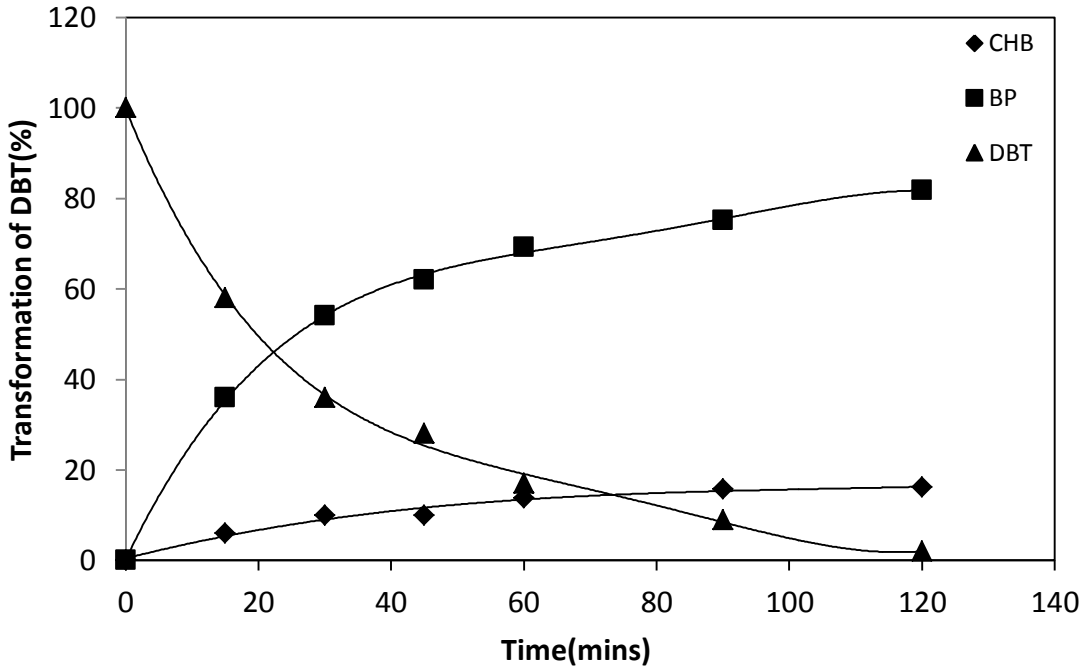

Figure 4.7.3 Transformation of DBT over NiMoP (0.5)/Al_2O_3 catalyst.

The HDS of 4,6-DMBDT were found to predominantly took place by hydrogenation pathway because more than 50% of desulfurization took place by hydrogenation pathway. The main product for HDS of 4,6-DMDBT were methyl cyclohexyl benzene(MCHT) and dimethyl biphenyl(DMBP). The maximum conversion of 4,6-DMDBT were 41.2% and the formation of MCHT and DMBP were 22.5% and 18.7% respectively. At these same conditions over CoMoP(0.5)/Al_2O_3 the conversion of 4,6-DMDBT, MCHT and DMBP were 30%, 14% and 15.8% respectively.

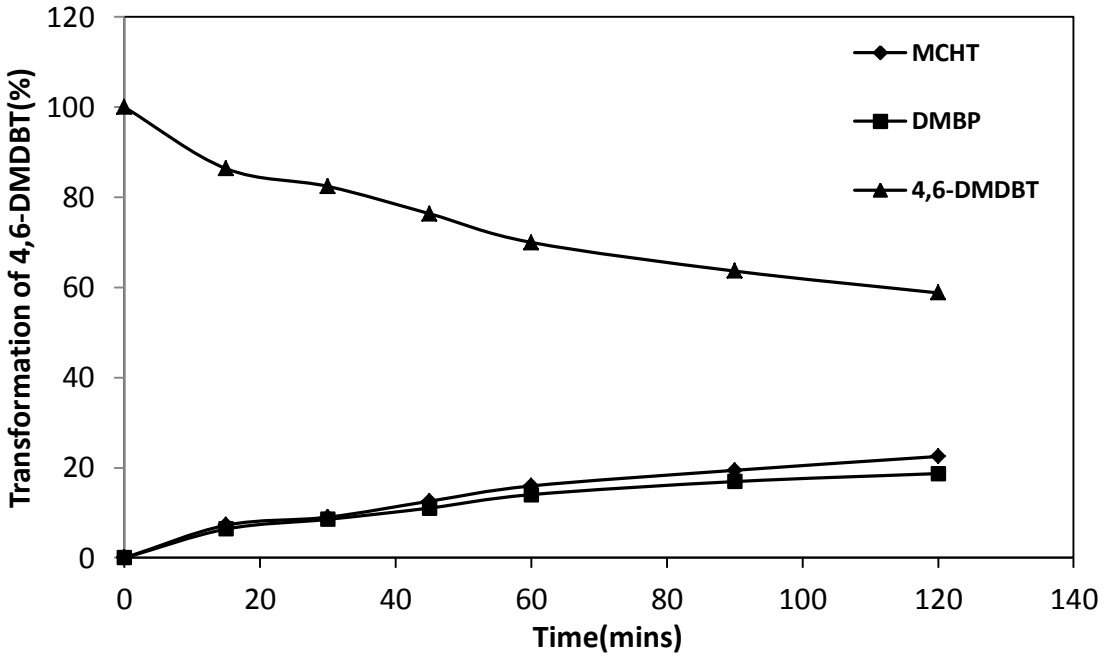

Figure 4.7.4 Transformation of 4,6-DMDBT over NiMoP(0.5)/Al_2O_3 catalyst.

The HDS of 4,6-DMBDT were found to predominantly took place by hydrogenation pathway because more than 50% of desulfurization tool placed by hydrogenation pathway. The main product for HDS of 4,6-DMDBT were methyl cyclohexyl benzene(MCHT) and dimethyl biphenyl(DMBP). The maximum conversion of 4,6-

DMDBT were 41.2% and the formation of MCHT and DMBP were 22.5% and 18.7% respectively. At these same conditions over CoMoP(0.5)/Al_2O_3 the conversion of 4,6-DMDBT, MCHT and DMBP were 30%, 14% and 15.8% respectively.

4.7.2 Rate of Formation for HDS product of DBT and 4,6-DMDBT

In order to investigate the reaction pathways individual rate constants were calculated from the plot of –ln(1-X) versus time. Where X is the conversion of DBT or 4,6-DMDBT into biphenyl, cyclohexyl benzene, methyl cyclohexyl benzene and methyl biphenyl. Figure 4.7.5 and 4.7.6 shows the rate constants of individual products obtained during the HDS reaction.

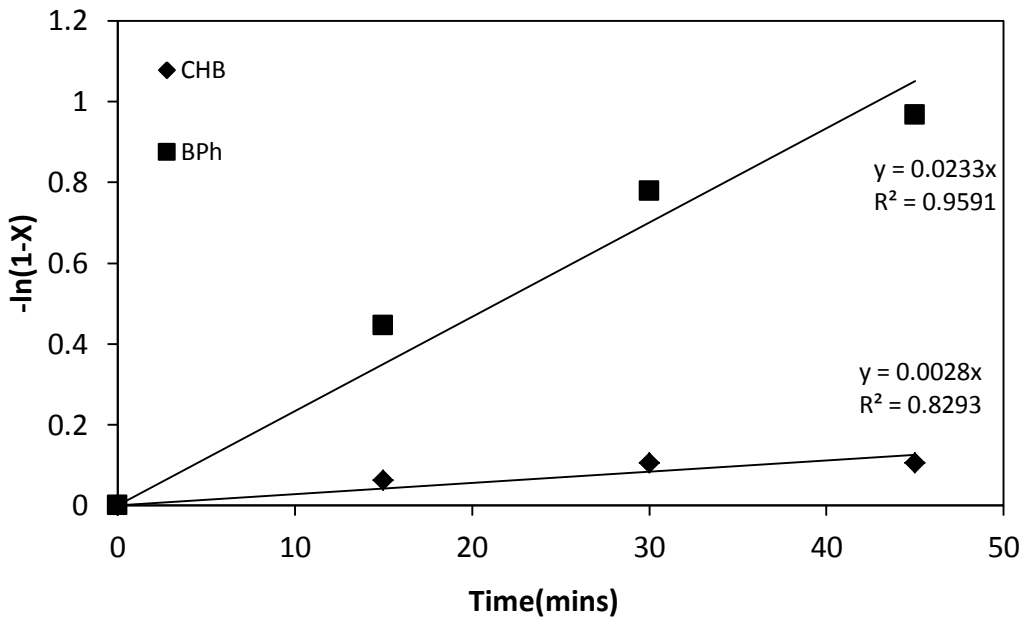

Figure 4.7.5 Formation rates of BP and CHBnover NiMoP(0.5)/Al_2O_3 catalyst.

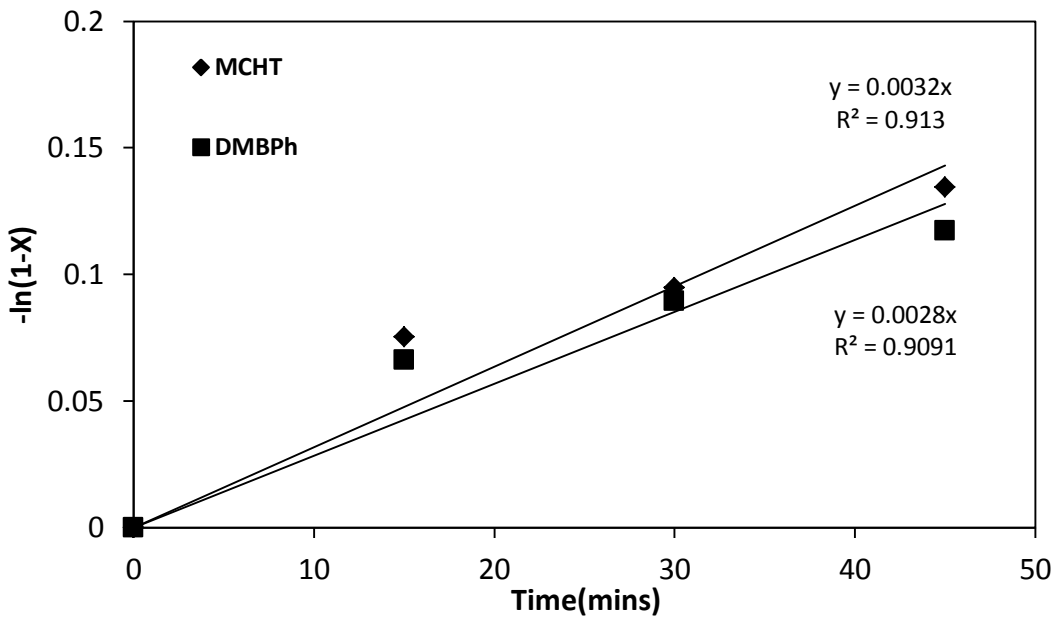

Figure 4.7.6 Formation rates of MBP and MCHB over NiMoP(1.5)/Al_2O_3 catalyst.

The rate of formations of biphenyl and cyclohexyl benzene is given in Table 4.7.3.

The rate constant for Biphenyl was found to be lower for reaction takes place over NiMoP(0.5)/Al_2O_3 and the CHB formations rates were about 1.75 times higher as compared to the rate of formations of these two compounds over CoMoP(0.5)/Al_2O_3.

Table 4.7.3 Foramtion rate constants k x1000 of Biphenyl and Cyclohexyl benzene and the ratio formation rate constants at 350°C.

Catalysts	BP	CHB	k_{BP}/k_{CHB}
CoMoP(0)/Al_2O_3	22	1.3	16.9
CoMoP(0.5)/Al_2O_3	24.8	1.6	15.5
NiMoP(0.5)/Al_2O_3	23.3	2.8	8.32

The rate of formation of MCHT was found to be higher than DMBP as 4,6-DMDBT desulfurized mainly by hydrogenation route as shown in the Table 4.7.4. The ratio of k_{DMBP}/k_{MCHT} were approximately same over the two catalyst but the formation rates of MCHT and MBP were higher over NiMoP(0.5)/Al_2O_3.

Table 4.7.4 Rate constant kx1000 and Relative rate of formation of dimethyl biphenyl and methyl cyclohexyl toluene.

Catalysts	DMBP	MCHT	k_{DMBP}/k_{MCHT}
CoMoP(0)/Al_2O_3	1.8	2.1	0.86
CoMoP(0.5)/Al_2O_3	1.8	2.1	0.86
NiMoP(0.5)/Al_2O_3	2.8	3.2	0.88

Chapter 5. CONCLUSIONS AND RECOMENDATIONS

5.1 Conclusions

1) The overall activity for Simultaneous HDS of Benzothiophene and Dibenzothiophene was higher over 0.4CoMo/Al_2O_3.
2) From the ratio of k_{BT}/k_{DBT} in the simultaneous HDS of BT and DBT, it was clear that the rate of BT HDS was more than 10 times as compared to DBT at 300^oC. At higher temperature (350 ^oC), the k_{BT}/k_{DBT} ratio decreased to 3.
3) From the formation rate constants of BP and CHB it can be concluded that the Co/Co+Mo ratio found to be only influenced the direct desulfurization pathway
4) HDS of benzothiophene comparatively took less time to desulfurize and 100% conversions were achieved at all temperatures and catalysts within 45 minutes.
5) For selectivity of DDS route 0.4CoMo/Al_2O_3 > 0.3CoMo/Al_2O_3>0.5 CoMo/Al_2O_3.
6) Phosphorus modification increases the pore radius of the catalysts.
7) X-ray diffraction analysis shows that phosphorus modification increases the active sites $CoMoO_4$ and MoO_3.
8) The HDS conversion was found to increase for all model compounds over all phosphorus modified catalysts. The maximum conversion was achieved over CoMoP(1)/Al_2O_3 as compared to other CoMo/Al_2O_3 catalysts.
9) The BPs/CHBs ratio decrease in the order of

   k_{BP}/k_{CHB} > k_{MBP}/k_{MCHB} > k_{DMBP}/k_{MCHT}
10) The HDS of DBT was also influenced by the competitive reactions with 4-MDBT and 4-6-DMDBT. The HDS conversion of DBT was higher when desulfurized in

a simultaneous HDS reaction with 4,6-DMDBT as compared to when desulfurized with 4-MDBT.

11) The DDS/HYD route of DBT was also affected in competition reaction a BP/CHB ratio was higher when desulfurized with 4,6-DMDBT compared to 4-MDBT.

5.2 Recommendations

1) In order to investigate the competition of DBT, 4-MDBT and 4,6-DMDBT the amount of catalyst can be varied to see the simultaneous HDS over the catalysts.
2) Nitrogen containing aromatic compounds can be used to see the effect of nitrogen compounds over HDS reaction.
3) Inhibition effects of H_2S can be studied over these same reaction conditions.

APPENDICES

APPENDIX A

SAMPLE CALCULATION FOR HDS ACTIVITY OF BENZOTHIOPHENE AND DIBENZOTHIOPHENE

Sample calculation for hydrodesulfurization activity of benzothiophene and dibenzothiophene are as follows.

Concentration of DBT (C_{DBT}) = Response Factor * A_{DBT}

Where

A_{DBT} is the area under the peak for unreacted benzothiophene or Dibenzothiophene

Response factor is calculated from

Response factor = Area of Phenyl sulfide / Concentration of Phenyl sulfide

Phenyl sulfide was added in the known concentration before injecting the sample in GC.

% conversion = $((C_A – C_{DBT}) / C_A) * 100$

C_A is the initial concentration of DBT before the reaction starts and in each case it was 500ppm.

C_{DBT} is the concentration of DBT at reaction time of t minutes.

For example

Response Factor = 325/4626

=0.07025

From the *chromatogram A* the area of DBT is 3057

C_{DBT} = 0.07025 * 3057

= 214ppm

So the percentage conversion of DBT is

% Conversion of DBT = ((500-214)/500) * 100

= 57.2

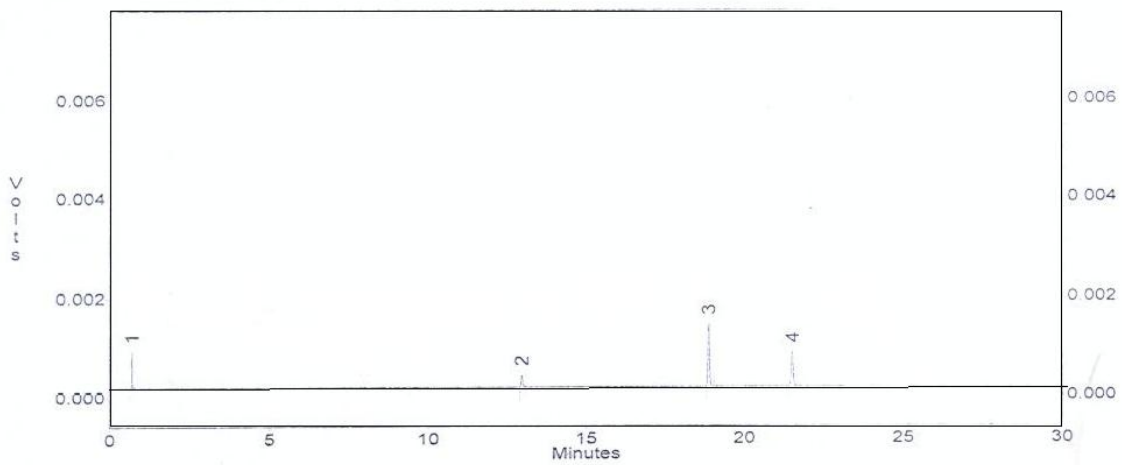

Channel A Results

NO.	NAME	TIME	AREA	CONC
1	H2S	0.71	872	0.00
--	thiophene	3.14	0	0.00
2	BT	12.96	850	0.00
3	Phen sulfide	18.87	4626	0.00
4	DBT	21.51	3057	0.00
--	4,6 DMDBT	25.00	0	0.00
Totals :			9405	0.00

Figure A-1. Chromatogram for the HDS of BT and DBT.

APPENDIX B

SAMPLE CALCULATION FOR THE CALCULATION OF CONCENTERATION OF BIPHENYL AND METHYL CYCLOHEXYL BEZNENE

$C_{BP} = (A_{BP}/(A_{BP} + A_{CHB})) * C_{DBT}$

$C_{CHB} = (A_{CHB}/(A_{CHB} + A_{CHB})) *C_{DBT}$

A_{BP} is the area under the peak for biphenyl.

A_{CHB} is the area under the peak for methyl cyclohexyl benzene.

C_{DBT} is the concentration of DBT at reaction time of t minutes.

C_{BP} is the concentration of biphenyl after the reaction time of t minutes.

C_{CHB} is the concentration of biphenyl after the reaction time of t minutes.

From Figure A-2

$A_{BP} = 21395$

$A_{CHB} = 2479$

$C_{BP} = (21395/(21395 + 2479)) * 214$

$C_{BP} = 191.77$

$C_{CHB} = (2479/(21395 + 2479)) * 57.2$

$C_{CHB} = 22.22$

% Conversion of DBT into biphenyl = $(C_{BP}/(C_{BP} + C_{CHB}))$ *%Conversion of DBT

% Conversion of DBT into biphenyl = (191.77/(191.77 + 22.22)) * 57.2

= 51.26

% Conversion of DBT into cyclohexyl benzene = $(C_{CHB}/(C_{BP} + C_{CHB}))$ *%Conversion of DBT

% Conversion of DBT into cyclohexyl benzene = (22.22/(191.77 + 22.22)) * 57.2

= 5.9

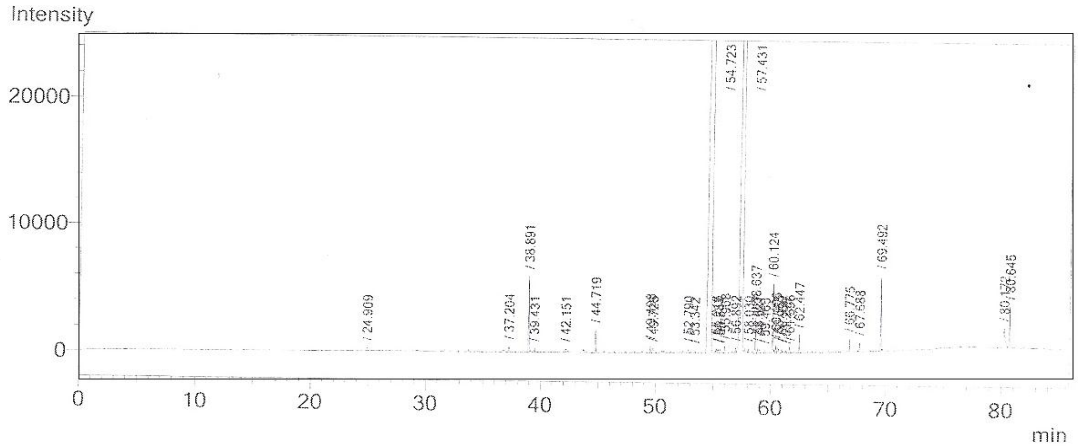

Peak Table - Channel 1

Peak#	Ret.Time	Area	Height	Conc.	Units	Mark	Name
1	24.909	1219	258	0.007			
2	37.204	2274	471	0.013			
3	38.891	24082	5959	0.137			
4	39.431	1123	292	0.006			
5	42.151	1125	296	0.006			
6	44.719	6862	1787	0.039			
7	49.498	2201	536	0.013			
8	49.725	1684	357	0.010		V	
9	52.790	1669	359	0.010			
10	53.342	1017	216	0.006			
11	54.723	10444076	929277	59.475			
12	55.216	1626	332	0.009		V	
13	55.387	1095	276	0.006		V	
14	55.544	1852	286	0.011			
15	55.968	2380	577	0.014		V	
16	56.892	1783	397	0.010			
17	57.431	6947340	728259	39.563		V	
18	58.030	1421	348	0.008			
19	58.637	11453	2801	0.065			
20	58.827	1775	412	0.010		V	
21	58.981	1832	366	0.010		V	
22	59.465	1368	210	0.008		V	
23	60.124	23191	5430	0.132		V	
24	60.406	2647	634	0.015		V	
25	60.585	2548	465	0.015			
26	60.930	1423	352	0.008			
27	61.298	1040	199	0.006		V	
28	61.596	1896	427	0.011			
29	62.447	5175	1425	0.029			
30	66.775	3118	1034	0.018			
31	67.688	2479	726	0.014		V	
32	69.492	21395	5888	0.122		V	
33	80.172	18831	1503	0.107			
34	80.645	15318	3214	0.087			
Total		17560318	1695369				

Figure B-1. Chromatogram for PIONA analysis for HDS of BT and DBT showing the Biphenyl and Cyclohexyl benzene peaks.

References

[1] F.L Plantenga, R.G. Leliveld, Applied Catalysis A: General., 248 (2003) 1-7.

[2] H. Topsøe, B.S. Clausen, F.E. Massoth Catalysis: Science and Technology., 11 (1996) 310.

[3] (a) US EPA Clean Air Act Tier 2; 1999; (b) Directive of European Parliament and of the Council. Brussels COM(2001) 11.05.2001 241 final

[4] R.G. Leliveld, S. E. Eijsbouts. Catalysis Today, 130 (2008) 183-189.

[5] D. R. Kilanowski, B.C. Gates, J.Chem., 41 (1996).

[6] P. J. Owens, C. H. Amberg, Adv. Chem Ser., 33 (1961) 182.

[7] P. Desikan , C .H. Amberg, Can. J. Chem., 42 (1964) 843.

[8] B. C. Gates, J. R. Katzer and G. C. A. Schuit, in: Chemistry of Catalytic Processes, p.390, McGraw-Hill: New York (1979).

[9] M. L. Vrinat, Appl. Catal, 6 (1983) 137.

[10] M. Houlla, N. K. Nag, A. V. Sapre, D. H. Broderick, B. C. Gates, AIChe J., 24 (1978) 1015.

[11] T.C. Ho, Hydrodenitrogenation Catalysis, Catal. Rev. Sci. Eng. 30 (1988) 117.

[12] R. Prins, V.H.J. de Beer and G.A. Somorjai, Catal. Rev. Sci. Eng. 31 (1989), p. 1.

[13] R. R. Chianelli, M. Daage, M.J. Ledoux, Adv. Catal. 40 (1994) 177.

[14] G. C. A. Schuit, B.C. Gates, AIChE J., 19 (1973) 417.

[15] F. E. Massoth, Adv. Catal., 27 (1978) 265.

[16] T. Lim, S.W. Weller, J. Catal., 108 (1987) 175.

[17] F.E. Massoth, J. Catal., 36 (1975) 164.

[18] H. Kraus, R. Prins, J. Catal., 164 (1996) 260.

[19] N.S. Chiu, S.H. Bauer, M.F.L. Johnson., J. Catal. 89 (1984) 226.

[20] T.G. Parham, R.P. Merrill, J. Catal., 85 (1984) 295.

[21] C. Li, Q. Xin, K.L. Wang, X.X. Guo, Appl. Spectrosc., 45 (1991) 874.

[22] C. Wivel, B.S. Clausen, R. Candia, S. Mørup, H. Topsøe, J. Catal., 87 (1984) 497.

[23] N. Topsøe, H. Topsøe, J. Catal. 84 (1983) 386.

[24] R. Prada Silvy, P. Grange, B. Delmon, Stud. Surf.Sci. Catal., 52 (1990).

[25] P. Arnoldy, J.A.M. van den Heijkant, G.D. de Bok, J.A. Moulijn, J. Catal., 92 (1985) 35.

[26] Y. Sakashita, T. Yoneda, J. Catal., 185 (1999) 487.

[27] M. J. Girgis and B. C. Gates, Ind. ENG. Chem., 30 (1991) 2021-2058.

[28] D. R. Kilanowski, H.Teeuwen, B. C. Gates, V. H. J. D. Beer, G. C. A. Schuit, H. Kwart, J. Catal., 55 (1978) 129.

[29] M. Houalla, D. H. Broderick, A. V. Sapre, N. K. Nag, V. H. J. D. Beer, J. Catal., 61 (1980) 523.

[30] X. L. Ma, K. Y. Sakanishi, I. Mochida, Ind. Eng. Chem. Res., 33 (1994) 218.

[31] Q. Zhang, A. Ishihara, T. Kabe, J. Jpn. Petrol. Inst., 39 (1996) 410.

[32] V. Lamuremeille, E. Schulz, M. Lemaire, M. Vrinat, Appl. Catal. A., 131 (1995) 143.

[33] F. Bataille, J. L. Lemberton, P.Michaud, G. Perot, M. Vrinat, M. Lemaire, E. Schulz, M. Breysse, S.Kasztelan, J. Catal., , 191 (2) (2000) 409.

[34] Landau, M. V.; Berger, D.; Herskowitz, J. Catal.1996, 159, 236.

[35]]Ma, X., Sakanishi, K.; Iosda, T.; Mochida, I.Ind.Eng.Chem. Res. 1995, 34,748.

[36] Isoda,T.; Nagao, S.; Ma, X.;Korai, Y.; Mochida, I. Energy Fuels 1996, 10, 1078.

[37] Lecrenay, E.; Sakanishi, K.; Mochida, I. Catal.Today 1997, 39, 13.

[38] Isoda, T.; Nagao, S.;Ma, X.; Korai, Y.;Mochida, I. Appl.Catal. A: General 1997, 150, 1.

[39] Lecrenay, E.; Sakanishi, K.; Nagamatsu, T.; Mochida, I.; Suzuka, T. Appl. Catal. B 1998, 18, 325.

[40] J. M. Lewis, R. A. Kydd, P. M. Boorman, P. H. Van Rhyn, Applied catalysis A General., 84 (1992).

[41] Usman, T. Yamamoto, Takeshi Kubota, Yasuaki Okamoto, Applied Catalysis A: General., 328 (2007) 219-225.

[42] C. Kwak, Mi. Y. Kim, K. Choi, S. H. Moon. Applied Catalysis A: General., 185 (1999) 19-27.

[43] J. M. Herrera, J. Reyes, P. Roquero, Tatiana Klimova Microporous and Mesoporous Materials 83 (2005) 283-291.

[44] B. Pawelec, J. L. G. Fierro, A. Montesinos, T. A Zepeda Applied Catalysis B: Environmental 80 (2008) 1-14.

[45] R.Nava, J. Morales, G. Alonso, C. Ornelas, B. Pawelec, J. L. G. Fierro Applied catalysis A: General 321 (2007) 58-70.

[46] F. Richard, T. Boita, G. Perot Applied Catalysis A: General 320 (2007) 69-79.

[47] Z. Tong-na, Y. Hai-Iiang, H. Shu-na, C. Yong-ming, L. Yun-ql, L. Chen-guang. Journal of Fuel Chemistry and Technology 37(3) (2009) 330-34.

[48] Do-W. Kim, D. K. Lee, Son-Ki Ihm, Catalysis Letters., 43 (1997) 91-95.

[49] G. Hagenbach, P.H. Courty, B. Delmon, J. Catal 31 (1973) 264.

[50] E. Lecerenany, K. Sakanishi, I. Mochida, Catalysis Today., 39 (1997) 13-20.

[51] M. Houlla, N.K. Nag, A.V. Sapre, D.H. Broderick, B.C. Gates AIChE J., 24 (1978) 1015.

[52] T. Kabe, A. Ishihara et al, Ind. Eng. Chem., 36 (1997). 5149.

[53] T. Isoda, S. Nagao, X. Ma, Y. Korai, I. Mochida, Energy & Fuel 10 (1996) 1078-1082.

[54] M. Egorova, R. Prins, J. Catal. 241 (2006) 162-172.

[55] F. Bataille, J. Lemberton, P. Michaud, G. Pérot, M. Vrinat, M. Lemaire, E. Schulz, M. Breysse, S. Kasztelan, J. Catal. 191 (2000) 409-422.

[56] T. Kabe, A. Ishihara, Q. Zhang, Appl. Catal. A: General. 97 (1993) L1-L9.

[57] V. Meille, E. Schulz, M. Lemaire, M. Vrinat, J. Catal. 170 (1997) 29-36.

VITAE

Name	Khaja Wahab Ahmed
Date of Birth	20th March 1985
Nationality	Pakistani
Religion	Islam
Educational Qualifications	BSc. Hons. in Applied Chemistry from University of Karachi .
	MSc. Applied Chemistry from University of Karachi.
	M.S. in Chemical Engineering KFUPM April 2011.
Present and Permanent Address	A-87 Rafa-e-Aam Society, Malir Halt, Karachi, Pakistan
Mobile Number	+966535654484
	+923332489760
Email address	kwahabahmed@gmail.com